University of Zurich UZH

Seasonal variability of rock glaciers kinematics using GNSS and UAV photogrammetry: four case studies in the Southern Swiss Alps, Canton Ticino.

GEO 511 Master's Thesis

Author
Giona Crivelli
18-706-275

Supervised by
Dr. Isabelle Gärtner-Roer
Prof. Dr. Cristian Scapozza (cristian.scapozza@supsi.ch)

Faculty representative
Prof. Dr. Andreas Vieli

30.04.2024
Department of Geography, University of Zurich

Abstract

The study of permafrost-related landforms such as rock glaciers is fundamental for gaining insights into the impacts of climate change on high mountain regions. Despite extensive research into the annual kinematics of these geomorphological forms over the past two decades, their behaviour on a seasonal scale remains poorly studied and understood. This thesis aims to address this research gap by investigating the intra-annual kinematics of four rock glaciers in the Southern Swiss Alps (Canton Ticino). Three dGNSS and UAV-photogrammetry surveys were conducted during the warm season on four selected sites: Stabbio di Largario, Piancabella, Monte Prosa and Ganoni di Schenadüi. Horizontal displacements between surveys were computed using dGNSS punctual measurements on big boulders, while horizontal displacements and thickness changes were derived for all the surface from UAV-photogrammetry products, orthomosaics and dense point clouds, using the NCC algorithm (CIAS) and M3C2 algorithm (CloudCompare), respectively.

The integration of UAV-photogrammetry together with dGNSS measurements allowed to gain more and reliable information on the intra-annual kinematics, highlighting significant spatial and temporal differences in velocity within individual rock glaciers and among them. Notably, Ganoni di Schenadüi exhibited rapid response after snowmelt at the onset of summer, while Stabbio di Largario and Monte Prosa displayed delayed reactions, with gradual acceleration observed during the early autumn. A noteworthy subsidence up to 50-60 cm over three months was detected close to a longitudinal furrow in the upper part of Monte Prosa. At the same time, a partial collapse of the front was documented at Stabbio di Largario.

These observations, consistent with previous research, offer preliminary insight into the potential triggers of these dynamic responses, which include, for example, the structure of rock glaciers themselves and their microtopography, as well as their internal thermal conditions and external climate-related factors such as snow cover, temperature variations and precipitations. This makes it possible to make initial assumptions about the condition of individual rock glaciers and the processes that might occur, such as ice melting or deformation due to material loading.

Continuing this type of measurement in the coming years, together with geophysical and hydrological investigations, will be crucial for a better understanding of the processes and factors that influence rock glacier kinematics.

Acknowledgements

During this past year, I have received great support from many people without whom this work would not have been possible. First of all, I would like to express my gratitude to my supervisors, Dr. Isabelle Gärtner-Roer and Prof. Dr. Cristian Scapozza, for giving me the opportunity to conduct this type of work and for guiding me along the way. In particular, I would like to thank Prof. Dr. Cristian Scapozza for his great enthusiasm and passion, for sharing data and for his support on the field and helpful advice before and during the writing of the thesis.

I would like to sincerely thank several other people, including:

- Chantal Del Siro (SUPSI), for the great collaboration and support during planning, field work and processing of the collected data. Her presence was crucial.
- Boris Ouvry (UZH), for the introduction to UAV-photogrammetry and help in the field work.
- Matteo Roncoroni (INRS), Alessio Spataro (SUPSI), Sebastian Vivero (UNIFR) and Andrea Rebba, who dedicated me several hours and gave me helpful advice regarding UAV-photogrammetry and the related software.
- The Institute of Earth Sciences (IST) of the SUPSI, for the financing of a helicopter flight and for the use of the "Daniel Bernoulli" cartography laboratory with the computer and photogrammetry software.
- The Glaciology and Geomorphodynamics Group of the UZH, for the financing of a helicopter flight.
- The Remote Sensing Group of the UZH, especially Prof. Dr. Felix Morsdorf and Nicole Manser, for borrowing the drone and giving me access to the flight planning software.
- Prof. Dr. Reynald Delaloye, for sharing GNSS data measured on the Monte Prosa rock glacier.
- My faculty member Prof. Dr. Andreas Vieli, for the valuable knowledge imparted during my studies.
- My family, Elisa and my friends for the enormous support throughout my studies and for always believing in me. Special thanks to my father for his help on the field and to Elisa for proofreading my thesis.
- The SUPSI IST employees, particularly Andrea, Aron, Chantal, Alessandro, Dorota, Filippo, Cristian for all the coffee and lunch breaks spent together during the last year.

List of figures

List of tables

List of abbreviations

GNSS	Global Navigation Satellite System
UAV	Unmanned Aerial Vehicle
GCPs	Ground Control Points
CPs	Check Points
LoD	Limit of Detection
GST	Ground Surface Temperature
MAGST	Mean Annual Ground Surface Temperature
MAAT	Mean Annual Air Temperature
LIA	Little Ice Age
SDL	Stabbio di Largario rock glacier
PB	Piancabella rock glacier
MP	Monte Prosa rock glacier
GA	Ganoni di Schenadüi rock glacier

Contents

1   Introduction

1.1   General context

High mountain regions, characterised by glacial and periglacial environments, constitute some of the Earth's most vulnerable and dynamic environments (Terzi *et al*., 2019; Immerzeel *et al*., 2020; Chakraborty, 2021). In these areas, elements like glaciers and permafrost are significantly impacted by climatic forcing due to their proximity to melting conditions and have recently changed at a rate never seen during the Holocene, therefore suggesting a dominant anthropogenic component (Haeberli & Beniston, 1998; Haeberli & Hohmann, 2008; Abermann *et al*., 2010; Brighenti *et al*., 2019; Cusicanqui *et al*., 2021; Haeberli *et al*., 2024). European Alps, which lie at a climatic crossroad, including continental, oceanic, polar, Mediterranean and sometimes Saharan influences (Beniston, 2006), experienced a temperature rise of about 2°C between the late 1800s and the beginning of the 21st century, which is twice the global and European average (Brighenti *et al*., 2019). This indicates that these environments are essentially unstable and undergo significant changes over geologically short time intervals in response to climatic events (Rahbek *et al*., 2019). For this reason, mountain environments are considered early warning areas of global warming (Brighenti *et al*., 2019). Given the significant vulnerability of these environments and following future climate scenarios, these regions will continue their changing processes (Terzi *et al*., 2019). It is estimated that in the first half of the 21st century, air temperature in the Alpine arc will increase by a further 1.5°C and by 3.3°C by the end of the century, with the most significant changes at higher altitudes (Brighenti *et al*., 2019). Overall, by the end of the century, there will be consequences both for the environment and consequently also for society, such as changes in the landscape, water cycle, loss of biodiversity and ecosystem services, as well as damage to the local economy (Beniston *et al*., 2018; Terzi *et al*., 2019). Climate change and the resulting changes in snow and ice melt will cause runoff regimes to move from glacial to nival and from nival to pluvial, as well as create a shift in the timing of discharge maxima (Beniston *et al*., 2018). This will have a significant effect on the seasonality of high-altitude water availability which, in turn, will have implications on managing and storing water in reservoirs for irrigation, hydropower generation, and drinking (Beniston *et al*., 2018; Brighenti *et al*., 2019). Moreover, human safety, which is related to the risk of natural hazards, is also increasingly threatened. Mountain slopes have become unstable due to glacier retreat and permafrost thawing, posing a threat to human facilities and inhabitants (Buchli *et al*., 2018; Cusicanqui *et al*., 2021). In such mountainous areas, the interaction of various processes relating to snow, ice melting, permafrost thawing, and water availability, which are frequently exacerbated by the steepness of the terrain, will probably cause mass movements and process chains that have not been documented in historical times (Beniston *et al*., 2018; Cusicanqui *et al*., 2021).

If the impact of ongoing climate change is easily visible and measurable for glaciers, the same cannot be said for permafrost. In fact, unlike glaciers, permafrost is less connected to the atmosphere because its thermal regime is mediated by topography, surface water, groundwater, soil properties, vegetation, and snow. The different interactions between these components can lead to positive and negative feedbacks regarding permafrost stability (Jorgenson *et al.*, 2010).

This master thesis is part of the study of permafrost and its degradation, which is exacerbated by ongoing climate change. It aims to improve the knowledge of the intra-annual kinematics of rock glaciers and the possible factors and mechanisms that can influence their variability.

1.2   Permafrost

Permafrost refers to ground material (soil, loose debris or rock unrelated to the ice content and organic material) that has remained at or below 0°C for two or more consecutive years (Kaufmann *et al.*, 2021). Since the definition is purely thermal, permafrost may, but does not have to, contain water in a liquid or solid state (Gruber & Haeberli, 2008). Above the permafrost body lies an active layer that shows a seasonal cycle of freezing and thawing and, on average, measures a few centimetres but can reach depths of several meters (Haeberli *et al.*, 2006; Dobiński, 2020). Permafrost is typical of glacial and periglacial regions. Therefore, it can be found at high latitudes and high alpine altitudes (Figure 1). According to Krautblatter *et al.* (2018), at Alpine level, permafrost covers approximately 6200 km^2, compared to approximately 2000 km^2 covered by glaciers. In Switzerland, which is the Alpine country with the highest percentage of permafrost (about 35%), this proportion is estimated to be between 3% (Haberkorn *et al.*, 2021) and 5% (Federal Office for the Environment FOEN, 2005) of the surface area. In the Southern Swiss Alps (Canton Ticino and Region Moesa in Canton Graubünden), it has been calculated that approximately 265 km^2, i.e. 9% of the surface area, have a probability of permafrost occurrence of more than 50% (Deluigi & Scapozza, 2020) (Figure 2).
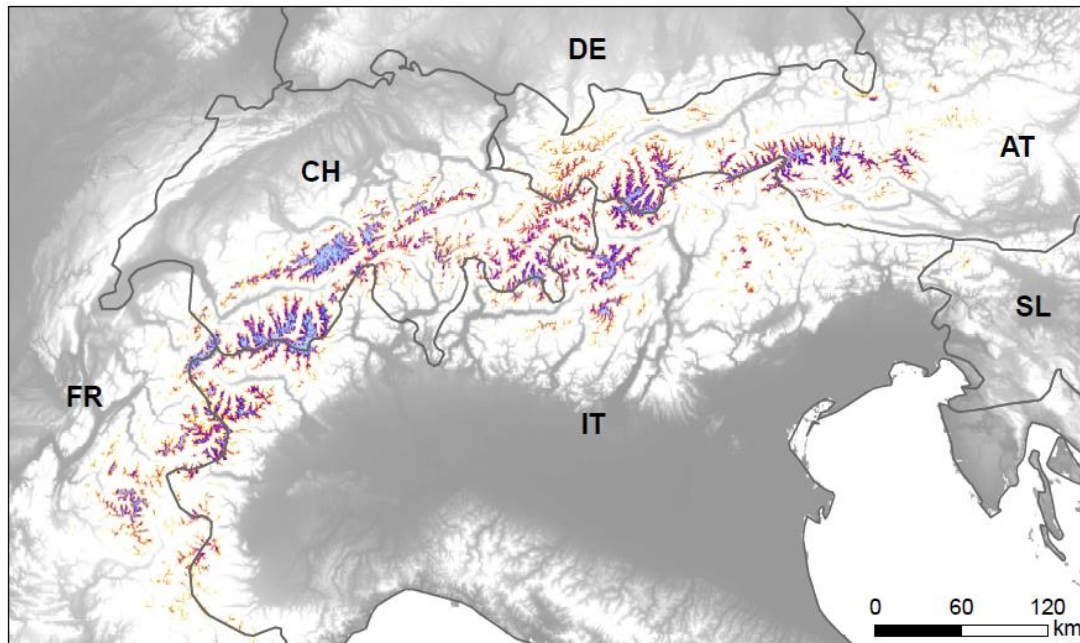
Figure 1: Permafrost distribution in the Alps (Boeckli et al., 2012).
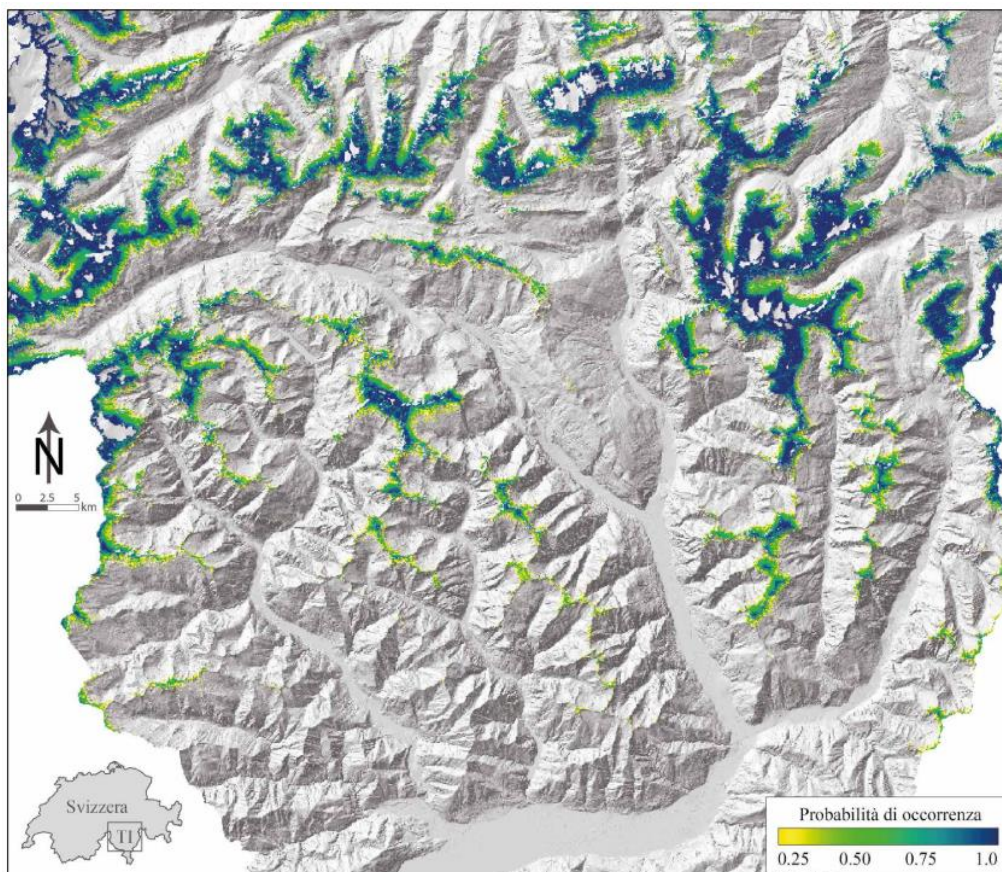
Figure 2: Probability of permafrost occurrence in the Southern Swiss Alps (Deluigi & Scapozza 2020).

Permafrost in mountain regions is considered to have a strong spatial variability that depends on many factors such as (1) elevation and other geometric factors such as slope, aspect and roughness, (2) composition and

thickness of subsurface material, (3) water availability, (4) snow cover as well as (5) surface micro-climatology (Gruber & Haeberli, 2008). The occurrence and characteristics of permafrost, which depend on these elements, are significantly impacted by atmospheric temperature rise because of its thermal conditions, which are closed to melting or thawing temperatures and seem to be more prominent in cold mountain regions than on a global average (Gärtner-Roer *et al.*, 2022). In fact, in the last two decades, the (Swiss) Alps have experienced increased ground temperatures, active layer thickening and varying ice- and water contents (Haberkorn *et al.*, 2021). For example, over the past decade, the mean ground surface temperature measured in the Southern Swiss Alps has increased by 0.7°C (Del Siro *et al.*, 2023a).

Since the end of the last century, and since permafrost was identified as one of the six cryospheric indicators of global climate change within the Global Climate Observing System (GCOS) monitoring framework of the World Meteorological Organization (Harris *et al.*, 2003), there has been a need to improve knowledge about the distribution of mountain permafrost, its thermal state and thickness, and how it might react in a constantly changing climate (Etzelmüller *et al.*, 2020). For this reason, in the 1990s and through a pilot phase in the early 2000s, the Swiss Permafrost Monitoring Network, known as PERMOS, took shape (Vonder Mühll *et al.*, 2008). This network ensures long-term mountain permafrost monitoring through a variety of methods, including ground surface temperature observations, borehole temperature logging, geophysical investigations (electrical resistivity tomography), and terrestrial geodetical slope deformation monitoring using devices like total stations and Global Navigation Satellite System (GNSS) receivers (Haberkorn *et al.*, 2021; Kellerer-Pirklbauer *et al.*, 2024). Data are sent to PERMOS by six Swiss research institutes responsible for monitoring permafrost in different regions of the country. In Southern Swiss Alps, the "Gruppo Permafrost Ticino", consisting of researchers from the SUPSI Institute of Earth Sciences in Mendrisio and the Cantonal administration, is responsible for monitoring this cryosphere component.

1.3   Rock glaciers

1.3.1 Rock glacier definition

The rock glacier is one of the most visible manifestations of permafrost in the high mountains (Haeberli, 1985; Barsch, 1996) (Figure 3). Rock glaciers, which are generated by unconsolidated and ice-supersaturated debris under permafrost conditions, are commonly recognised as creep phenomena of mountain permafrost (Wirz *et al.*, 2016; Zahs *et al.*, 2019; RGIK, 2021). They are believed to hold a significant portion of mountain ground ice, making them significant geomorphological markers of the existence and extent of mountain permafrost and a crucial component of the periglacial cryosphere landscape in high mountain areas (Zahs *et al.*, 2019). They are classified as active, transitional and relict based on their activity and ice content (Fey & Krainer, 2020). The active ones are composed of a mixture of ice and debris and creep downslope. Generally, the ice

content varies between 50-90%, and the body of the rock glacier is permeable, meaning air voids occur inside it, and water can flow through it (Wirz *et al*., 2016). These landforms are defined by their characteristic morphology, which includes long-term cohesive creep with reduced internal friction (RGIK, 2021; Gärtner-Roer *et al*., 2022), convex shape with oversteepened fronts as well as longitudinal and transverse furrows and ridges (Wirz *et al*., 2016; Kaufmann *et al*., 2021) caused by continued advance. Furthermore, they are characterised by their composition of talus or debris with variable but generally high (excess) ice contents and their complex flow behaviour is affected by negative subsurface temperatures and highly anisotropic material properties (Gärtner-Roer *et al*., 2022). A graphical illustration made by Cicoira *et al*. (2021) can be seen in Figure 4. The transitional rock glaciers still contain ice and debris but no longer move. In contrast, the relicts no longer contain ice, are generally covered by vegetation and show collapse structures on the surface (Barsch, 1996).

Figure 3: Drone image of the Ganoni di Scheandüi rock glacier, Cadlimo Valley. Date: 01.09.2023
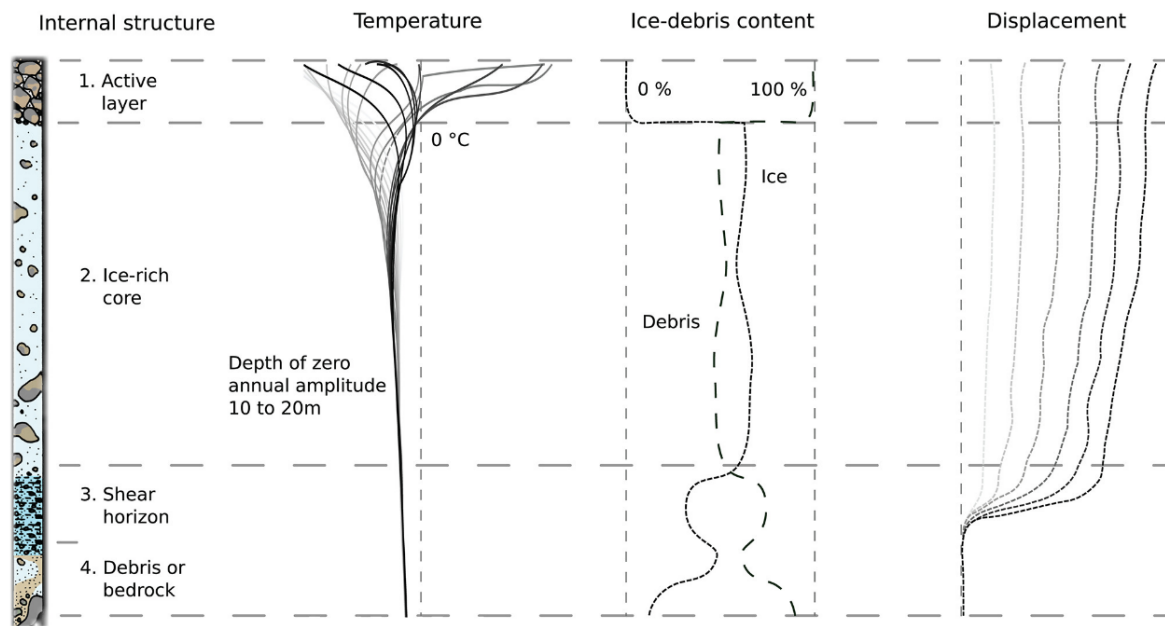
Figure 4: Graphical illustration of conceptualised vertical profiles in a rock glacier. From left to right internal structure, ground temperatures, material composition and displacements profiles are shown (Cicoira *et al.*, 2021)*.*

In Switzerland, the first detailed description of a rock glacier, then seen as a strange relief shape and called a "block flow", was made by André Chaix about a century ago (Chaix, 1923). He observed these geomorphological figures in the Lower Engadin region. It was mainly a qualitative description. However, Chaix (1923) observed and calculated the movement of these "block flows" using basic methods. The researcher understood that progression occurs as in glaciers (or fluids in general) but curiously did not assume the presence of ice within these forms. After Chaix's observations, over decades, rock glaciers were assumed to move down the slope at a steady rate, moved by gravity and nearly wholly independent of any external effect. It is only since the 1980s that kinematic investigations have shown strong interannual and seasonal variability in rock glacier flow velocities (Haeberli, 1985), renewing the interest in their dynamics and their driving processes (Cicoira *et al.*, 2021). At that time, PERMOS took shape, and towards the beginning of the 2000s, systematic monitoring of a significant number of scattered rock glaciers in the Swiss Alps began. At present, there is no complete inventory of all rock glaciers in the Alps; however, considering only the Swiss Alps, more than 2000 active landforms are estimated (Delaloye *et al.*, 2010).

1.3.2 Rock glacier kinematics

Monitoring rock glacier kinematics involves observing the viscous flow of these geomorphological landforms, visible on its surface, and its variability over time (RGIK, 2021). This means quantifying movement, which, in the case of rock glaciers, is determined by changes in surface geometry, horizontal and vertical (Delaloye *et al.*, 2010). Permafrost creep, permafrost slide, zonal thinning or thickening, advection of surface

microtopography, three-dimensional (3D) straining, general mass changes (heaving or settlement), and horizontal shearing and rotation are all examples of rock glacier deformation processes (Delaloye *et al.*, 2010; Zahs *et al.*, 2019).

Typically, rock glaciers creep downwards with horizontal velocities in the range of centimetres to metres per year (Zahs *et al.*, 2019; Gärtner-Roer *et al.*, 2022), and these displacements, that can vary over time and space and in magnitude (Vivero & Lambiel, 2019), are thought to depend on a combination of factors such as slope, ice content, differential sediment evacuation or accumulation rates, deformation layer thickness, water input, internal composition, temperatures (which influence the rheological behaviour) and shear stresses (Zahs *et al.*, 2019; Cicoira *et al.*, 2021), with some of them influenced by external factors associated with the climatic variables (Bertone *et al.*, 2023). However, it is essential to underline that not all parts of the rock glacier deform similarly. According to Wirz *et al.* (2015), studies on borehole deformation measurements in rock glaciers show that within the permafrost body, there are thin layers called shear horizons, with very different rheological properties, for example, with low viscosity, where 50-97% of the horizontal deformation occurs (Figure 4). It is also argued that the internal deformation process does not occur below these shear horizons, while only limited internal deformation occurs above them. Statistical and numerical modelling based on comprehensive kinematic data have been utilised to link the observed temporal variations in creep velocities to climate forcing such as air and ground temperature, snow melt, and liquid precipitation (Cicoira *et al.*, 2021).

1.3.3 Importance of monitoring rock glacier kinematics

In addition to the mentioned mechanical processes, there are different scientific reasons for monitoring rock glacier kinematics. These include climate change impact assessment, sediment transfer balance, geological hazard management and mass balance study, namely ice storage evolution (RGIK, 2021; Gärtner-Roer *et al.*, 2022). As slopes with potential instability and reservoirs of frozen water, rock glaciers and their dynamics have increased in importance in climate change investigations over recent years. Anticipated increases in average annual temperatures are believed to cause alterations to surface and subsurface dynamics at various time scales (ranging from weekly to decadal), depending on the conditions found at each different site (Zahs *et al.*, 2019).

The climate change impact assessment probably remains the most important reason to monitor rock glacier kinematics, with climate influencing most of the abovementioned processes. Indeed, as argued by RGIK (2022), the movement of rock glaciers is susceptible to changes in permafrost temperature. They are important features in understanding the response of the high-altitude cryosphere to climate change since they are abundant in many weakly glaciated mountain locations worldwide (Bodin *et al.*, 2018). By updating

and comparing the inventories of various rock glaciers of different regions, which usually include information on the kinematics in a well-defined time frame, the impact of ongoing climate change on the mountain periglacial environment can be assessed (Haberkorn *et al.*, 2021). Recognising and understanding how permafrost responds to climate change is very important for the scientific community and society as a whole (Bodin *et al.*, 2015).

Closely related to permafrost temperature change are geological hazards, which can threaten society and its activities and infrastructures (RGIK, 2022). Any change in the flow rate of permafrost can alter the supply of loose material at the rock glacier front and influence the frequency, the magnitude and even the nature of associated slope instabilities (Delaloye *et al.*, 2008). In this context, and considering the climate warming trend, there is an increasing demand for reliable and up-to-date data on the development of the permafrost environment at high altitudes (Delaloye *et al.*, 2008). The study of rock glaciers, although insufficient to fully understand the complex issue of permafrost degradation in periglacial regions, can provide clues to the presence or absence of permafrost in a given area (RGIK, 2022). This could also help in understanding how much water is stored underground. Indeed, with the reduction of glaciers and snow cover in the Alpine arc, the supply of water from rock glaciers (and periglacial areas in general), which are believed to be more resilient to climate change (Pruessner *et al.*, 2022), could play a critical role. In fact, from the middle of the current century, in the European Alps, the ice volume present in the ground could be greater than the volume of surface ice (Haeberli et al., 2017). Furthermore, as suggested by Pruessner *et al.* (2022), by the end of the 21st century, runoff from thawing permafrost could represent between 5-12% of the monthly runoff of a catchment, reaching peaks of 50% in the most extreme years.

1.3.4 Temporal variability of rock glacier kinematics

The measurement and interpretation of the surface kinematics of rock glaciers on different time scales have been an important field of research for several decades (Cusicanqui *et al.*, 2021). Three types of temporal variability of surface movement are superimposed and respond to variations in different environmental variables such as temperature and water supply: decadal or multi-decadal fluctuations, inter-annual variations and seasonal or intra-annual trends (Delaloye *et al.*, 2008). In recent decades, the kinematics of rock glaciers have been studied mainly through tachymetric surveying and differential GPS. More recently, with the rapid development of sensors and software and the increase in computing capabilities, remote sensing techniques such as differential interferometry, terrestrial laser scanning and unmanned aerial vehicle (UAV) have been used increasingly (Fey & Krainer, 2020).

High-resolution kinematic measurements reveal significant seasonal and interannual fluctuations in rock glacier creep. These variations, along with the shearing process, are impacted by how climate affects

subsurface water conditions and ground temperature (Cicoira *et al.*, 2019; Kaufmann *et al.*, 2021). An increase in shear temperatures causes a rise in the amount of unfrozen water, which amplifies the lubricating action and releases more shear stress (Wang *et al.*, 2023). According to Haberkorn *et al.* (2021), short-term acceleration is due to an increased water content within rock glaciers caused by intense summer precipitation. In contrast, throughout the year, the speed of rock glaciers is determined more by the freezing duration of the active layer, which controls the water balance. Despite these explanations concerning the role of temperature and water, clear evidence of the processes and the mechanisms linking them to rock glacier acceleration remains rare (Kenner *et al.*, 2017). Similarly, Delaloye *et al.* (2008) highlight the need for more documentation of short-term (interannual and seasonal) variations to improve the understanding of how fast, where and how they deform (Bodin *et al.*, 2018). To date, much importance has been given to rock glaciers creeping or surface height changes, whereas volume changes have received less attention (e.g., Halla *et al.*, 2021; Kaufmann *et al.*, 2021; Vivero *et al.*, 2021; Vivero and Lambiel, 2019). According to Abermann *et al.* (2010), volumetric changes are mainly due to the dynamics of the rock glaciers themselves. However, the thinning of these geomorphological forms is generally attributed to ice melt, although the contribution of rocks from the above walls can play a very important role (Cusicanqui *et al.*, 2021).

As seen, the processes and interactions that lead to observable changes in the surface topography of a rock glacier have different spatial, temporal and magnitude characteristics (Zahs *et al.*, 2019). Quantifying these changes, as well as knowing the relationship between the aforementioned processes, requires multi-temporal datasets spanning from decades to several months or days (depending on the purpose) and which can capture processes down to a few centimetres. This requires measurements and 3D reconstructions of the surface that are sufficiently accurate and precise (Zahs *et al.*, 2019).

1.4   Regional rock glacier and permafrost studies

The thermal state and kinematics of rock glaciers in Canton Ticino have been monitored annually since 2006 and 2009 respectively. It was first monitored by the Geography Institute of the University of Lausanne (until 2012), and later by the Earth Sciences Institute of SUPSI, with the support of PERMOS and the Cantonal Museum of Natural History in Lugano (Del Siro *et al.*, 2023a). As far as the Monte Prosa A rock glacier is concerned, it is still monitored by the geomorphology research group of the University of Fribourg. The data collected and the consequent results (excluding those of Monte Prosa A) are summarised in six reports entitled "Il Permafrost nelle Alpi Ticinesi" (Mari et al., 2012; Scapozza et al., 2014b, 2016, 2018, 2020; Del Siro et al., 2023a). During these years, mainly two types of measurements were carried out: geodetic point measurements and thermal measurements of the ground surface. In addition, in 2011, an attempt was made to compile a cadastre of ground movements in permafrost zones in the Swiss Southern Alps, in particular in

Canton Ticino, using satellite radar interferometry (InSAR) (Mari *et al*., 2011). This work made it possible to inventory 178 active areas, 76 of which are in the Alpine permafrost zone, catalogued as active rock glaciers. A few years later, Scapozza *et al*. (2014b), using the Schmidt-Hammer technique, as well as monophotogrammetry, calculated the age and horizontal velocities for the rock glacier Stabbio di Largario on a very long time scale. They estimated a front age of 5.05 ± 0.57 ka cal BP, thus situating its formation during or right at the end of the Mid-Holocene climate optimum (9.5-6.3 ka cal BP). Furthermore, they saw how during the Medieval Warm Period (MWP) and since the end of the Little Ice Age (LIA) there have been accelerations, which have become more important since the late 1990s, leading to signs of possible destabilisation of the rock glacier, such as the formation of crevasses. Drone flights were also carried out in 2014 and 2016 with the aim of calculating horizontal velocities and surface changes of two rock glaciers using photogrammetry. The only studies in Ticino on the intra-annual kinematics of rock glaciers were carried out by Ramelli *et al*. (2011) and Mari *et al.* (2012), where a comparison of summer displacements (measured by dGPS) of rock glaciers revealed important differences between them. However, the absence of boreholes in the Ticino rock glaciers does not allow direct observations of their internal conditions and, thus, their thermal state at depth.

1.5 UAV Photogrammetry for geomorphological research

Considering the effects of continuous global warming, especially in mountain regions where permafrost thawing is accelerating, accurate analyses of geomorphological landforms and geo-hazards is becoming increasingly important (Clapuyt *et al*., 2017). Unmanned aerial vehicles (UAVs) are increasingly being employed to automatically collect high-resolution airborne imagery for these purposes, as well as for a range of other geomorphological and environmental contexts such as fluvial, coastal, or agricultural studies. The collected images are typically used to generate comprehensive high-resolution orthomosaics and digital elevation models (DEMs) to derive surface changes (James *et al*., 2017). The fast proliferation of Structure-from-Motion Multiview Stereo (SfM-MVS) software, which offers far easier image processing procedures than classic aerial photogrammetry approaches, has additionally helped in DEMs creation (Abermann *et al*., 2010; James & Robson, 2014; Martínez-Fernández *et al*., 2022) and have enabled the assessment of surface motion on rock glaciers, as well as other landforms such as glaciers and landslide (Bearzot *et al*. 2022), with remarkable resolution, accuracy, and spatial coverage, resulting in a variety of new insights into rock glaciers development and behaviour (Haeberli *et al*., 2006). Using the photogrammetric technique, changes in thickness and surface displacements can be calculated through repeated stereo-imagery (Haeberli *et al*., 2006). In the field of research on rock glaciers, and more specifically on their kinematics, the integration of the classic dGNSS method with point measurements and UAV photogrammetry has been found to be very interesting in several cases (Dall'Asta *et al*., 2015; Fey & Krainer, 2020; Bearzot *et al*. 2022). Point data

measured using dGNSS allows having ground control points, hence "absolute truths", which are used to georeference the products of the photogrammetric process and which would otherwise not be available if only aerial images were used. On the other hand, the great advantage of UAV photogrammetry is to have spatialised kinematic information over the entire surface of the rock glacier. The advantages of this method, compared to other remote sensing techniques such as LiDAR, are mainly flexibility and ease of use, which add up to excellent results with relatively low-cost equipment (Hayamizu & Nakata, 2021; Martínez-Fernández *et al.*, 2022).

1.6   Research questions and hypothesis

Despite a considerable number of studies that have focused on rock glaciers, it is still unclear what factors and how they influence their kinematics, especially over a short period of time. In this sense, observations of changes in kinematics over periods of a few months can be a good starting point for trying to understand these processes. In this regard, the aim of this thesis is to extend the historical information on kinematics already collected over the last 15 years through point geodetic measurements and to investigate its seasonal variability on four rock glaciers located in the Southern Swiss Alps (Canton Ticino) during the hydrological year 2023 using dGNSS measurements and UAV photogrammetry. To do so, the following objectives were defined:

- Contextualise the kinematics of the four investigated rock glaciers within their interannual evolution thanks to the historical series of dGNSS measurements.

- Quantify through the use of dGNSS the displacements that occurred in summer 2023 and identify differences in velocities:
    o For all four rock glaciers together between the different periods (regional trend)
    o For each individual rock glacier between the different periods (local trend)
    o Among the four rock glaciers for each individual period (comparison)

- Compare dGNSS measurements with UAV-based surveys in order to verify their possible complementarity for the spatialisation of kinematic information.

- Quantify horizontal displacements and thickness changes (with an approximation of the volume lost/gained) using photogrammetry products during the hydrological year 2023, particularly during the warm season 2023, as well as between 2016 and 2023 for the rock glaciers of Stabbio di Largario and Piancabella.

- Interpret and discuss the evolution of kinematics and its variability at the intra-annual and inter-annual level by analysing the obtained results through the relevant literature.

These information could be valuable for a better understanding of the internal state of individual rock glaciers and how they react to changing external factors such as temperature, snow conditions and precipitation events during different periods of the year.

In 2022, measurements showed that rock glaciers in the Ticino Alps have slowed down significantly (Del Siro *et al.*, 2023a). This result is somewhat surprising, given that 2022 was the warmest year since the beginning of the measurements (MeteoSchweiz, 2023a). The air temperature at high altitudes, for example, at the Matro measuring station (2271 m a.s.l.), reached peaks of 20°C between July and August (MeteoSchweiz, 2023a). However, as already seen, factors that are not (directly) related to temperature can also play a very important role in influencing the creep rate. The effect of topography, for example, especially on longer time scales, or the effect of snowmelt water infiltration, subpermafrost groundwater (Delaloye *et al.*, 2008), as well as rainfall on shorter time scales (Kenner *et al.*, 2017) could play a role. Following this reasoning and analysing the snowfall and precipitation data for the hydrological year 2022, it can be seen that the values are clearly below the norm from 1991-2020 (MeteoSchweiz, 2023a). The lack of snow cover (insulating effect in winter and source of water in spring/early summer) and precipitation could be the cause, despite the high temperatures, of the decreasing horizontal velocities of rock glaciers compared to the previous year. Going back three years, i.e. to the hydrological year 2021, snowfall during winter had been abundant (the ground was insulated from the cold temperatures), as well as summer precipitation (MeteoSchweiz, 2023a). The sum of these two factors may, therefore, be the cause for the downstream acceleration of the Ticino rock glaciers during that period.

Looking at the weather data for the winter of 2022-2023, the sum of precipitation was only between 40-65% of the 1990-2020 norm (MeteoSchweiz, 2023b). This means that the ground had again relatively little insulation that winter. Furthermore, there was little meltwater. As mentioned, especially on the time scale this research is interested in, the intra-annual/seasonal one, spring and summer precipitation will play a very important role. Based on the results of Wirz *et al.* (2015), the seasonal acceleration and velocity peaks correspond to water infiltration, which causes thermal advection and increased pore water pressure. Cicoira *et al.* (2019) also suggest that the major cause of rock glacier creep variations is not air temperature but water from liquid precipitation and snow melt. Indeed, the conductive energy injected onto the surface of the rock glacier (as the air temperature rises) reaches the shear layer tens of metres below the surface with a considerable delay (Kenner *et al.*, 2017).

Concerning volume changes, it is unclear how these are related to changes in climatic and environmental factors and how they affect rock glacier dynamics. Cusicanqui *et al.* (2021) suggest that the surface mass

balance predominantly controls thickness changes and that changes in geometry do not affect flow velocities. Furthermore, the same authors hypothesise that the acceleration of rock glaciers is due to a general thinning of the rock glaciers that have caused changes in conditions (thermal and liquid water content) in the shear layer and at the base.

The hypothesis, based on the previous studies by Ramelli *et al*. (2011), Mari *et al*. (2012) and Scapozza & Ambrosi (2017), is that during the warm season, rock glaciers of the southern Swiss Alps will experiment horizontal displacements in the range of tens of decimetres, with spatial differences depending on the rock glacier. Thickness changes are also expected, although their magnitude is uncertain. Furthermore, based on other studies (Perruchoud & Delaloye, 2007; Wirz *et al*., 2016; Cicoira *et al*., 2019), time-varying velocities are expected, with a probable increase in displacements during the summer as a result of water infiltration due to snow melt (Wirz *et al*., 2016; Cicoira *et al*., 2019), and a further increase during the early autumn, when the temperature signal will have had more time to reach depth. Therefore, depending on weather conditions, but also on thermal state, ice quantity, structure and microtopography, differences could be seen between periods of the year and between rock glaciers. The use of photogrammetry, which has proven effective in other studies (Scapozza *et al*., 2018; Vivero & Lambiel, 2019; Bearzot *et al*. 2022), should help in the spatialisation of information also at the seasonal level, adding important information on the intra-annual kinematics of the four investigated rock glaciers.

2 Study sites and available data

2.1 Studied rock glaciers

The thesis focuses on four active rock glaciers in the Lepontine Alps of Ticino, Switzerland: Stabbio di Largario, Piancabella (Valle di Sceru), Monte Prosa, and Ganoni di Schenadüi. Figure 5 shows their geographical locations.
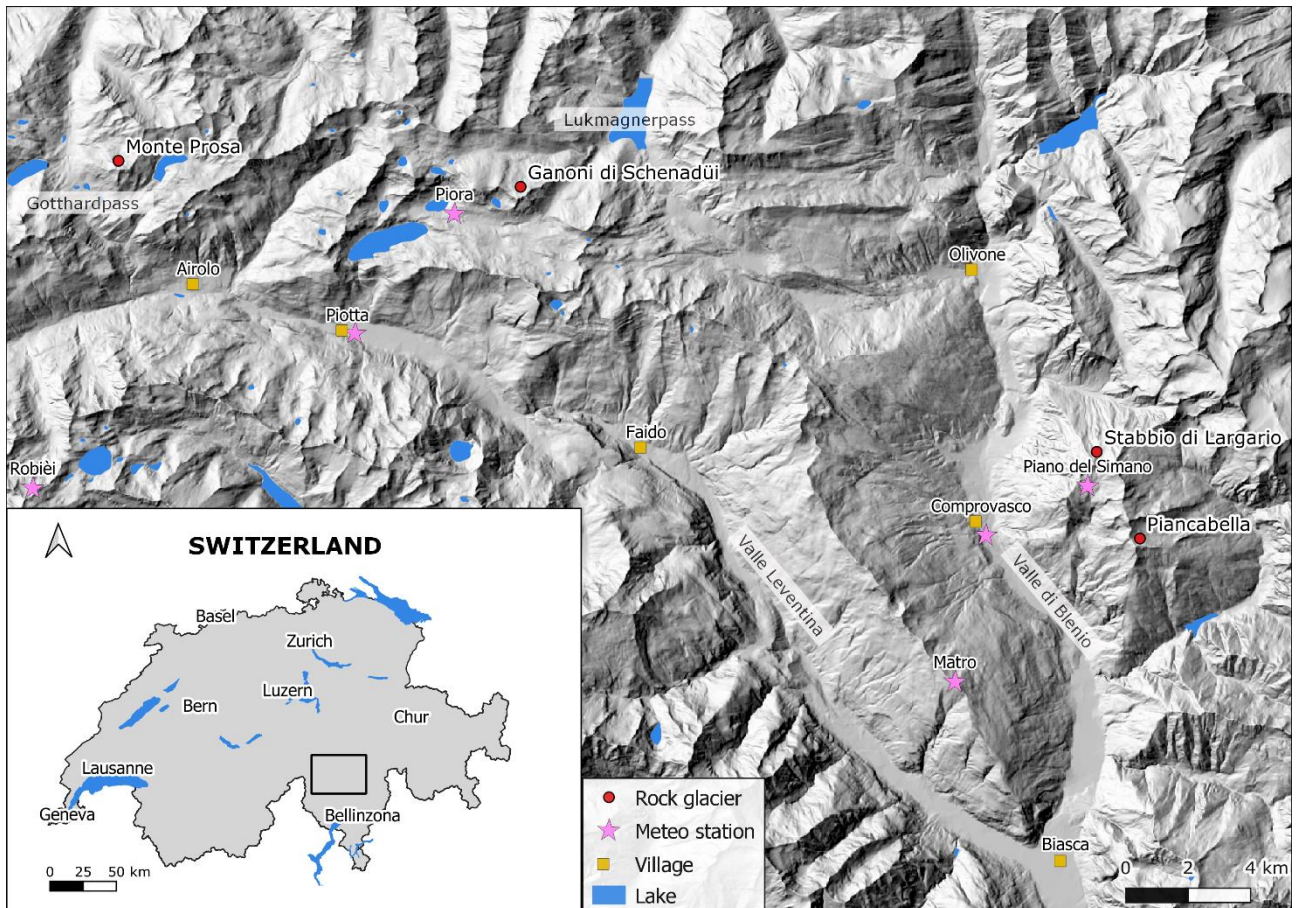
Figure 5: Location of the study sites. Data source: swisstopo.

The active rock glacier of Stabbio di Largario (abbreviated SDL), visible in Figure 6, is located on the orographic left-hand side of the Soia Valley (Blenio Valley, Ticino, Switzerland). It stretches from 2240 to 2500 m a.s.l, is approximately 500 m long and 250 m wide, and has an area of about 11 ha. The unit consists of 3 lobes: an east lobe and a west lobe, as well as a smaller lobe in the upper part. Tectonically, it is located in the Simano nappe and is characterised mainly by of Augengneiss boulders (Federal Office of Topography swisstopo, 2022) coming from the two peaks above, Cima di Gana Bianca and Cima dei Toroi. Its shape does not remind one of the typical rounded and convex shape with longitudinal and transverse furrows and ridges of classic rock glaciers. However, very steep fronts are visible. Since 2009, it has been part of the PERMOS network.

In terms of measurements taken annually on this rock glacier, there are six points where ground surface temperature (GST) is measured, as well as 33 points where dGNSS measurements are taken to calculate surface displacement. In addition, two fixed mono-frequency GPS antennas have been installed for several years, which can constantly monitor the movements of the rock glacier at the location where they are fixed. However, the antenna placed on the western lobe was destroyed by an avalanche, so only one remains located in the eastern lobe. In addition to these data, there are products obtained employing a fixed-wing drone (eBee Sensefly) in 2014 and 2016 (Scapozza *et al.*, 2018). These are orthophotos and point clouds that allow the creation of a digital elevation model (DEM). Data tell us that this rock glacier is generally the second fastest in Ticino, behind the Monte Prosa rock glacier. Its highest horizontal surface velocity ever recorded was 1.44 m on the eastern lobe in 2015, as well as in 2020 and 2021 (Del Siro *et al.*, 2023a).
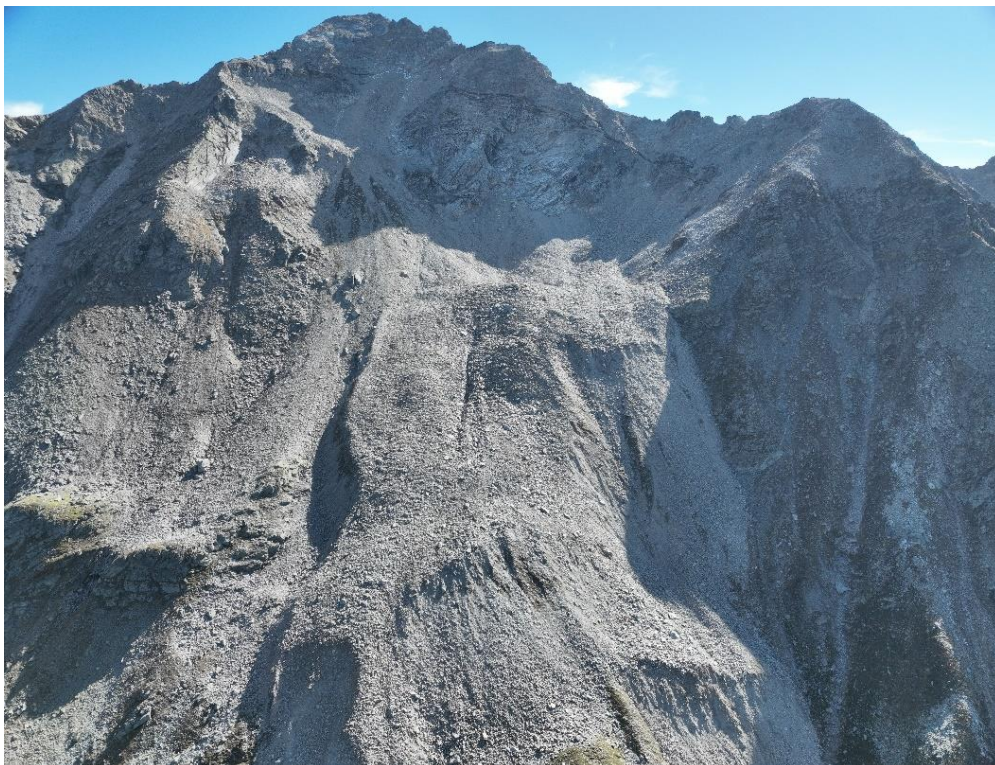
Figure 6: Drone image of the Stabbio di Largario rock glacier, Soia Valley. Date: 12.10.2023.

2.1.2 Piancabella

The Piancabella (PB) rock glacier, visible in Figure 7, is also part of the PERMOS network and is located in the Blenio Valley and, more precisely, in the Sceru Valley, at an altitude between 2440 and 2550 m a.s.l. It is approximately 250 metres long and has a maximum width of about 150 metres, with an area of about 3 ha. From a tectonic point of view, as for the previous site, this valley is located in the Simano nappe, which represents the former southern margin of the European continent before the Alpine orogeny and is mainly characterised by biotite-rich paragneisses and polycyclic gneisses of variable composition (Federal Office of Topography swisstopo, 2022). The Sceru Valley offers a complex and extensive Alpine periglacial environment of approximately 37 ha, where various geomorphological forms such as protalus ramparts and active and inactive rock glaciers are present (Scapozza *et al*., 2011). Also here, two measurements are carried out annually: thermal, since 2006, and geodetic, since 2009. GST is calculated using 10 sensors distributed on the rock glacier, and 22 points are used to detect movements using dGNSS. In addition, as in the previous case, in 2014 and 2016 two surveys were carried out using a fixed-wing drone (eBee), which made it possible to create orthophotos and DEMs and thus to calculate horizontal velocities and changes in thickness over two years (Scapozza *et al*., 2018).

Figure 7: Drone image of the Piancabella rock glacier, Sceru Valley. Date: 05.10.2023.

2.1.3 Monte Prosa

The Monte Prosa (MP) rock glacier, added to the PERMOS network in 2010, is located about 1 km north of the Gotthard Pass. The area comprises two active rock glaciers that are very close to each other and are known as A and B. The first, the one considered for this work and shown in Figure 8, extends from 2430 m a.s.l. at the front to 2570 m a.s.l. at the top. It is characterised by large boulders of Gotthard Nappe granites and orthogneiss coming from the north wall of Monte Prosa (Hafner *et al.*, 1975). Interestingly, this rock glacier was classified as "recent and sub-recent moraine" and is still considered as such according to the Geological Atlas.

As in the case of the other sites, GST and precise coordinates of boulders are measured and monitored at several points. This rock glacier is, on average, the fastest monitored in Ticino and could show average annual horizontal velocities of more than 50 cm·a⁻¹ with max velocity peaks of about 150 cm·a⁻¹ (Swiss Permafrost Monitoring Network PERMOS, n.d.).

Figure 8: Drone image of the Monte Prosa (A) rock glacier. Date: 03.10.2023.

2.1.4 Ganoni di Schenadüi

The Ganoni di Schenadüi (GA) rock glacier (Figure 9) was first mentioned and described in literature by the geographer Valentin Binggeli in 1965, in the sixth volume of the journal "Regio Basiliensis: Hefte für Jurassische und Oberrheinische Landeskunde"(Binggeli, 1965). Binggeli described it as a relatively large 'block stream', about 450 metres long and 150 metres wide, ending in an almost ideal streamline-shaped tongue with a slightly convex 25 m high frontal wall. It is located in the Cadlimo Valley, between the Lukmanier Pass and the Gotthard Pass. It covers an altitude range between 2470 and 2600 m a.s.l. and features an area of about 7 ha. Two lobes compose the central body of the rock glacier: the one to the west is more pronounced, and its front extends further down until it reaches a flat area at about 2470 m a.s.l., while the one to the east remains higher, with a very steep front that reaches 2520 m a.s.l. The research area is situated in the Gotthard crystalline massif, part of the Helvetic domain and is distinguished mainly by orthogneisses, paragneisses, and amphibolites. More specifically, the Ganoni di Schenadüi region is composed of "Streifengneis," a leucocratic gneiss which contains muscovite and alkali feldspar (Bianconi *et al*., 2014).

For this rock glacier also, GST measurements are conducted (at four points) and displacements are calculated using dGNSS at 36 points.

Figure 9: Drone image of the Ganoni di Schenadüi rock glacier, Cadlimo Valley. Date: 01.09.2023

2.2. Available historical data

2.2.1 dGNSS measurements

In Canton Ticino, the monitoring of rock glacier kinematics made by the Institute of Earth Sciences of SUPSI is based on the periodic measurement of the three-dimensional position of several points placed on large boulders on the surface. These measurements are carried out using GNSS (Global Navigational Satellite System) through the GEOMAX Zenith 25 Pro equipment, which supports GPS, GLONASS, Galileo, BeiDou, and SBAS systems (GeoMax AG, n.d.). This type of measurement works via the Real-Time Kinematics (RTK) technique, explained in more detail in Chapter 0. The base, fixed on a tripod (Figure 10) and placed alongside the rock glacier (as in the case of the rock glacier of Stabbio di Largario) or placed further downstream (as in the other cases), allows the coordinates measured by the rover to be corrected in real-time, and thus the coordinates of the points to be measured with extreme precision. The accuracy of this instrumentation is between 0.5 and 2 cm on the horizontal position. The periodicity and number of measured points may vary depending on the rock glacier. In the case of the four rock glaciers under consideration, measurements are made annually between 22 and 37 points. The difference between the two-dimensional positions between two surveys is made to calculate the horizontal displacement of these points. This displacement is then normalised over 365 days to derive an annual average horizontal surface velocity (Del Siro *et al.*, 2023a).

Figure 10: Installation of the base station on a stable terrain outside the rock glacier. Photo: S. Crivelli. Date: 26.06.2023.

2.2.2 GST measurements

GST monitoring, performed for the first time in the Swiss Alps by Hoelzle et al. (1999), consists of the automatic measurement at regular intervals of the ground surface temperature, which partly reflects that of the underground and thus makes it possible to obtain information on the thermal state of the ground surface at a high temporal and long-term resolution (Scapozza *et al.*, 2014b). These measurements are carried out using UTL-3 mini-loggers (GEOTest AG) with an accuracy of ±0.1°C. They are programmed to measure temperature every two hours and are placed at depths varying between 10 and 50 cm, sheltered from the sun (Scapozza *et al.*, 2014b). Thanks to these two-hourly measurements, it is possible to obtain an average of the daily GST temperatures. However, in order to show the evolution of GST over a longer period, the Mean Annual Ground Surface Temperature (MAGST), calculated by means of a moving average of the daily temperatures over 365 days, is taken into account, which provides a record of the cumulative effect of the climatic trends of the previous 365 days (Scapozza *et al.*, 2014b, 2020). This measure makes it possible to quantify seasonal and annual fluctuations in GST and to observe its correlation with variations in rock glacier kinematics (Scapozza *et al.*, 2020). It should be emphasised that MAGST not only reflects air temperature variations but also incorporates two important thermal offsets that determine heat transfer from the atmosphere to the permafrost body: the snow thermal offset and the surface thermal offset. The first is determined by variations in thickness, density, and duration of the snow cover. The second depends on albedo, roughness, and permeability of the ground surface as well as the surface part of the active layer. MAGST can, therefore, be considered a good indicator of temperature variations in the upper part of the rock glacier body (Scapozza *et al.*, 2016).

2.2.3 Temperatures and Precipitations

Atmospheric temperature and precipitation data are available for weather stations located in the vicinity of the four rock glaciers (Figure 5). For this thesis, the GST values (from temperature loggers) of the individual rock glaciers were directly used to compare the thermal state between periods and between sites. For a comparison of precipitation, data from two weather stations were used: Acquarossa/Comprovasco (MeteoSwiss), located at 575 m a.s.l. and Piora (Dipartimento del Territorio, Cantone Ticino) located at 1960 m a.s.l. The former was used to approximate the precipitation of the rock glaciers of Stabbio di Largario and Piancabella. In fact, they are only a few kilometres apart. For Ganoni di Schenadüi and Monte Prosa, the latter was used for the same reason.

3 Methods

3.1 Introduction to the methods

dGNSS measurements and drone photogrammetry were used to analyse the intra-annual kinematics of the four rock glaciers under study. Table 1 shows the dates of the measurements while Figure 11 briefly summarises the most important steps required to obtain horizontal displacements and thickness changes by means of the Structure from Motion and Multiview-Stereo photogrammetry method.
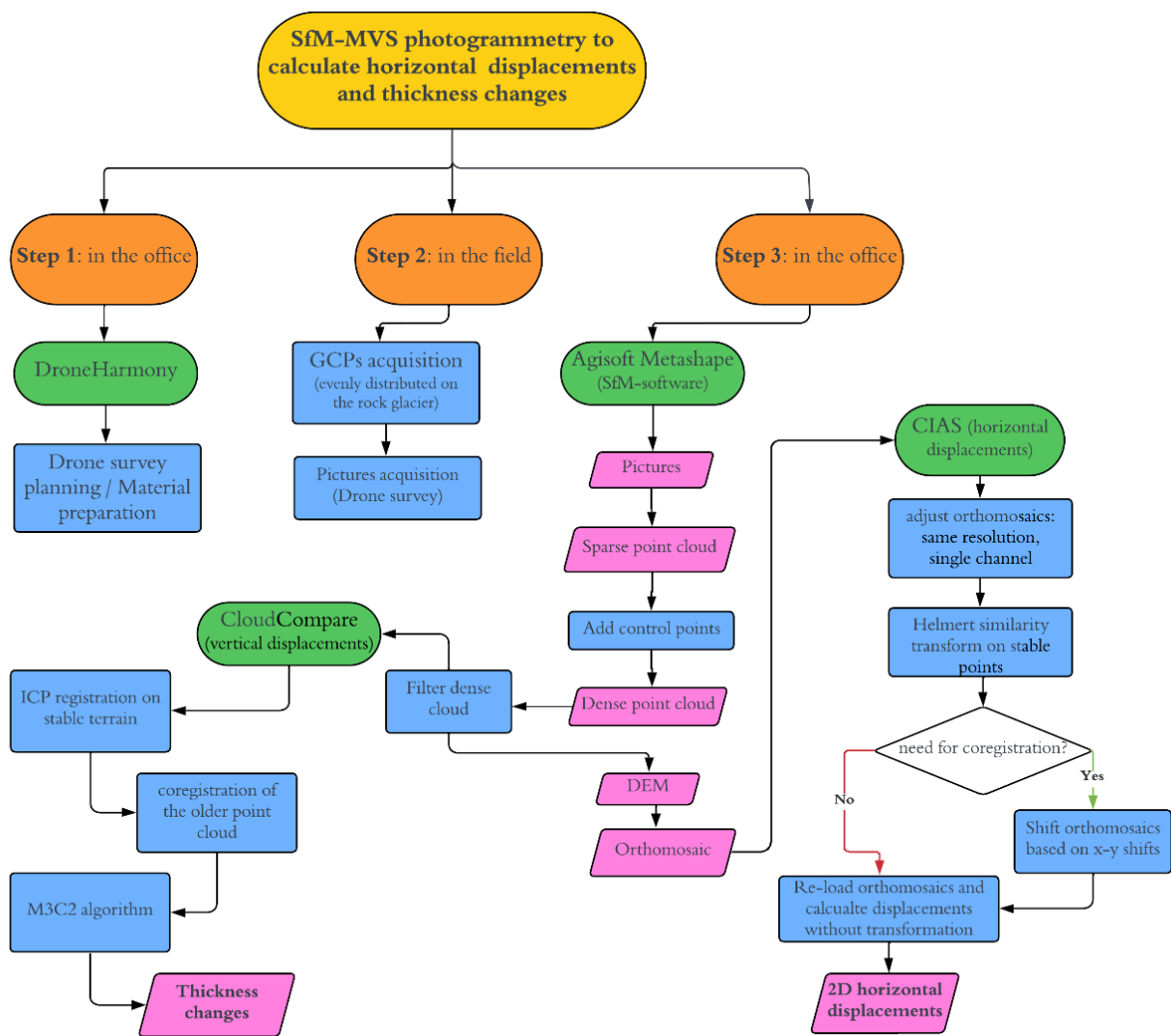
Figure 11: Flowchart summarising the main steps necessary for creating photogrammetric products and calculating horizontal displacements and thickness changes.

Table 1: Dates of dGNSS and drone surveys.

	Survey 2022 (only dGNSS)	**Survey 1**	**Survey 2**	**Survey 3**
SDL	23rd September 2022	21st June 2023	31st August 2023	12th October 2023
PB	20th September 2022	26th June 2023	24th August 2023	5th October 2023
MP	26th September 2022	10th July 2023	25th August 2023	3rd October 2023
GA	22nd September 2022	11th July 2023	1st September 2023	10th October 2023

For convenience, in the analysis and discussion, the periods between measurements will be referred to as 'Cold season', 'Summer', 'Early autumn' and 'Warm season'. The first refers to the period between the end of September 2022 and the first measurements at the end of June/beginning of July 2023. The second refers to the period between the first and second measurements in 2023 (late June/early July until the end of August). The third refers to the time between the second and the last 2023 survey, which occurred in early/middle October. ' Warm season', on the other hand, refers to the entire summer period, i.e. June/July 2023 to October 2023.

3.2   Structure from Motion and Multiview Stereo (SfM-MVS) photogrammetry

3.2.1 Fundamentals of the SfM-MVS photogrammetry

In geosciences, digital terrain models (DTMs) have become standard tools for characterising topographic surfaces, particularly for examining the spatial and temporal evolution of geomorphic change in various contexts (Mosbrucker *et al*., 2017). To create these digital terrain models and orthophotos, which are required for the purposes of this research, the Structure from Motion (SfM) and Multiview stereo (MVS) photogrammetry technique, generally abbreviated as SfM-photogrammetry, was used within the commercial software Agisoft Metashape (version 1.8.3). For the past couple of decades, this low-cost method has enabled the creation of high-resolution topographic reconstructions from overlapping randomly oriented photographs of uncalibrated cameras (Westoby *et al*., 2012; Cook, 2017; Dinkov, 2023). Combined with unmanned aerial vehicle (UAV) platforms, which have evolved enormously and become much more available, it is particularly suitable for surveying remote and hard-to-reach areas (Westoby *et al*., 2012; Cook, 2017). The SfM-MVS technique differs from the classical photogrammetric method since the geometry of the scene as well as the positions and orientation of the camera are calculated directly without having to specify a priori the 3D position and pose of the camera or certain control points (Westoby *et al*., 2012; Gienko & Terry, 2014;

Iglhaut *et al*., 2019). In more detail, in the SfM reconstruction process, all images are processed by an automatic algorithm (e.g. SIFT), which identifies features (called key points or tie points) that are present in a photo and are likely to be identifiable in other photos taken at different points (James & Robson, 2012). To reconstruct the geometry, the software uses the network of matched features, and starting with a pair of images and incrementally adding more, it calculates the parameters of the camera model (e.g. focal length) as well as the orientation of the camera, i.e. position and direction, and simultaneously optimises these values through a process known as 'bundle adjustment'. The result is a sparse point cloud representing the tie points, with associated camera parameters that are self-consistent and minimise the overall residual error (James & Robson, 2012, 2014). The number of tie points in the sparse point cloud depends mainly on the texture and resolution of the images (Westoby *et al*., 2012), as well as their geometry and lighting conditions (Mosbrucker *et al*., 2017), and is usually better with complex images and better resolution (Westoby *et al*., 2012). To refer the point cloud to a real system, it is necessary to know ground control points or the position of the camera, which are typically recorded or measured on the field using dGNSS equipment during image acquisition. When ground control points are included in the bundle adjustment, they represent observations outside the image set and must be fulfilled during the subsequent adjustment process. On the other hand, the features identified within the pictures (in the case of rock glaciers, these may be the edges of boulders) and their relative correspondences are internal measurements within the image set and must also be fulfilled. Thus, including these independent internal and external constraints in the bundle adjustment determines the shape, scale and orientation of a 3D model (James & Robson, 2014).
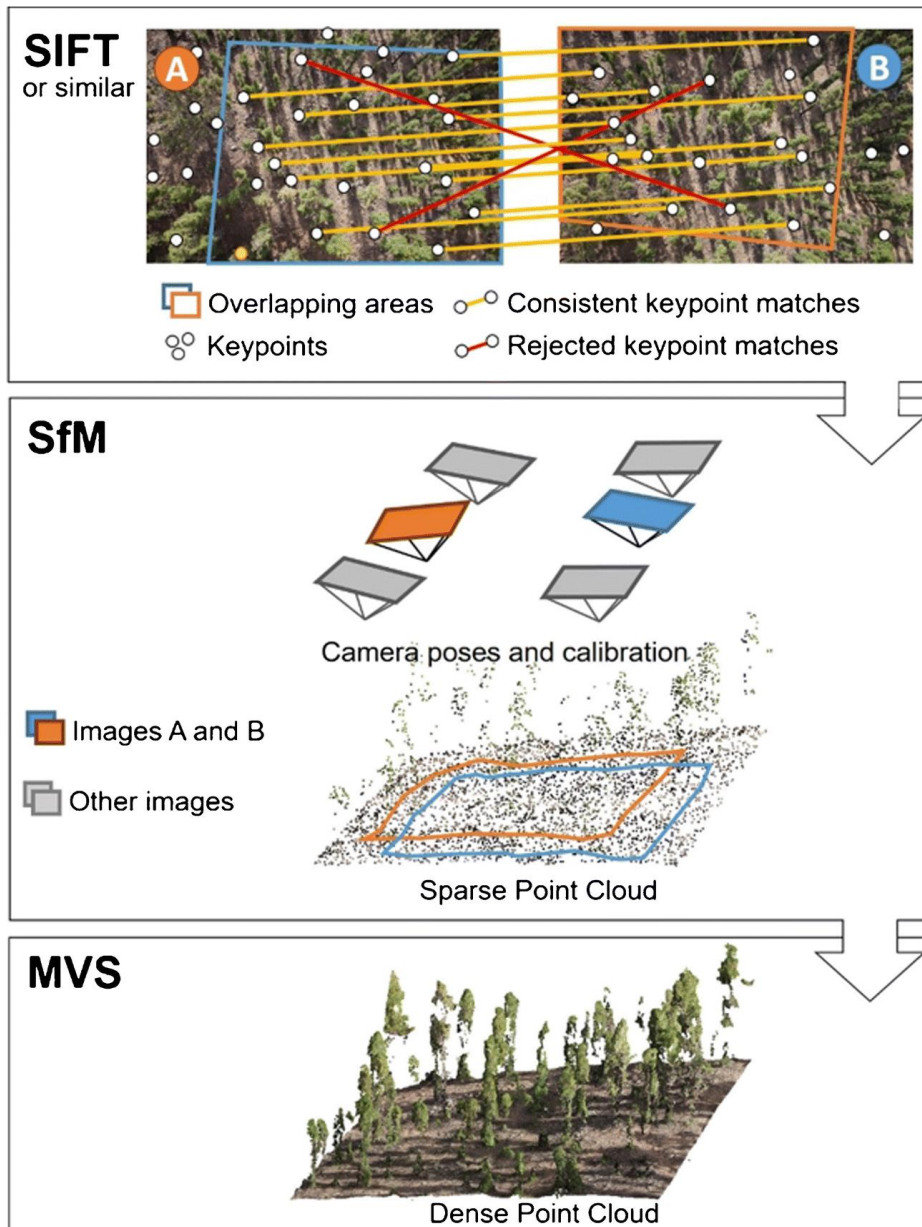
Figure 12: Three key steps of the SfM-MVS Workflow (Iglhaut et al., 2019).

A second step, the dense MVS matching process, creates the detailed 3D terrain model, i.e., the dense cloud. The algorithm creates a huge number of points from a grid of pixels of an image and searches for the best matches for each of these cells (James & Robson, 2012). These steps are clearly visible in Figure 12. Once the dense point cloud has been created, the final two steps are the creation of a terrain elevation model (DEM) and successively an orthomosaic.

To achieve effective image processing with SfM photogrammetry, the flight design must include an adequate frontal and lateral overlap, a constant altitude above the ground and homogeneous coverage over the entire area (Sanz-Ablanedo *et al.*, 2018). There is a positive relationship between image overlap and accuracy of digital elevation models, i.e., the higher this percentage, the better the result. To achieve an optimised object

shape, photogrammetric software generally recommends a front overlap of at least 80% and a minimum side overlap of 60% (Jiménez-Jiménez *et al.*, 2021). In addition to this configuration, the UAV must be equipped with a good-quality camera.

One significant advantage of SfM photogrammetry is that the image acquisition and subsequent processing are significantly faster and simpler than the traditional method (Mosbrucker *et al.*, 2017). They are also cheaper than using terrestrial or airborne laser scanners or other methods that require the use of more expensive and complex instrumentation while still maintaining a very high quality of results.

3.2.2 Image acquisition

Based on the above indications, the images were acquired during three campaigns between June 2023 and October 2023 using a DJI Mavic 3E quadrocopter. The drone is equipped with a 20 MP RGB camera with wide-angle 4/3 CMOS and a mechanical shutter that prevents motion blur (DJI, n.d.). In addition, a built-in Real-Time Kinematics (RTK) module supporting GPS, Galileo, BeiDou and GLONASS was mounted on the drone. It enabled the use of Post-Processing Kinematics (PPK) technology, explained in Chapter 0. The drone can perform terrain-following missions, i.e. following the topography of the terrain and constantly flying at a given altitude, thus maintaining a constant resolution of the acquired images. The missions were prepared using the Drone Harmony software (version 2.4.0). It allows drones to prepare various missions via a web interface and execute them automatically. To achieve the best possible result with four batteries available, three flight types with different parameters were planned. Each survey aimed to obtain nadiral images (90-degree camera), oblique images (75-degree camera) and images that could improve the 3D model, i.e., additional 70-degree oblique photographs. To do this, a simple mission covering the entire rock glacier was first created, and the altitude was set at 50 m above the ground (60 m for Stabbio di Largario because of the more extensive area), an 85% front overlap and 75% side overlap, as well as the camera at a 90-degree inclination, i.e. perpendicular to the axis of the drone. The second type of mission is essentially the same as the first. The only differences are the orientation of the mission perpendicular to the previous one and the camera tilt set at 75°. The reason why oblique images have been acquired is that these favour the significant reduction of systematic error and, especially in areas with complex reliefs (as in the case of rock glaciers), reduce the variation of patterns and thus errors in geomorphic interpretations (James & Robson, 2014; Hendrickx *et al.*, 2019). Finally, several circular missions (2-4 depending on the rock glacier) were created at the same flight height but with the camera more inclined (70°) in order to cover the various areas of the rock glacier even better. Table 2 gives an overview of the survey data and Figure 13 shows the flight plans of the four rock glaciers.

Table 2: Principal drone survey parameters and products quality.

	Area (km^2)	flying altitude	n° images	GSD (cm/pix)	point density (m^2)	DEM resolution (cm/pix)
SDL 1			721	1.73	209	6.91
SDL 2	0.159	61	1628	1.88	176	7.53
SDL 3			1826	1.79	195	7.16
PB 1		57	1449	1.65	228	6.62
PB 2	0.0678	58	1497	1.67	223	6.69
PB 3		54	1337	1.57	254	6.27
MP 1		109	1879	2.91	74	11.6
MP 2	0.107	112	2078	3.17	62	12.7
MP 3		111	2010	3.14	63	12.6
GA 1		89	2167	2.52	98	10.1
GA 2	0.122	88	2196	2.47	103	9.87
GA 3		87	2217	2.46	103	9.86
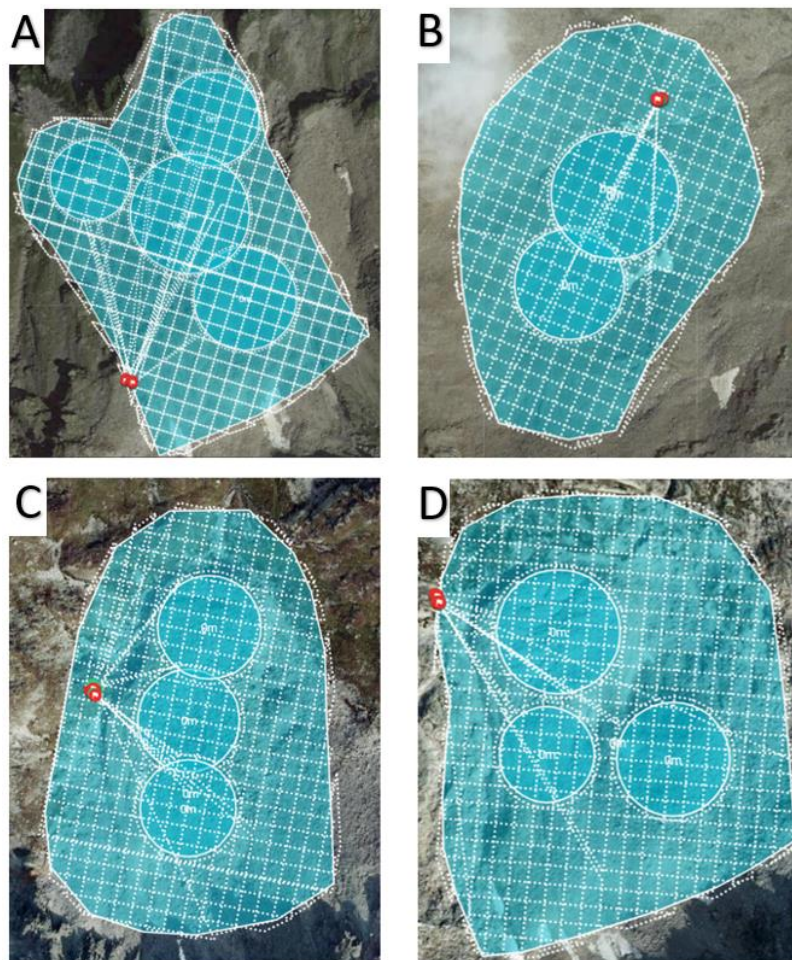
Figure 13: Drone flying plans prepared using DroneHarmony software.
A) Stabbio di Largario, B) Piancabella, C) Monte Prosa and D) Ganoni di Schenadüi.

3.2.3 Control point acquisition

In addition to image acquisition by drone, the exact position of ground control points (GCPs) located on the top of big boulders of the rock glaciers (Figure 14) was measured using the GNSS receivers presented in Chapter 2.2.1. They are required to geo-reference the photogrammetric products and control the quality of the latter. An attempt was made to distribute these points as evenly as possible on the surface of the rock glaciers to achieve better accuracy of the terrain models. It is well known that the spatial arrangement and amount of GCPs used considerably impact accuracy (Zhang *et al.*, 2019). Despite the fact that this is a time consuming operation and the targets are relatively heavy, their usefulness justifies their use. The downside is that it is time-consuming, besides the fact that these (rather heavy) targets have to be brought up to the rock glaciers.

Figure 14: Ground Control Point, drone, and controller.

3.3 Real Time Kinematics (RTK) and Post Processing Kinematics (PPK)

High-resolution topographic data products of SfM-photogrammetry are initially generated in an arbitrary reference frame. The process of georeferencing allows these initial arbitrary coordinates to be transformed into a predefined coordinate system, and this can be done in two ways: using the GCPs mentioned above (indirect georeferencing) or directly through known external parameters of the photographs (direct georeferencing) (Dinkov, 2023). The development of the direct georeferencing method has been possible in recent years thanks to the expansion of high-quality IMU and GNSS technology and RTK and PPK solutions for UAVs, which provide accurate measurements of external orientation parameters (Zhang *et al.*, 2019). The

principle of these technologies is based on the double differentiation of phase ambiguities between two GNSS receivers, a reference station with well-known coordinates (base) and a rover which collects simultaneous observations (Zhang *et al*., 2019; Türk *et al*., 2022). This allows the atmosphere propagation delay, as well as the clock errors of the two receivers, to be eliminated (Zhang *et al*., 2019). As visible in Figure 15, in the case of RTK technology, measurements and differential corrections transmitted from the base take place in real-time via a radio link (or internet link in the case of using the Swiss Positioning Service system *swipos* based on the Automatic GNSS Network Switzerland "AGNES"). The rover then calculates its relative position based on that of the reference station, combining its measurements with those received. Once its relative position has been calculated, it is able to calculate its absolute position in space with centimetre-level accuracy. This type of approach is very suitable when a mobile rover is used, and the accuracy of the measurements can be verified at the same time (Jemai *et al*., 2023). However, if RTK loses its connection even for seconds, it can cause problems in producing the correct outputs (Türk *et al*., 2022). As opposed to RTK, there is PPK. This approach can be used if the rover is equipped with a post-processed GNSS receiver (as in the case of the DJI Mavic 3E) that is able to collect and record raw data and information useful for retrieving the drone's position after the survey through separate software (Jemai *et al*., 2023). The main advantage of this approach over RTK is that it works even in the absence of network coverage or in the presence of radio wave interferences. However, good satellite coverage is required to achieve satisfactory results.
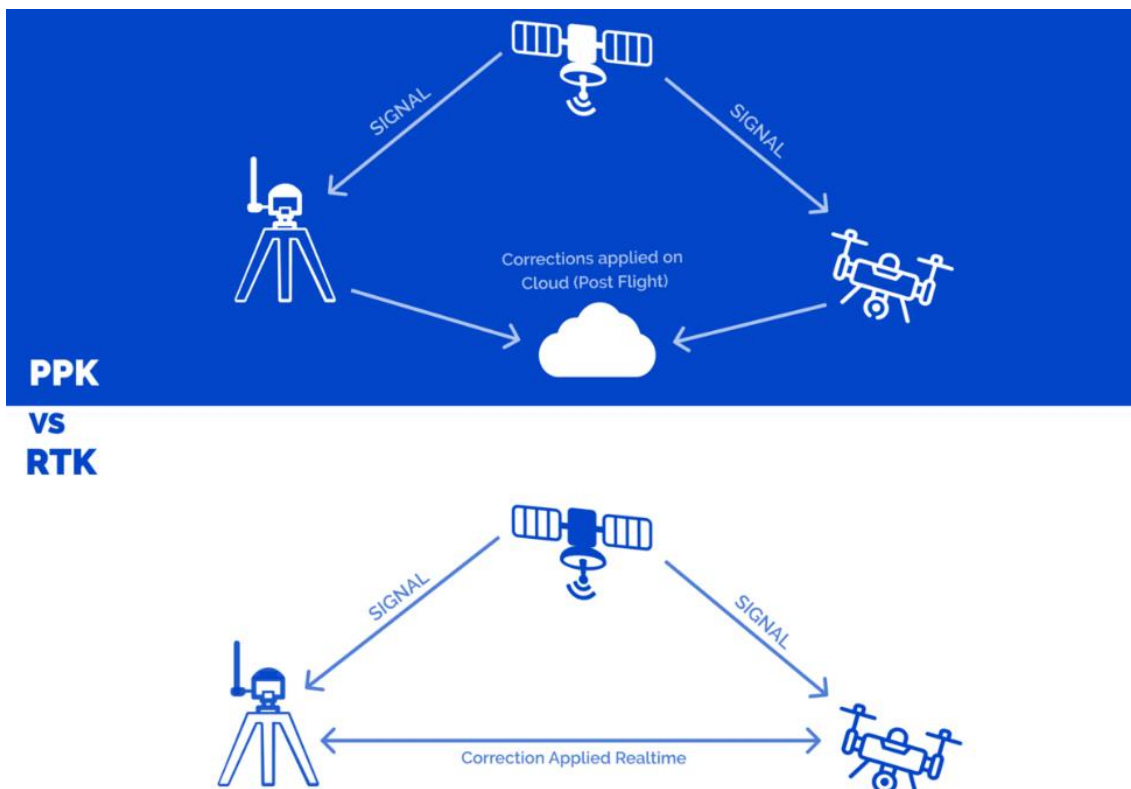
Figure 15: Post-processing Kinematics vs. Real-Time Kinematics (Indshine, n.d.).

For this work, it was decided to combine the PPK methods with GCPs (measured by RTK). This is because, in general, adding the PPK (or RTK) method to GCPs leads to an improvement in the result (McMahon *et al.*, 2021). Furthermore, through the use of PPK, the number of GCPs to be used to achieve the same accuracy is much lower (McMahon *et al.*, 2021). We, therefore, placed the Geomax Zenith 25 GNSS base outside the rock glaciers (depending on the location it was positioned further down the valley, at 1-2 km) which had a dual task: (1) Correcting in real-time (RTK) the rover data used to measure ground control points and (2) recording raw data and then merging them with the raw data from the GNSS module on the drone and georeferencing the photos in post-processing (PPK) using the free software kinematic and drone data processing Emlid Studio (version 1.5). The PPK technique was chosen mainly for three reasons, two of which are technical. Network coverage in these areas is very poor, so the use of the *swipos* system, which requires a stable internet connection, is unlikely. In addition, the use of a non-DJI base with the DJI Mavic 3E drone for RTK is not permitted. Not least, to avoid interference problems between drone and base that could have led to missed or incorrect georeferencing. The use of PPK alone without the support of GCPs after a test did not yield the desired results. Consequently, it was decided to integrate some GCPs. Other reasons for this choice were: (1) dGNSS measurements had to be made for the annual monitoring of rock glaciers anyway, (2) the sites are located in high mountains and are enclosed by mountains, and the base is not always close to the rock glacier. This factor can introduce several errors. Using GCPs ensures to have "absolute truths" in the model, which would not have been the case using only the PPK method. (3) The third reason is that we want GCPs that are not used within the photogrammetric process but are used to assess the accuracy of the models. These points become control points (CPs). The dGNSS measurements of the GCPs and all other points measured on the rock glaciers were then corrected by two or three control points placed outside the rock glacier and considered stable. These points were measured, and their coordinates were compared with those of the same points measured in the previous survey. The average of the difference between these two coordinates was then used to correct all points (in X, Y and Z). This procedure has been carried out from the beginning of the measurements. A local reference system was thus created where positions are corrected according to these stable points. As the photos processed in PPK contain absolute position information, they were used to create the first point cloud (sparse cloud) to position it precisely in space. In order to then create the dense cloud in the "local reference system" within the photogrammetry software, greater weight was given to the GCPs, which were corrected as described above. In this way, the point cloud, with the resulting DEMs and orthomosaics, were corrected and their accuracy could be compared and checked via the CPs.

3.4   Accuracy assessment of the photogrammetry products

Before moving on to calculating horizontal displacements and thickness changes, it is necessary to assess the accuracy of the individual models produced. This is done to determine whether there are systematic errors in the XY or Z direction, such as doming (convex deformation) or bowling (concave deformation) (James & Robson, 2014). To do this, as mentioned above, during the photogrammetric process, a few GCPs were not used to georeference the point cloud but rather to assess the final quality of the results and thus as CPs (Table 3).

Table 3: Summary of the number of GCPs, CPs and CPs RMSE of each drone survey.

	n° GCPs	n° CPs	CPs RMSE$_{xy}$ (cm)	CPs RMSE$_z$ (cm)
SDL 1	10	7	2.15	2.37
SDL 2	7	3	0.9	1.07
SDL 3	7	3	1.43	1.76
PB 1	6	3	1.83	2.77
PB 2	7	3	1.22	1.70
PB 3	7	3	1.41	2.64
MP 1	7	3	2.02	2.53
MP 2	7	3	1.36	2.02
MP 3	7	3	1.73	1.77
GA 1	9	3	0.56	1.62
GA 2	7	3	1.77	2.02
GA 3	7	3	1.07	1.98

Although for almost all the cases only 3 points were used, they were chosen to be representative of the entire surface of the rock glaciers: one at the bottom, one in the middle and one at the top near the rooting zone. The Root Mean Square Error (RMSE) derived from these points made it possible to calculate the goodness of the photogrammetric reconstruction and, thus, to estimate a spatially uniformly distributed error value.

3.5   Calculation of horizontal displacements (CIAS)

To correctly calculate rock glacier displacement vectors as well as the level of detection (LoD), i.e. the distance threshold that distinguishes between data uncertainties and real geomorphological displacements (Fey & Krainer, 2020), it was first necessary to assess whether the orthomosaics should be aligned with each other. The CIAS software (Kääb & Vollmer, 2000) was used to evaluate the quality of the alignment between the two epochs and thus detect possible systematic errors (bias). It has been used successfully in other studies on rock glaciers (Klug *et al*., 2012; Vivero *et al*., 2021, 2022; Bearzot *et al*. 2022). This software contains the image

matching algorithm, which uses the normalised cross-correlation (NCC) function. By comparing a window of reference pixel values (8-bit greyscale picture) taken from an initial image at time step 1 with a larger search window area contained in an overlapping image at time step 2, the NCC essentially identifies homologous points from the moving surface (Vivero *et al.*, 2022). To be able to use this function, orthomosaics must fulfil three basic requirements: (1) be coregistered with each other and in Geotiff or tiff-world format, (2) have exactly the same resolution, (3) be single channel (greyscale). Using the NCC function and the Helmert similarity transform available on CIAS, the systematic error between orthomosaics of different epochs was calculated on a total of 40-50 points placed on rock outcrops outside the rock glacier and, therefore, considered stable. Areas outside of the rock glacier with suspected surface displacements or possible deformations due to their location on the sides of the model were excluded from the alignment quality analysis. As stated by Vivero *et al.* (2022), the Helmert similarity transform can detect systematic rotations, translation (x-y-shift) and differences between two orthomosaics. In the case of the four rock glaciers studied, no differences in scale and rotation were found, and translation values were all less than 2 cm in both x- and y-shifts. After a careful qualitative analysis of the orthomosaics, it was concluded that these small shifts were not uniformly distributed and can, therefore, be seen as random errors. Thus, due to the absence of systematic errors, it was not necessary to correct/coregister the orthomosaics among themselves for almost all the pairs. The only exceptions, for which coregistration was necessary, were the 2016-2023 orthomosaic pairs (Stabbio di Largario and Piancabella) as well as those of August and October 2023 for the Stabbio di Largario rock glacier. In this case the older orthomosaic was shifted according to the values shown in Table 7 through the "shift" tool in the ArcMap software (Version 10.6.1).

After ensuring the absence of systematic errors, it was possible to proceed with the calculation of the horizontal displacement vectors using the CIAS software and the NCC function. For the intra-seasonal periods, a measurement of 32x32 pixels was chosen as the reference window on the oldest ortho mosaic and a search window of 64x64 pixels for the newer ortho mosaic, while for the calculation of the seasonal displacements 64x64 pixels was chosen as the reference window and 128x128 pixels as the search window. The grid size was set to 5 m. Having calculated the horizontal displacements and considering the Helmert similarity transform performed in the first step, it was possible to calculate LoD, i.e. the uncertainty of the displacement calculation (Redpath *et al.*, 2013). It is represented as standard deviation and is calculated for each individual displacement vector obtained via CIAS in the following way:

$$\sigma_l = \sqrt{\left(\frac{\Delta x}{l}\right)^2 \sigma_x^2 + \left(\frac{\Delta y}{l}\right)^2 \sigma_y^2}$$

where:

- σ_l : LoD of each single vector

- Δx : X displacement

- Δy : Y displacement

- l : XY displacement (named "length" in the CIAS output)

- σ_x : standard deviation in X derived from CIAS taking the stable ground (σ_x^2 = RMS$_x$ obtained in the Helmert similarity transform step)

- σ_y : standard deviation in Y derived from CIAS taking the stable ground (σ_y^2 = RMS$_y$ obtained in the Helmert similarity transform step)

The spatial uncertainty associated with the orthorectification and mosaicking procedures, as well as the automated image matching via correlation, is represented by the variances σ^2_x and σ^2_y (Redpath *et al*., 2013; Vivero *et al*., 2022).

The result of the equation was then multiplied by 1.96 (i.e. a confidence limit of 95%) and was used to establish the minimum detection limit for each displacement vector. In the results, the minimum value, the maximum value, and the mean of all values were calculated. The latter was rounded to the whole number and used as the LoD of horizontal displacement vectors. All displacement maps were then produced using the open source software QGIS.

3.6   Calculation of 3D surface changes

3.6.1 Surface thickness changes using M3C2

Several studies and research have relied on the difference between two digital elevation models (DoD) to calculate changes in thickness at the surface of rock glaciers (Bollmann *et al*., 2012; Klug *et al*., 2012; Kaufmann *et al*., 2021). However, according to Ulrich *et al*. (2021), this technique is limited when representing vertical changes in steep and complex terrain. For this reason, the Multiscale Model to Model Cloud Comparison (M3C2) algorithm (Lague *et al*., 2013) implemented in the CloudCompare software (v. 2.13) and already widely used for study in the geomorphological domain was used in this work (Clapuyt *et al*., 2017; Cook, 2017; Midgley & Tonkin, 2017; Vivero & Lambiel, 2019; Zahs *et al*., 2019; Ulrich *et al*., 2021; Bearzot *et al*. 2022; Kaiser *et al*., 2022). Unlike the DoD, it calculates the distances between two point clouds in a direction perpendicular to the local surface (Ulrich *et al*., 2021). The results of this 3D Cloud-to-Cloud comparison between the two surveys are more robust and allow for the measurement of differences between surface normals (Cook, 2017). In other words, this algorithm finds for each point the most suitable direction of the normal. Then it calculates the 3D distance between the two point clouds along a cylinder of defined

radius projected in the direction of the normal (Lague *et al.*, 2013; Cook, 2017) (see Figure 16, part a). In the case of complex topography (see Figure 16, part b) where the degree of surface roughness is rather high (as in the case of a rock glacier), the point cloud may possess occlusion patterns (i.e. missing data) that can make comparisons between them complicated (Lague *et al.*, 2013). Furthermore, according to the same authors, in the case of a high degree of roughness, it must be considered that the calculation and orientation of surface normals depends on the scale at which it is performed. In this study, to respect the variation of roughness in the study areas, the "multi-scale" method was used to calculate the normal, in which the normal for each core point is calculated on different scales (D, see Figure 16) and the "flattest" one is used (Lague *et al.*, 2013). To define these values, the "Guess params" option implemented in M3C2 was used, which estimated the minimum and maximum values of the scale (D) for each rock glacier based on roughness values. The minimum values varied between 0.16 m at Piancabella and 0.4 m at Monte Prosa, with the maximums ranging between 0.65 m and 1.6 m (i.e. four times the minimum). As a projection value (d, see Figure 16), values between 0.16 m and 1.6 m were used, which were also automatically estimated by the algorithm. To speed up the process, subsamples of the clouds with a uniform distribution of 0.05 m were used as core points. Finally, the global registration error (RMSE) calculated during the co-registration of the point clouds was entered to take it into account during the confidence computation calculated by the algorithm for each point.
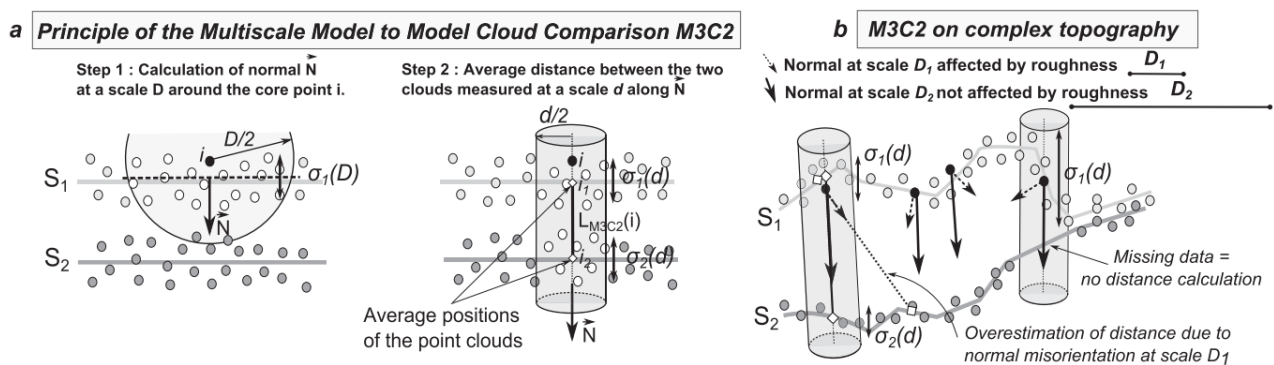
Figure 16: Description of the M3C2 algorithm and the two user-defined parameters D (normal scale) and d (projection scale). For more detailed description see Lague et al. (2013).

Before using the M3C2 algorithm, the point clouds were co-registered, using one cloud as a reference and the other as "to be co-registered". To do this, between 6 and 8 different polygons representing the stable terrain (equal between the three epochs) were cut out of the rock glacier for each point cloud. The number of points representing the stable areas varies between 5'000 (for the Piancabella rock glacier, where few are considered stable) to around 60'000 at Monte Prosa. Then, in these stable areas, the iterative closest point (ICP) algorithm, also called "fine registration", proposed by Chen and Medioni (1991), was used. To be able to use this algorithm, the point clouds must fulfil two requirements, namely, they must already be approximately aligned, and they must depict the same features or shapes (Kaiser *et al.*, 2022). As explained

by Micheletti *et al*. (2017), to find the best overall fit with regard to the reference surface, the ICP uses least-squares minimisation of residuals to adjust the orientation and position of scan points. The distance between every data point in the cloud being co-registered and its nearest point on the reference surface is known as its residual. Every time this process is repeated, the nearest point search, as well as the adjustment parameters, are updated until the best fit is determined (Table 4).

Table 4: RMSE after the coregistration (Iterative closest point ICP) of point cloud pairs over stable terrain.

	RMSE Summer (cm)	RMSE Early autumn (cm)	RMSE Warm season (cm)	RMSE 2016 – 2023 (cm)
SDL	3	3.3	2.9	14.4
PB	2.7	2.6	2.6	14.5
MP	4.9	4.9	5	-
GA	4.8	4.8	4	-

In this work, the most recent cloud was always used as the reference cloud, and at the same time, both clouds were always subsampled at 0.05 m minimum point spacing to define the core points. This step is necessary to make the process faster. The result of the ICP on the stable zones, therefore, includes the residual distances expressed as RMSE values that are used to determine the quality of the co-registration (registration error), as well as a matrix containing translation, rotation and scaling values (Vivero & Lambiel, 2019). These values indicate how much the point cloud has been translated, rotated, and scaled to be accurately recorded with the reference cloud. The values obtained for the stable zones are then applied to the entire point cloud so that it is best co-registered with the reference cloud.

After this step, the distance between the two point clouds can be calculated using the M3C2 algorithm explained previously. It also automatically provides a confidence assessment of the minimum detectable change, namely the LoD (95%). For each point in the cloud, it calculates LoD following the formula below of Lague, Brodu and Leroux (2013):

$$LOD_{95\%}(d) = \pm 1.96 \left(\sqrt{\frac{\sigma_1(d)^2}{n_1} + \frac{\sigma_2(d)^2}{n_2}} + reg \right)$$

where:

- σ_1 (d), σ_2 (d): local roughness for each point measured along the normal direction
- n_1, n_2 : size of the sub-clouds taken to compute the normal
- reg: registration error (RMSE obtained during clouds co-registration)

This calculation allows the accuracy of the distance measurements between the two point clouds to be measured locally and is therefore also used to define whether a measured value is statistically significant or not (also calculated automatically in M3C2). The higher the standard deviation of the residual distances of the points, the lower the confidence. Conversely, the greater the number of points within the neighbourhood, the more robust the position of the centroid will be and thus the greater the confidence (Lague *et al.*, 2013). In order to have a single LoD value to be used when visualising three-dimensional changes between the two point clouds, the average of all LoD values is taken. This value provides a fairly accurate estimate of the limit above, which makes it possible to say if there have been real changes in the surface.

3.6.2 Volume change analysis

In contrast to glaciers, in the case of rock glaciers it is difficult to carry out a 'surface mass balance', as the complex internal structure (consisting of a mix of ice and debris) makes it practically impossible to establish density values (Kaufmann *et al.*, 2021). However, in order to estimate possible changes in surface thickness and consequently to calculate possible changes in volume ('surface volume balance'), digital terrain models or point clouds can be used. Despite the complex dynamics associated with rock glaciers, with superimposed horizontal and vertical movements, the information extracted from these models can be useful in order to identify possible ice losses related to permafrost degradation.

The calculation of volume changes has rarely been performed for rock glaciers and a DoD has almost always been used (Fleischer *et al.*, 2021, 2023; Kaufmann *et al.*, 2021; Vivero *et al.*, 2022). However, effectively monitoring geomorphological changes in highly complex areas such as rock glaciers requires the development of change detection algorithms using 3D point clouds (Nourbakhshbeidokhti *et al.*, 2019). This is because the use of DoD represents a further simplification of the surface caused by the shift to 2.5D and consequently increases the error of volumetric calculations (Nourbakhshbeidokhti *et al.*, 2019). Furthermore, given the horizontal displacement of the rock glacier surface, the DoD values could deviate significantly from the actual ones. For this reason, in order to better estimate intra-annual volume changes, the values obtained via the M3C2 algorithm were used, without considering the values below LoD. As seen above, they in fact do not represent vertical distances as in DoDs, but rather consider local surface roughness and local slope variability and consequently better represent thickness changes (Lague *et al.*, 2013; Clapuyt *et al.*, 2017; Vivero & Lambiel, 2019). Areas covered by snow during the various periods were excluded from this analysis.

The M3C2 results obtained on CloudCompare were first exported to QGIS. An interpolation was then carried out using the "Fill nodata" tool in order to obtain values for all cells of the rock glacier. Finally, the rasters containing thickness changes were exported as a matrix into the MATLAB software. Within it, all values below LoD were set to zero so they would not affect the calculations. Afterwards, all remaining values were

multiplied by the pixel area and the results were added together. This resulted in the net volume change. For the calculation of volume gain and volume loss, the same procedure was performed, resetting the negative and positive values to zero respectively. The uncertainty values associated with these calculations are incorporated in the result as the calculation of M3C2 already considers the root mean square error (RMSE) obtained during the co-registration process (ICP) as well as the roughness of the terrain.

3.7   Statistical analysis

To investigate in detail the displacements obtained through dGNSS measurements on the reference points, visual representations and statistical tests were carried out using the RStudio software (version 2021.09.0). Their main objective was to better visualise the data and find out whether there are significant differences in the displacements on the total of all points, within each rock glacier, and between different sites. Since the distance between surveys is not identical on a temporal level, absolute displacement values cannot be used to assess the difference between seasons and between rock glaciers. Consequently, the velocity of each point was calculated and expressed in cm·month^{-1}.

To assess whether the mean value of velocity between more than two groups differs, the analysis of variance test (ANOVA) is used. To be able to use this test, specific prerequisites must be fulfilled, such as that the variances between the groups must be homogeneous or that the dependent variable is normally distributed in all groups. When these prerequisites are not met, the Kruskal-Wallis test, which is the non-parametric equivalent of the ANOVA test, can be used. The Kruskal-Wallis test can also be calculated in the case of small samples and outliers (Methodenberatung UZH, n.d.). If the p-value obtained through ANOVA or Kruskal-Wallis tests is less than 0.05 (95% CI), there is at least a significant difference between two groups. However, these two tests do not allow to tell between which groups this difference exists. Therefore, it is necessary to carry out post-hoc pairwise comparisons, which can be done using various tests, such as Tukey's HSD test. This can be used to identify between which groups the mean values differ significantly. In the case of a rejected Kruskal-Wallis test, the most appropriate procedure is a nonparametric pairwise multiple comparison through a Dunn's test (Dinno, 2015), which can be seen as a test for medians difference. These statistical tests were carried out using the *ggbetweenstats* package.

The same tests were conducted to assess possible differences in GST, which in the warm season directly reflects changes in atmospheric temperature.

4   Results

4.1   Inter-annual horizontal velocities

Before analysing the intra-annual kinematics in detail, it is worth to observe and comment the kinematics of the last 15 years for better contextualise the measurements carried out during the warm season 2023. The annual measurements clearly show that the kinematics of rock glaciers can vary significantly from year to year (see e.g. Kellerer-Pirklbauer *et al.*, 2024). Figure 17, which illustrates the average annual horizontal velocity of the four rock glaciers analysed in this thesis, clearly shows that two of them, namely Monte Prosa and Stabbio di Largario, are generally much faster than those of Piancabella and Ganoni di Schenadüi.
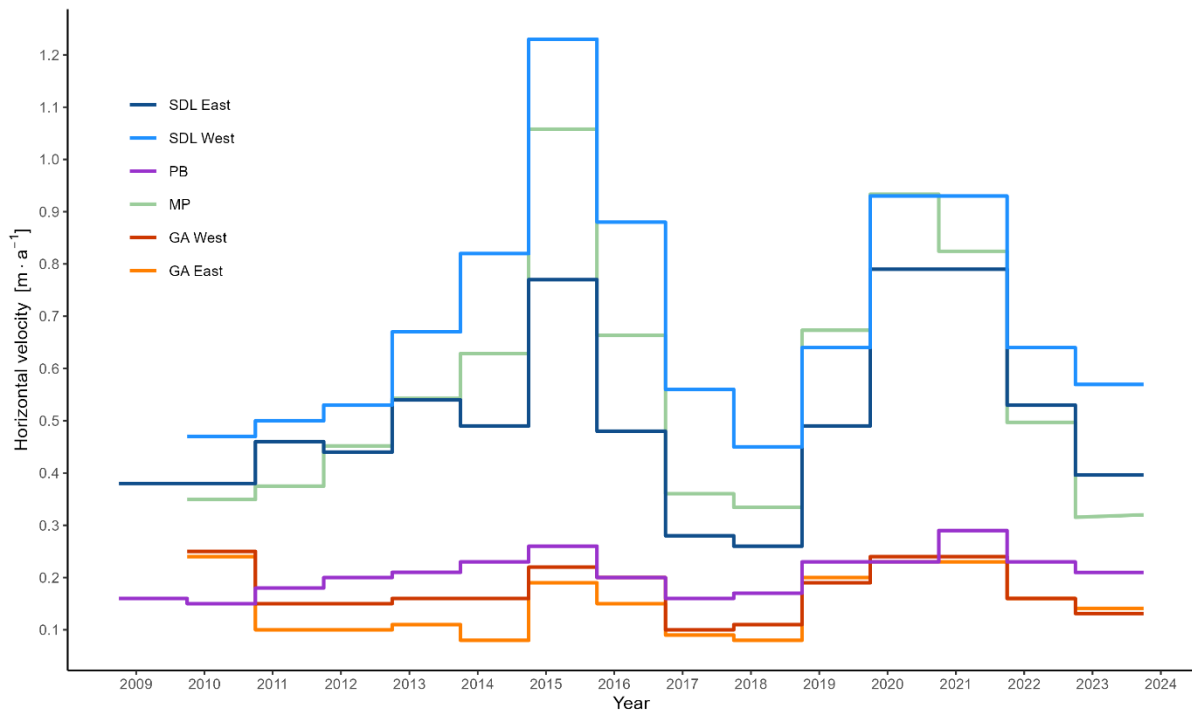
Figure 17: Graph of the mean annual horizontal velocities of the four rock glaciers since 2009. Data: SUPSI-IST and PERMOS.

The first two have reached speeds of over 1 m·a⁻¹in the past, while the other two have never averaged more than 0.3 m·a⁻¹m·a⁻¹. The inter-annual variation of these rock glaciers during the last three decades has been very large. In the space of a few years, e.g. from 2010 to 2015, velocities have increased significantly, and in the case of Monte Prosa A and Stabbio di Largario they have practically tripled, from 35 cm and 47 cm in 2009 to 106 cm and 123 cm in 2015 respectively. A close look at the graph shows that in the case of Stabbio di Largario, there are important differences between the west and east lobes. The trends are very similar, but the former is always slower. In the first years of measurements and up to 2014, the horizontal velocity measured on the Piancabella rock glacier also increased, albeit more slowly. It rose from 16 cm in 2008 to 26

cm in 2015. As far as Ganoni di Schenadüi is concerned, it first showed a slowdown on both lobes between 2009 and 2010, falling from 24 cm and 25 cm of the east and west lobes, respectively, to 10 cm and 15 cm, and then increased slightly until 2015, but without reaching the velocities measured in 2009. This positive trend of horizontal velocities underwent an abrupt deceleration between the years 2016 and 2018, where all measured average velocities decreased significantly, between 39% and 64%, especially regarding Stabbio di Largario and Monte Prosa, with 2017 average velocities being the lowest since 2009 (Scapozza *et al.*, 2020).

As already mentioned, straddling this peak in velocities measured in 2015, two fixed-wing drone (eBee) surveys were carried out on the rock glaciers of Stabbio di Largario and Piancabella: one in 2014 and one in 2016. Using the photogrammetric process, these surveys made it possible to calculate the displacements over the entire surface of the two rock glaciers over the two years (Figure 18 and Figure 19). In both cases, significant variations in surface velocity could be observed depending on the area of the rock glacier. In the case of Stabbio di Largario, two distinct flows can be observed near the two fronts, with relatively high velocities precisely at these points (between 0.5 m and 2 m for the west lobe and between 0.5 m and above 2 m in the east lobe). In the central and rooting zone, the velocities were more moderate. In the case of the Piancabella rock glacier, the differences in speed are smaller. In the central part and in the rooting zone, they were between 0.2 and 0.5 $m \cdot a^{-1}$. The most remarkable difference was found between the eastern and western parts of the front. The east side generally showed lower velocities, between 0.1 and 0.2 $m \cdot a^{-1}$, while the west side showed relatively high velocities, up to 0.5 to 1 $m \cdot a^{-1}$. These velocities measured using the photogrammetry seem to confirm what was measured by dGNSS measurements visible in Figure 17. From the hydrological year 2018-2019 onwards, there was then a second major acceleration, with peak velocities measured in 2020 and 2021. Velocities returned to the levels measured during the previous peak in 2015, except for Stabbio di Largario and Monte Prosa, where the 1 $m \cdot a^{-1}$ threshold was not exceeded. All four rock glaciers studied experienced a new major deceleration in 2022. The latest measurements taken in October 2023 confirm the deceleration trend for all sites, with horizontal average velocities between 0.13 $m \cdot a^{-1}$ for the west lobe of Ganoni di Schenadüi and 0.57 $m \cdot a^{-1}$ for the east lobe of Stabbio di Largario. In general, when looking at all the lines in the graph, it can be seen that the trend has been similar for all rock glaciers since the beginning of the measurements. However, the percentage variations can vary significantly between sites.
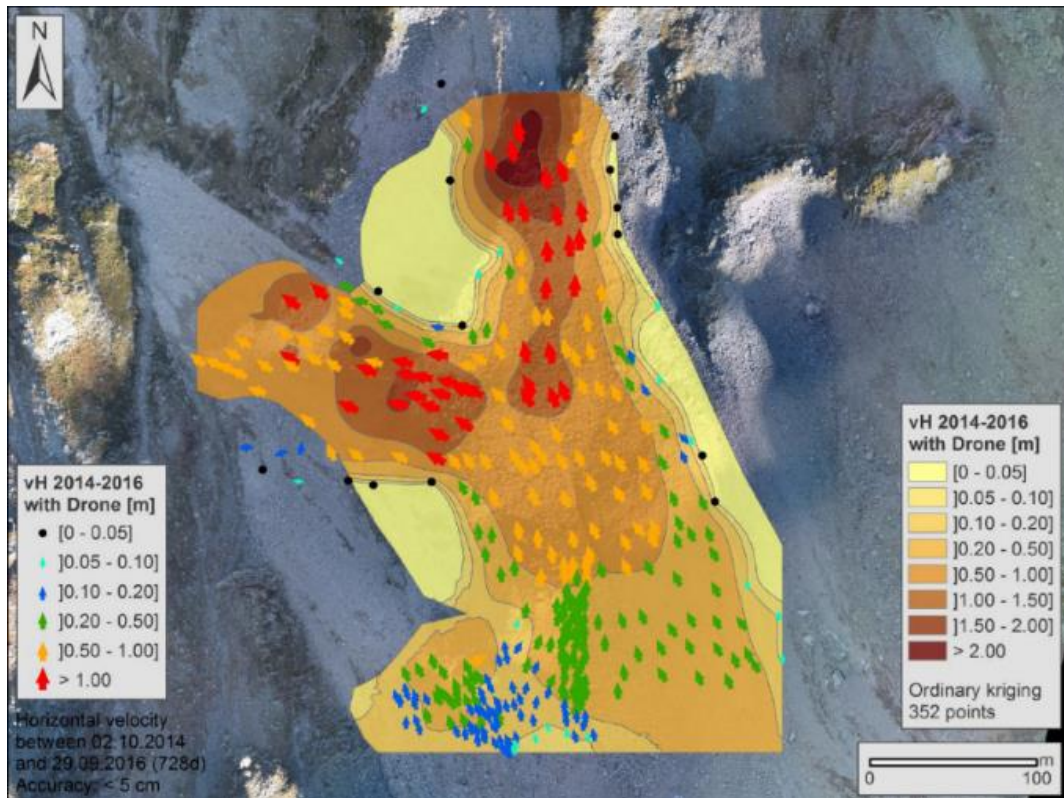
Figure 18: Stabbio di Largario horizontal velocities calculated between 2014 and 2016 using UAV photogrammetry (Scapozza and Ambrosi 2017).
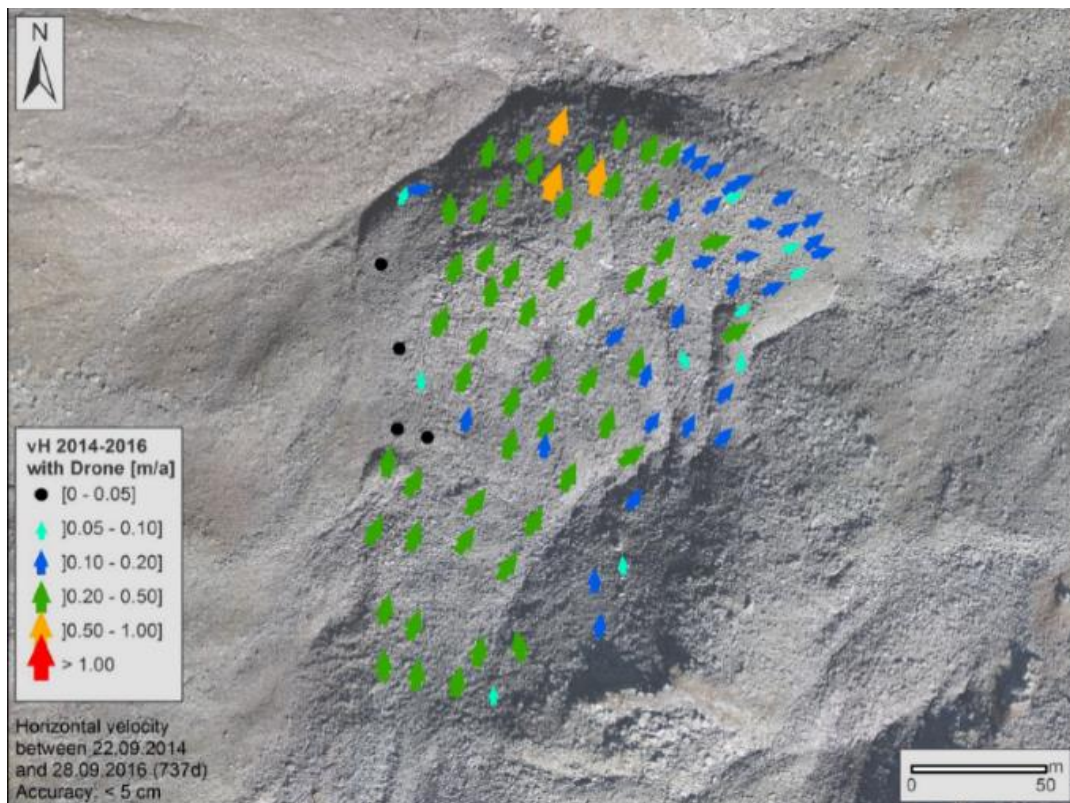
Figure 19: Piancabella horizontal velocities calculated between 2014 and 2016 using UAV photogrammetry (Scapozza and Ambrosi 2017).

4.2 Ground surface temperature (GST) and Mean annual ground surface temperature (MAGST)

4.2.1 Inter-annual evolution of kinematics

The evolution of MAGST since the beginning of the measurements clearly shows four positive peaks in the years 2015, 2019, 2020 and 2023, which are the cause of the clear warming trend in GST. Indeed, the mean MAGST of all monitored sites in the southern Ticino Alps (excluding Monte Prosa A) has warmed between 0.8 and 1.1°C in the decade 2010-2019 (Scapozza *et al.*, 2020). Although there is a warming trend in MAGST, there are important fluctuations between years. These are mainly due to the effect of cold winters or warm summers on the soil surface, as well as the presence or absence of winter snow cover, which in winter prevents the soil from cooling down excessively while, on the contrary, in summer, allows it to insulate it from external heat. Looking at Figure 20, we can see that the 2015 peak resulted from a previous year with very high temperatures. Temperatures remained high the following winter, but poor snow cover allowed the ground to cool and consequently decreased MAGST (Scapozza *et al.*, 2018). Concerning the 2019 peak, it can be seen that it was due to a combination of two factors: the warming of air temperature that occurred between September 2018 and May 2019, as well as the presence of snow on the ground that remained until early summer (Scapozza *et al.*, 2020). The peak recorded in 2020 is most likely the result of the combination of the very hot summer and autumn 2019 with the very high winter and spring temperatures 2020, with respective values of 3°C and 1.8°C above the 1981-2010 norm (MeteoSchweiz, 2021). The peak observed in the summer of 2023, similarly to the one before, also appears to be due to the exceptionally high-temperature values measured especially in winter and spring, combined with the high temperatures of summer and autumn 2022, among the hottest since the beginning of measurements (MeteoSchweiz, 2023a, 2024).
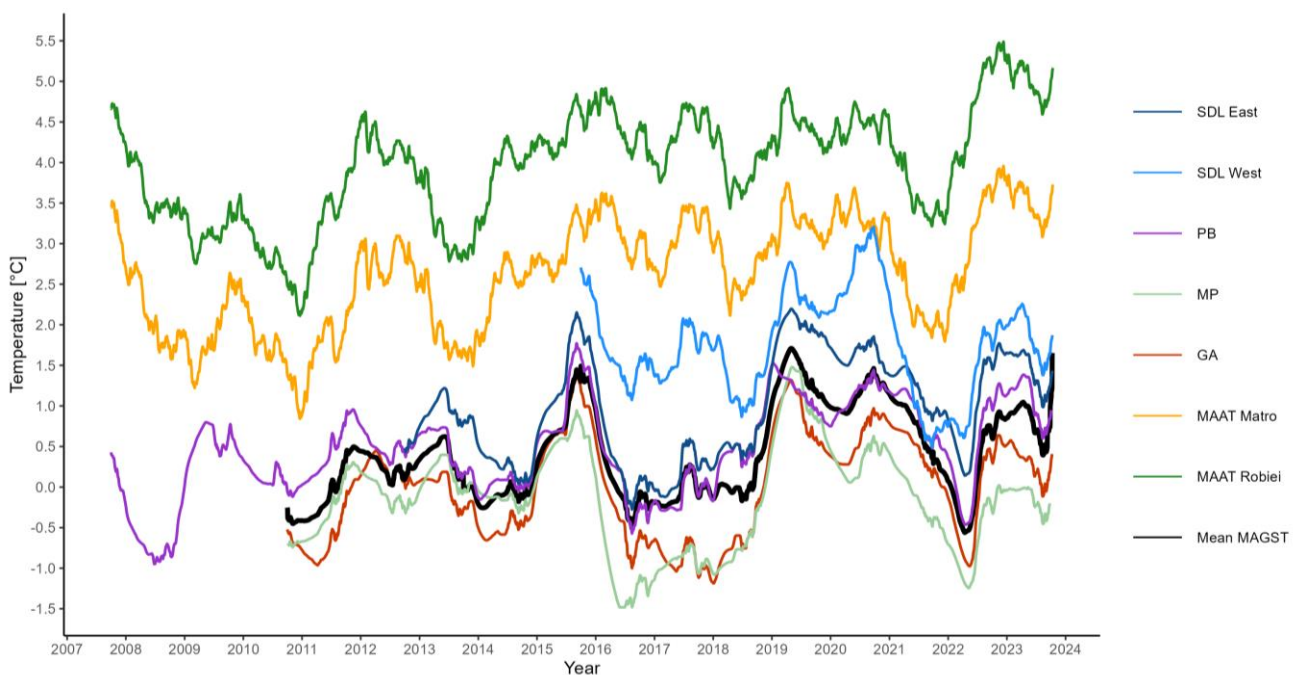
Figure 20: rock glaciers MAGST and MAAT of 2 meteo stations Matro and Robièi. Data: SUPSI-IST, PERMOS and MeteoSwiss.

To analyse land surface temperature trends in more detail over a year, it makes more sense to look at direct changes in GST, which reacts directly to changes in external factors such as snow conditions and temperature variations during the year. The hydrological year 2023 was quite interesting in this respect. Between the middle and the end of September 2022, there was a major drop in atmospheric temperature, which immediately affected the ground surface temperatures of all four rock glaciers. This resulted in an important and early cooling of the ground, with GST values at the end of September dropping below 0°C. Given the lack of snowfall, the GST trend in October continued to substantially follow that of the air temperature, again reaching temperatures up to around 4°C. At the beginning of November, there was a sharp drop in GST values, interspersed with a slight increase, again due to the atmospheric temperatures, which fell steadily below 0°C. At the same time, the little snow that fell (around 20-25 cm) was not enough to prevent the cold temperatures from reaching the ground surface, which was already tending to be cold anyway. Between the end of November and the month of December, partly due to the snowfall at the beginning of the month and the slight increase in atmospheric temperature in the second half of the month, GST rose slightly. However, the lack of significant new snowfall and a significant drop in air temperature led to a new drop in GST that lasted until around mid-February. From that time until the beginning of May, GST continued to increase following the air temperature trend, although with markedly smaller fluctuations due to the presence of about 50 cm of snow. The late snowfall in mid-April, which resulted in a snow thickness of over a metre, did not have a significant effect on GST, which continued to increase as it reached the zero-curtain period, i.e. melting of snow, where GST remains for several days/weeks almost equal to 0°C due to the latent heat required for the change of state from snow (solid) to water (liquid).

The snowmelt period, which varied in duration, was not synchronous for the four rock glaciers. It first began at Stabbio di Largario, located at a slightly lower altitude than the other three, and occurred between 10 May and 26 May by averaging the temperature loggers. A little later, Piancabella and Ganoni di Schenadüi also experienced snow disappearance between 15 May and 10 June for the former and between 21 May and 4 June for the latter. The snow remained longer on the rock glacier of Monte Prosa. It disappeared between 24 May and 14 June. This is visible in Figure 21, where, in a staggered manner, the four rock glaciers began to show GSTs above 0°C. It is important to emphasise that for practically all four rock glaciers, there are areas where the snow remained much longer, beyond the beginning of summer.

The first summer period saw rather high GSTs, which varied between about 6°C and 15°C, with the greatest fluctuations found at Ganoni di Schenadüi and Stabbio di Largario. The following period was characterised by great meteorological variations, alternating short periods with intense rain events and temperatures well below the seasonal average, with sunny periods also characterised by very high air temperatures (Figure 22 - Figure 23). There were three periods in particular: the first occurred at the end of July and the first few days

of August, with air temperatures dropping to daily averages below 5 °C at high altitudes. Subsequently, the atmospheric temperature rose again to reach very high average values of around 18 °C towards the middle/end of August. These values then plummeted for a second time due to the sudden change in weather conditions, which brought a rainfall of around 180 mm (Piora station) within three days. Towards the end of September, after a rather warm period, another cold front caused a major rainfall event (110 mm in 5 days) and again brought air temperatures down to around 0°C. These major changes in the weather conditions can be seen by observing the trend in GST during that period, with daily averages dropping from around 16°C to as low as 0°C within a few days, as in the case of Ganoni di Schenadüi.
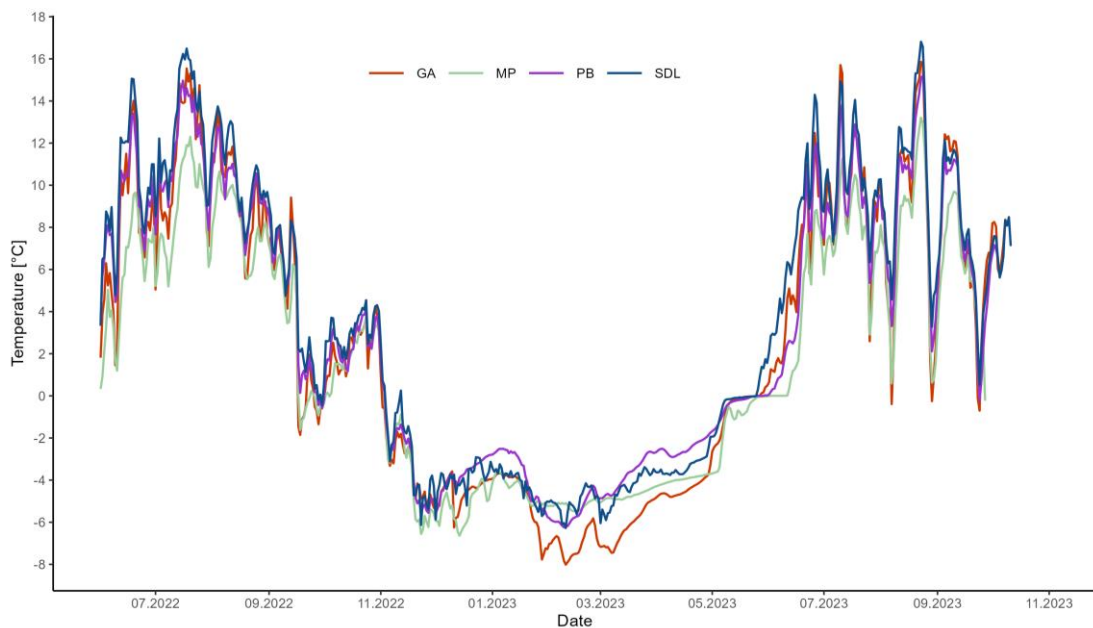
Figure 21: GST of the four rock glaciers from June 2022 to November 2023. Data: SUPSI-IST and PERMOS.
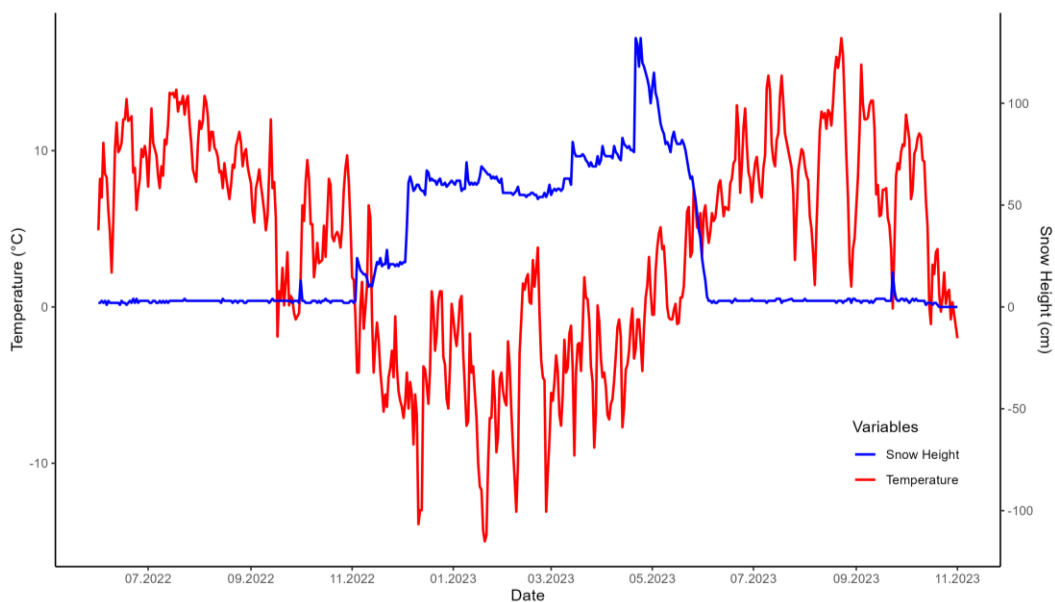
Figure 22: Air temperature and snow height from June 2022 to November 2023, SLF meteo station Piano del Simano. Data: WSL.
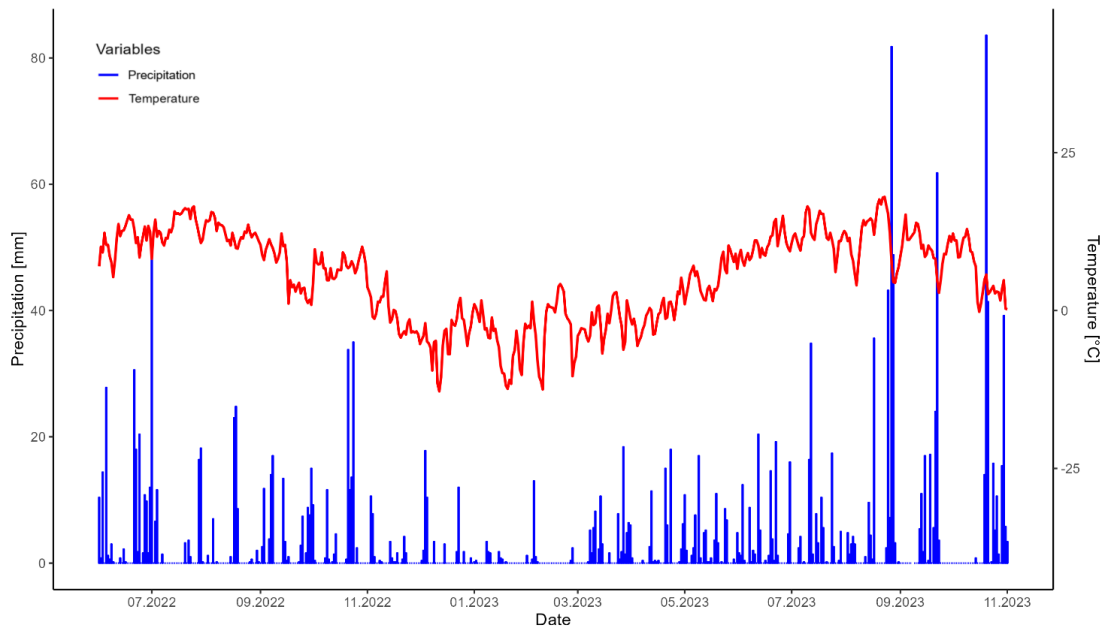
Figure 23: Precipitation and air temperature measured by the Piora meteo station between June 2022 and October 2023. Data: Cantone Ticino, Dipartimento del territorio.

The results of statistical tests performed to assess possible differences in GST (which in summer reflect atmospheric temperature trends) and precipitation between periods and between rock glaciers are shown below (Figure 24 - Figure 25 - Figure 26 - Figure 27 - Figure 28 - Figure 29 - Figure 30). This information will be relevant for discussing possible differences in their kinematics.
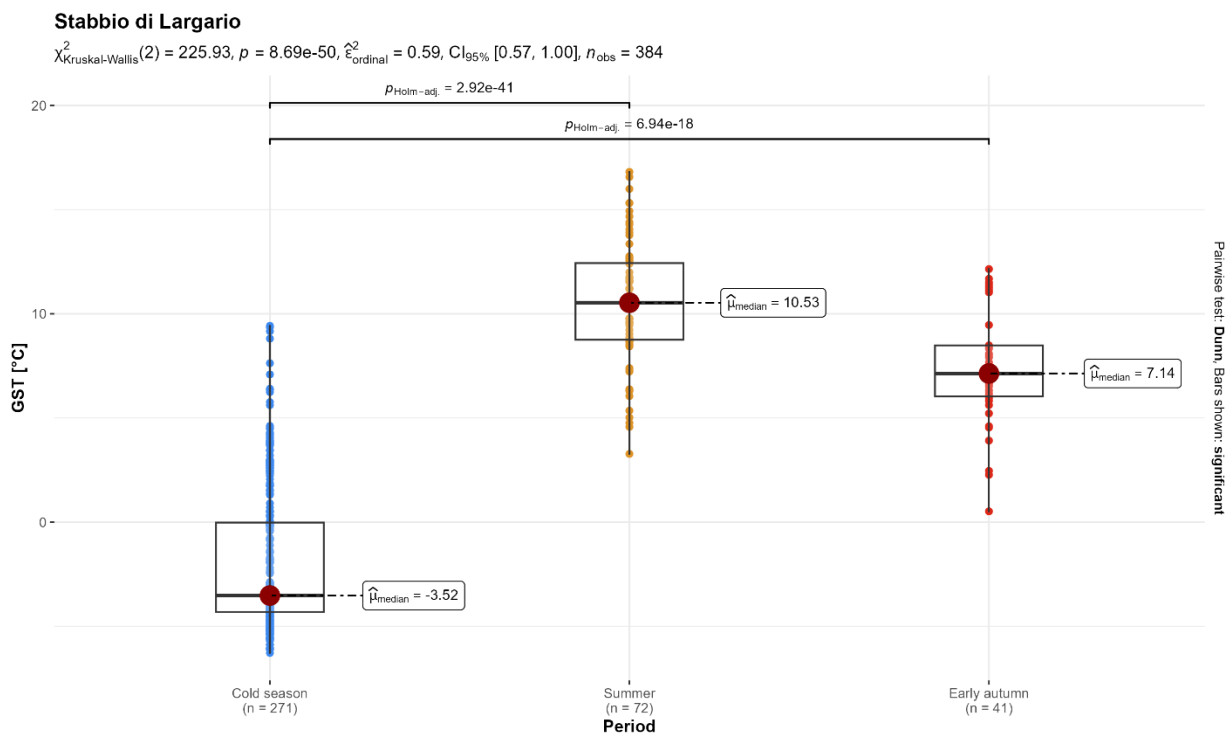
Figure 24: Statistical tests on GST differences between periods for Stabbio di Largario.

Piancabella

$\chi^2_{\text{Kruskal-Wallis}}(2) = 205.06$, $p = 2.97\text{e-}45$, $\hat{\varepsilon}^2_{\text{ordinal}} = 0.54$, $\text{CI}_{95\%}$ [0.52, 1.00], $n_{\text{obs}} = 380$
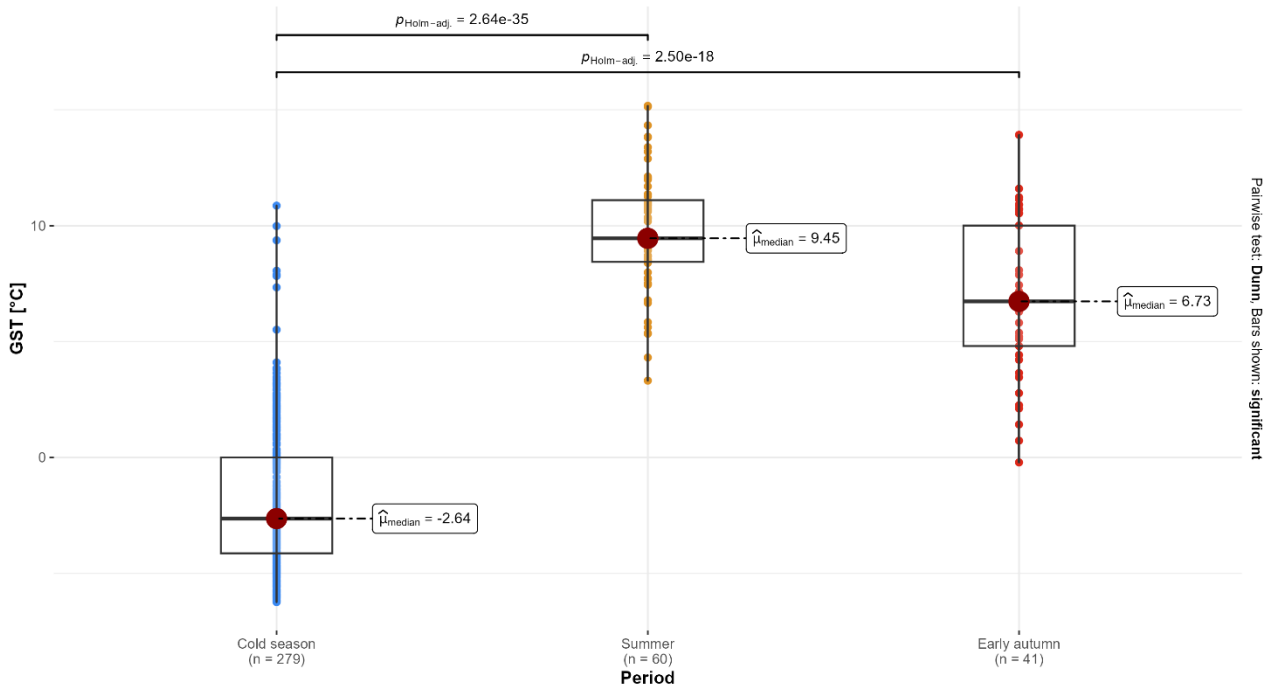
Figure 25: Statistical tests on GST differences between periods for Piancabella.

Monte Prosa

$\chi^2_{\text{Kruskal-Wallis}}(2) = 152.69$, $p = 6.96\text{e-}34$, $\hat{\varepsilon}^2_{\text{ordinal}} = 0.42$, $\text{CI}_{95\%}$ [0.39, 1.00], $n_{\text{obs}} = 367$
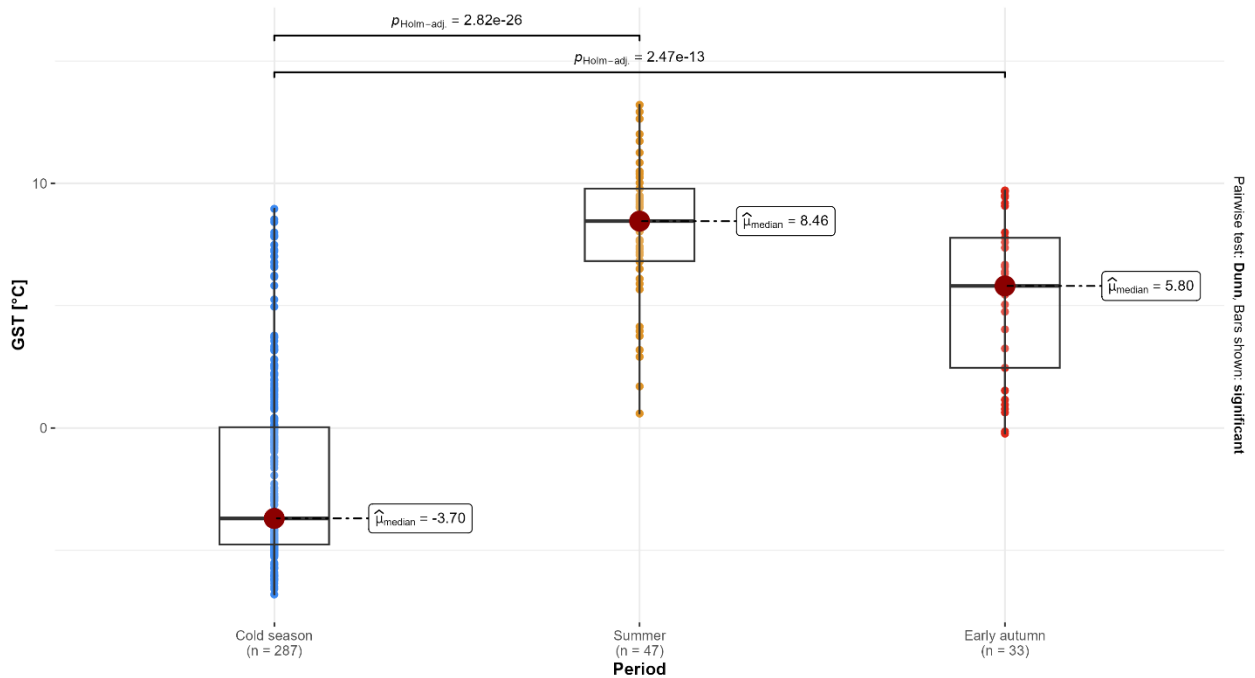
Figure 26: Statistical tests on GST differences between periods for Monte Prosa.

Ganoni di Schenadüi

$\chi^2_{\text{Kruskal-Wallis}}(2) = 157.10$, $p = 7.70\text{e-}35$, $\hat{\epsilon}^2_{\text{ordinal}} = 0.41$, $\text{CI}_{95\%}$ [0.38, 1.00], $n_{\text{obs}} = 383$
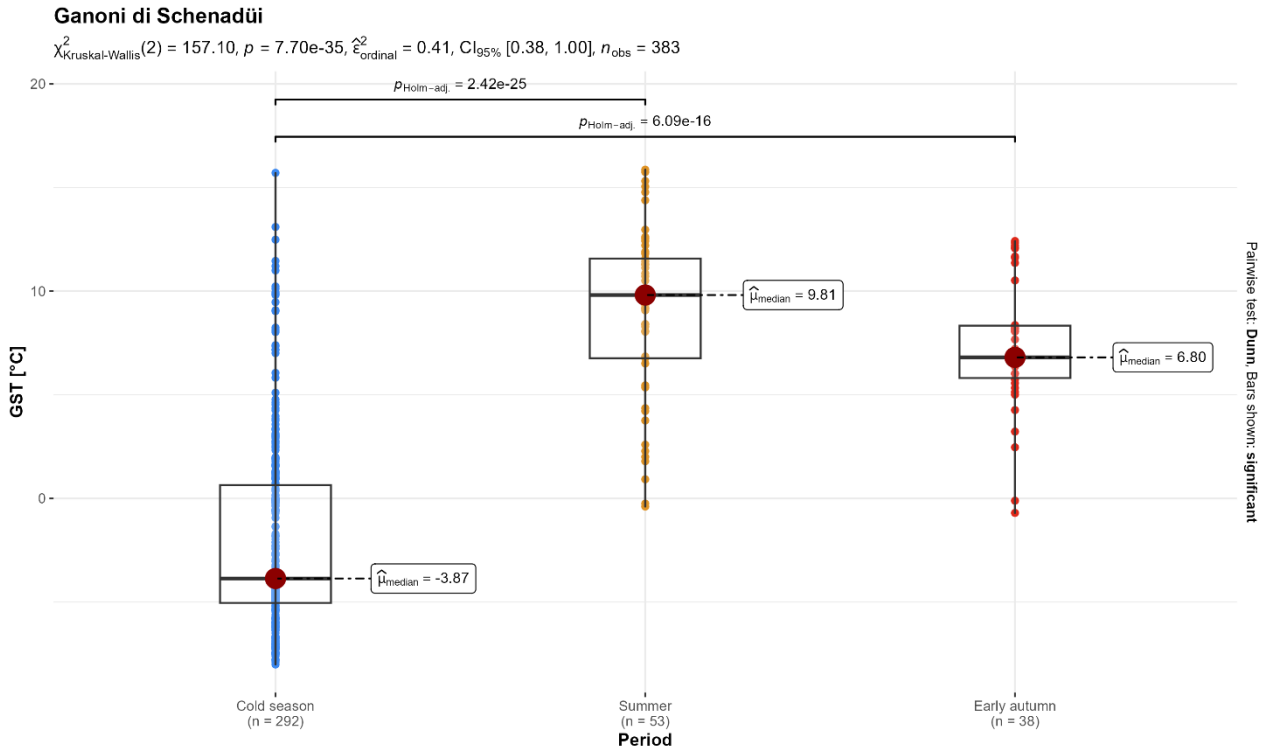
Figure 27: Statistical tests on GST differences between periods for Ganoni di Schenadüi.

Cold season

$\chi^2_{\text{Kruskal-Wallis}}(3) = 13.59$, $p = 3.52\text{e-}03$, $\hat{\epsilon}^2_{\text{ordinal}} = 0.01$, $\text{CI}_{95\%}$ [5.51e-03, 1.00], $n_{\text{obs}} = 1,127$
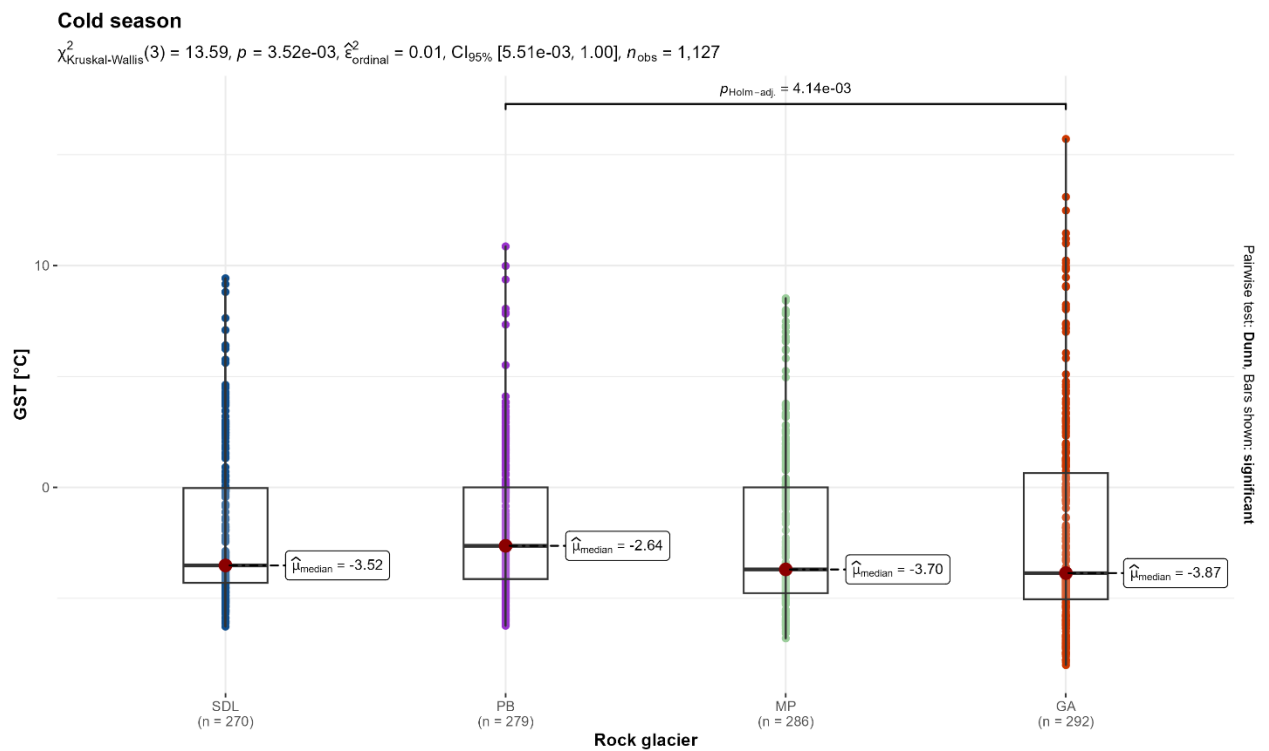
Figure 28: Statistical tests on possible cold season GST differences between rock glaciers

Summary

Summer

$\chi^2_{\text{Kruskal-Wallis}}(3) = 16.93$, $p = 7.31\text{e-}04$, $\hat{\epsilon}^2_{\text{ordinal}} = 0.07$, $\text{CI}_{95\%}$ [0.03, 1.00], $n_{\text{obs}} = 232$

$p_{\text{Holm-adj.}} = 2.47\text{e-}04$

$\hat{\mu}_{\text{median}} = 10.53$

$\hat{\mu}_{\text{median}} = 9.45$

$\hat{\mu}_{\text{median}} = 8.46$

$\hat{\mu}_{\text{median}} = 9.81$

GST [°C]

SDL (n = 72)   PB (n = 60)   MP (n = 47)   GA (n = 53)

Rock glacier

Pairwise test: **Dunn**, Bars shown: **significant**
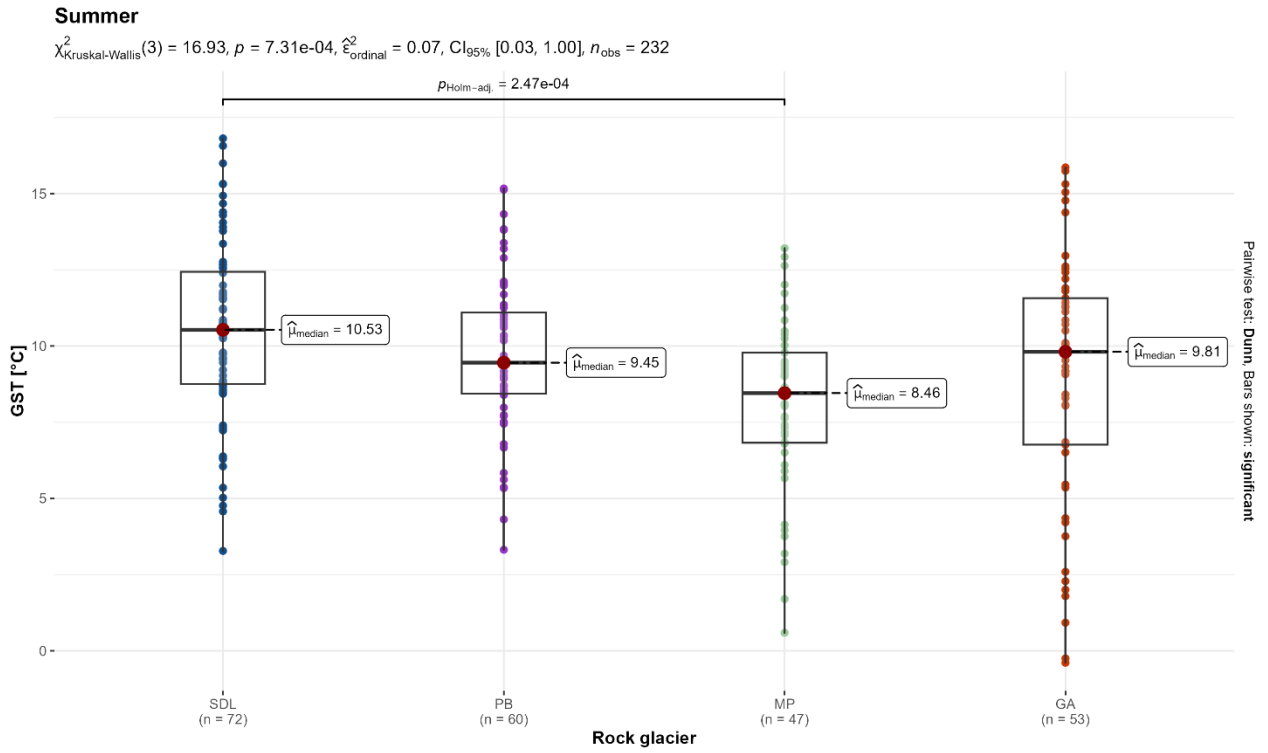
Figure 29: Statistical tests on possible summer GST differences between rock glaciers

Early autumn

$\chi^2_{\text{Kruskal-Wallis}}(3) = 9.09$, $p = 0.03$, $\hat{\epsilon}^2_{\text{ordinal}} = 0.06$, $\text{CI}_{95\%}$ [0.02, 1.00], $n_{\text{obs}} = 152$

$p_{\text{Holm-adj.}} = 0.03$

$\hat{\mu}_{\text{median}} = 7.14$

$\hat{\mu}_{\text{median}} = 6.73$

$\hat{\mu}_{\text{median}} = 5.78$

$\hat{\mu}_{\text{median}} = 6.80$

GST [°C]

SDL (n = 41)   PB (n = 41)   MP (n = 32)   GA (n = 38)

Rock glacier

Pairwise test: **Dunn**, Bars shown: **significant**
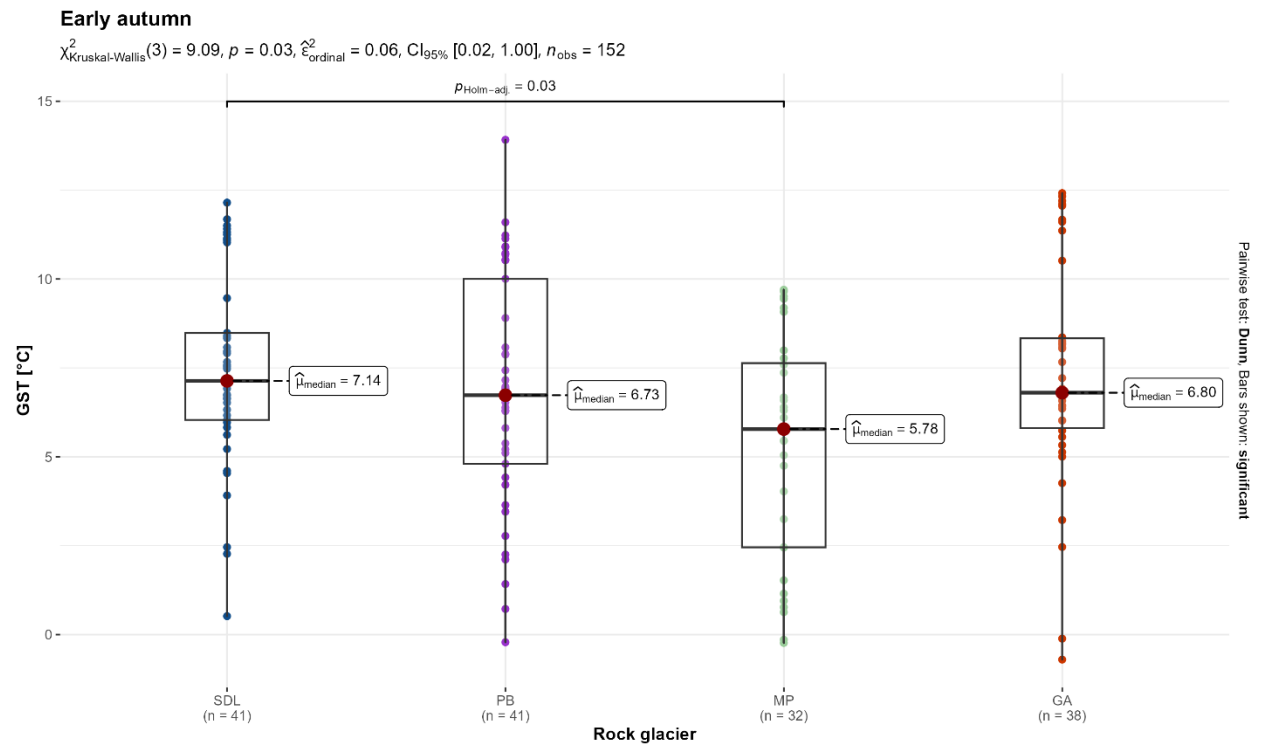
Figure 30: Statistical tests on possible early autumn GST differences between rock glaciers

Starting with the GST statistical tests (Figure 24 - Figure 25 - Figure 26 - Figure 27), the significant differences are only between cold season and the two periods of the warm season. Regarding the difference between the latter two, there seems to be a slight decrease during the early autumn, probably due to the alternation of hot and very cold periods compared to the norm. However, this difference is not statistically significant.

It is interesting to note the differences in GST between individual rock glaciers (Figure 28 - Figure 29 - Figure 30). During the cold season, there is a difference between Piancabella and Ganoni di Schenadüi, with median values of -3.87 °C and -2.64°C, respectively. During the summer, the medians of GST between Monte Prosa and Stabbio di Largario are statistically different, with values of 8.55°C for the former and 10.74°C for the latter. As in the previous case, the only significant difference in the early autumn is observed between Monte Prosa (5.78°C) and Stabbio di Largario (7.14°C).

Regarding precipitation (Table 5), there are important differences between periods and between rock glaciers. Since the two meteo stations are located at lower altitudes than the rock glaciers, and since in winter at those altitudes most of the precipitation falls in the form of snow, only summer precipitation was considered in the analysis. The large differences between summer and early autumn are mainly due to the timing of the second survey, which occurred in the middle of a period of heavy precipitation in northern Ticino. This event occurred between 26 and 28 August. Looking at the dates of the surveys, it can be seen that those of Monte Prosa and Piancabella had already been carried out, while those of Stabbio di Largario and Ganoni di Schenadüi had not yet. This is why, for these last two rock glaciers, the period between first and second survey was the one with the greatest water supply. On the contrary, for the other two, the period with the greatest water supply from precipitation was the one between the second and third survey of 2023.

Table 5: Cold season, summer and early autumn precipitation for each rock glacier normalized in mm/month. Data: Piora meteo station, Cantone Ticino, Dipartimento del Territorio.

	Cold season precipitation [mm/month]	Summer precipitation [mm/month]	Early autumn precipitation [mm/month]
SDL	44	153	144
PB	44	78	281
MP	69	117	222
GA	67	207	114

4.3 Intra-annual horizontal velocities (based on GNSS surveys only)

4.3.1 Introduction to the results

In the following chapter, based on the RGIK guidelines (RGIK, 2023), comparisons are made between seasonal (normalised over one year) reference velocities of all rock glaciers and their annual velocities, measured by dGNSS (Figure 31). These are the periods between the end of September 2022 and the beginning of October 2023. This comparison makes it possible to understand for the sites considered in the study the relationship between seasonal and overall annual velocities and, thus, to understand the extent to which the seasonal signal is more or less pronounced than the year-round signal. Furthermore, to better visualise and quantify these seasonal differences in velocity, Figure 32 was prepared, where on the y-axis, the ratio of seasonal to annual velocity was plotted in percentages and on the x-axis, the annual velocity in m·a⁻¹ (e.g. RGIK, 2023). Considering all the reference points of all four sites, the mean, median and standard deviation (in percentage terms) were then extracted. This allows for better quantification and understanding of the kinematics of these rock glaciers on an intra-annual level. However, the graphs proposed by RGIK (2023) do not allow us to assess whether the differences between one period and the next are statistically significant. For this purpose, statistical tests were carried out on the velocities measured in the three periods based on what is explained in the methods section. In the first step, the results of all four rock glaciers together will be presented, while in the second step, the variations within and between them will be described.

4.3.2 All the rock glaciers together

The first graph of Figure 31 shows cold season velocities versus annual velocities and is very close to the 2022-2023 yearly trend. Almost all points lie close to the dashed line representing the bisector, suggesting that most of that season's velocities are in line with the annual ones. However, while there are elements above and below the line, there seems to be a slight tendency towards lower speeds, with some points lying well below the line representing the 1:1 speed ratio. In fact, looking at the corresponding graph in Figure 32, the one representing the deviation of the cold season speed ratio from the annual one, one can see that there is generally a variability between the different points, with values ranging from +90% to -75%. This variation is evident at points with rather low annual velocities, i.e. up to 0.1-0.2 m·a⁻¹. Moving to the right in the graph, i.e. towards the points with the most significant annual movements, this variability decreases significantly. Considering all points together, the average value is -3% (median of -6%), which indicates an overall average cold season velocity slightly lower than the annual one.

The distribution of points during the summer is somewhat different from the previous period, i.e. less uniform and more distant from the bisector. This generally indicates a greater difference between the velocities measured during this period and those measured throughout the year. The graph can be divided into two

parts. In the first one, where there are the points with lower velocities, about up to 0.2 m·a⁻¹, the seasonal velocities in summer are higher than the annual ones. In the second part, where the points have shifted the most, summer velocities average below annual velocities. The graph representing the deviation of the summer velocity ratio from the annual one shows significantly higher values than those seen above. As in the previous case, the most significant variability is observed at points with annual movements below 0.2 m·a⁻¹ with some values above 400%, i.e. four times the annual velocity. Looking at the points with larger displacements, a lower variability is also observed in this case. Moreover, most of the values are negative in that portion of the graph. This confirms what is seen in Figure 31, where the seasonal velocity of the slowest points is much greater than the annual one, while that of the fastest points is slightly slower. The median value of 70% is influenced by the very high value of a few points (see SD of 121%) and would indicate a rather high seasonal speed of the first part of summer. On the other hand, looking at the median value of 22%, one can see that it is definitely lower and seems to represent the speeds of this period better than the annual one.

The early autumn, between the second and third survey, clearly shows that the horizontal velocities are in the vast majority of cases above the annual velocities. Only a few points show values below the annual speed. This can also be seen very clearly in the graph showing the deviation of the seasonal/annual ratio. It shows a similar trend to the previous one but with higher values, some between 400% and 1000%, indicating speeds of 4 to 10 times the annual speed. Variability also decreases here, moving towards the largest movements, where most points are below 200%. The mean of 120% and the median of 75% indicate an early autumn velocity about twice as fast as the annual one.

In the graph showing the points over the entire summer period, most of the points are above the bisector, indicating higher summer speeds compared to the annual ones. The trend is similar to that of the early autumn. However, the velocities over the warm season are lower than during that period, as they are balanced by a season start with velocities several points below the annual ones. The graph in Figure 32 illustrates very well how, in contrast to the two separate summer periods, the deviation of the values (SD of 72%) is significantly lower. However, the trend remains similar, with higher values for points with smaller movements and lower values for points with higher speeds. Looking at the mean and median values, it can be stated that generally, the velocity over the entire summer is about 30-50% higher than the annual velocity, again considering all four rock glaciers together.
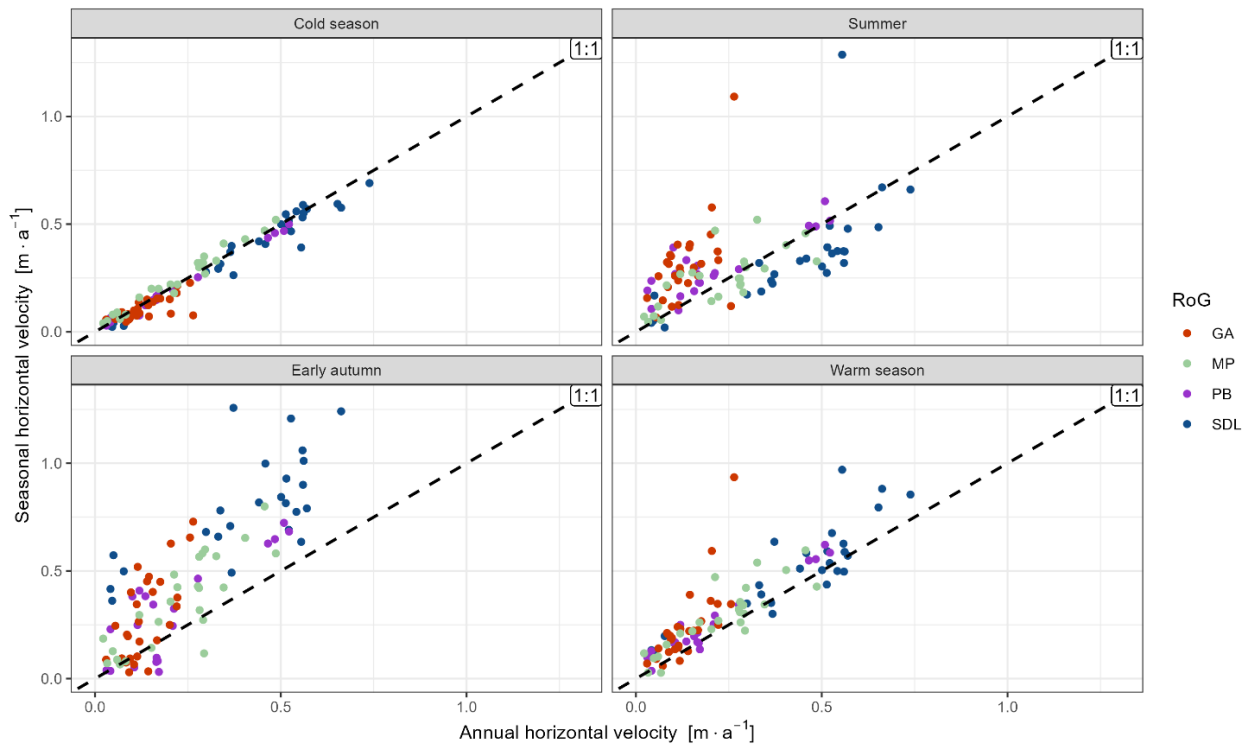
Figure 31: Seasonal horizontal velocities (normalized in m·a⁻¹) over annual horizontal velocities for the reference points of the four rock glaciers.
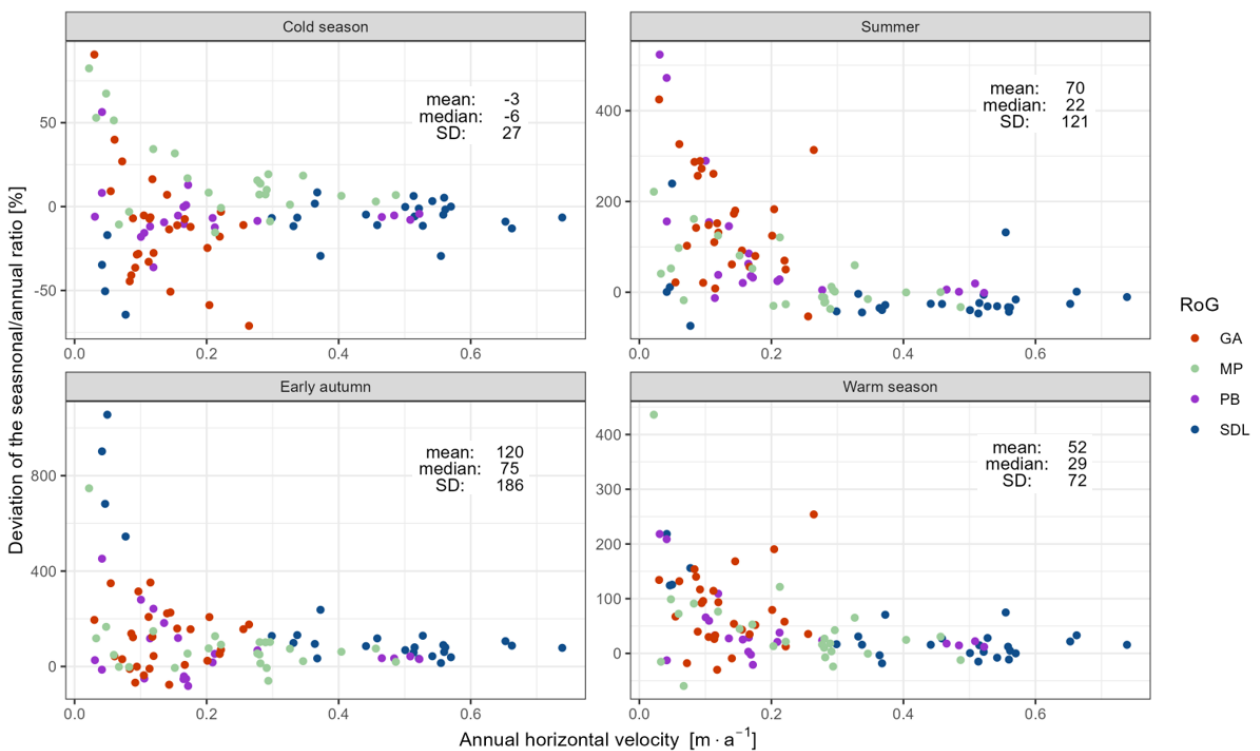
Figure 32: Deviation of the seasonal/annual ratio over the annual horizontal velocity for the reference points of the four rock glaciers.

The result of the non-parametric Kruskall-Wallis test, visible in Figure 33, statistically confirmed the difference between the velocities, expressed in cm·month⁻¹, of at least two periods (p = 1.16e-05). This was already relatively clear from what we saw earlier. What is interesting to note, however, from the pairwise comparisons using Dunn's test, is that the significant differences are only between summer and early autumn (p = 1.58e-03) and between cold season and early autumn (p = 1.21e-05). Surprisingly, the differences observed between cold season and summer cannot be regarded as statistically significant. Therefore, considering the reference points of all four rock glaciers combined, although a trend is observed, it cannot be rejected the fact that cold season velocity is equal to the summer one.

$\chi^2_{\text{Kruskal-Wallis}}(2) = 22.72$, $p = 1.16e-05$, $\hat{\epsilon}^2_{\text{ordinal}} = 0.08$, $CI_{95\%}$ [0.04, 1.00], $n_{\text{obs}} = 273$
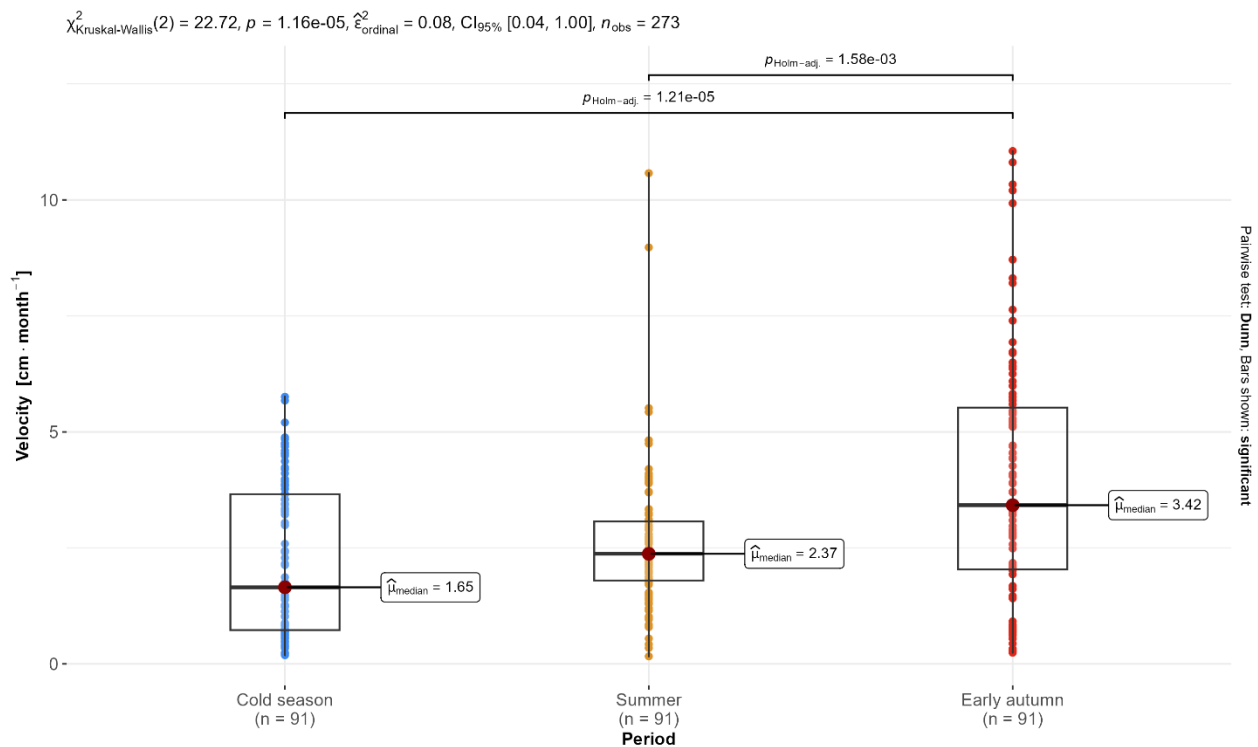
Figure 33: Statistical test to check for seasonal velocity differences between periods for all the reference points together.

4.3.3 Differences between and within rock glaciers

This chapter shows the differences in seasonal contributions to the annual total and, consequently, the differences in velocity between periods of the year for each rock glacier (Figure 34 - Figure 35 - Figure 36 - Figure 37) and between the four rock glaciers (Figure 38 - Figure 39 - Figure 40). Table 6 clearly shows how, depending on the season, the seasonal displacement contribution to the annual total can vary between sites. It refers to the average displacement contribution from one survey to the next, expressed as a percentage of the total displacement. This allows a better comparison between different periods between different rock glaciers. In addition, as done in the previous chapter, statistical tests were carried out to quantify these differences. Since data do not meet the assumptions for an ANOVA test (not normally distributed or absence

of homogeneity of the variances), Kruskal-Wallis tests were carried out, resulting in Dunn's pairwise comparisons.

Starting with the cold season, Stabbio di Largario shows displacements that account for about 60% of the total, with median velocities of 2.67 cm·month^{-1}. The contribution of the first part of the summer, until the end of August, is rather limited to the total, about 14%. The Kruskal-Wallis statistical test performed on the velocities showed no significant differences between cold season and summer. On the other hand, a significant increase (p = 1.77e-08) is observed in the latter part of summer and early autumn, with a higher percentage contribution in a shorter period. Although the trend of the two lobes is somewhat similar, it is interesting to note that in the case of the year 2022-2023, during the cold season, the west lobe contributes more to the total displacement than the east lobe. The contribution was virtually identical in the warm season and increased more in the east lobe during the early autumn.

The Piancabella rock glacier also shows a cold season contribution of about 60%, with a median velocity of 1.38 cm·month^{-1}. The beginning of summer seems to cause an increase in speed, which contributes about 25% of the total, with a median value of 2.14 cm·month^{-1}. However, the differences in velocities between these two periods are not statistically significant. The second part of the summer also sees a further increase in the median velocity to 2.58 cm·month^{-1}. Still, as in the previous case, this cannot be regarded as statistically significant. It should be noted that the result of the Kruskal-Wallis test for Piancabella gave a p-value of 0.07, i.e. very close to the significance level of 0.05. These are, therefore, non-significant differences that, however, suggest a trend.

The cold season contribution of Monte Prosa is high compared to the other three rock glaciers, with almost 80% of the annual contribution and a median rate of 3.54 cm·month^{-1}. Consequently, the contribution of the two warm season periods is relatively small in the total. Another peculiarity from the statistical tests is that the summer rate is significantly slower (p = 8.25e-04) than the cold season rate, with a median value of 2.36 cm·month^{-1} and 3.54 cm·month^{-1}, respectively. This is the only case among the four analysed. Early autumn velocities, on the other hand, are on par with cold season velocities with no significant differences.

Ganoni di Schenadüi also represents a very interesting case, which is opposite to what we have just seen. It shows a much lower cold season contribution of between 45% and 58% (east and west lobes). This means that the contribution of the nine months of the cold season period is roughly equivalent to the three summer months between July and the beginning of October. In the first part of summer, it shows significantly higher velocities than in the cold season (p=1.70e-06), with a median value of 2.45 cm·month^{-1} compared to 0.73 cm·month^{-1}. Even in the early autumn, the velocity values remain significantly higher than in the cold season but do not differ much from those of the summer.

Table 6: Seasonal contribution on the total horizontal displacement (expressed in %).

	Cold season [%]	Summer [%]	Early autumn [%]
SDL West	68.5	14.2	17.3
SDL East	57.0	14.4	28.6
PB	60.5	24.4	15.1
MP	78.1	10.1	11.8
GA West	58.3	26.0	15.7
GA East	45.6	32.7	21.8

SDL

$\chi^2_{\text{Kruskal-Wallis}}(2) = 37.55$, $p = 7.01\text{e-}09$, $\hat{\varepsilon}^2_{\text{ordinal}} = 0.49$, $\text{CI}_{95\%}$ [0.36, 1.00], $n_{\text{obs}} = 78$
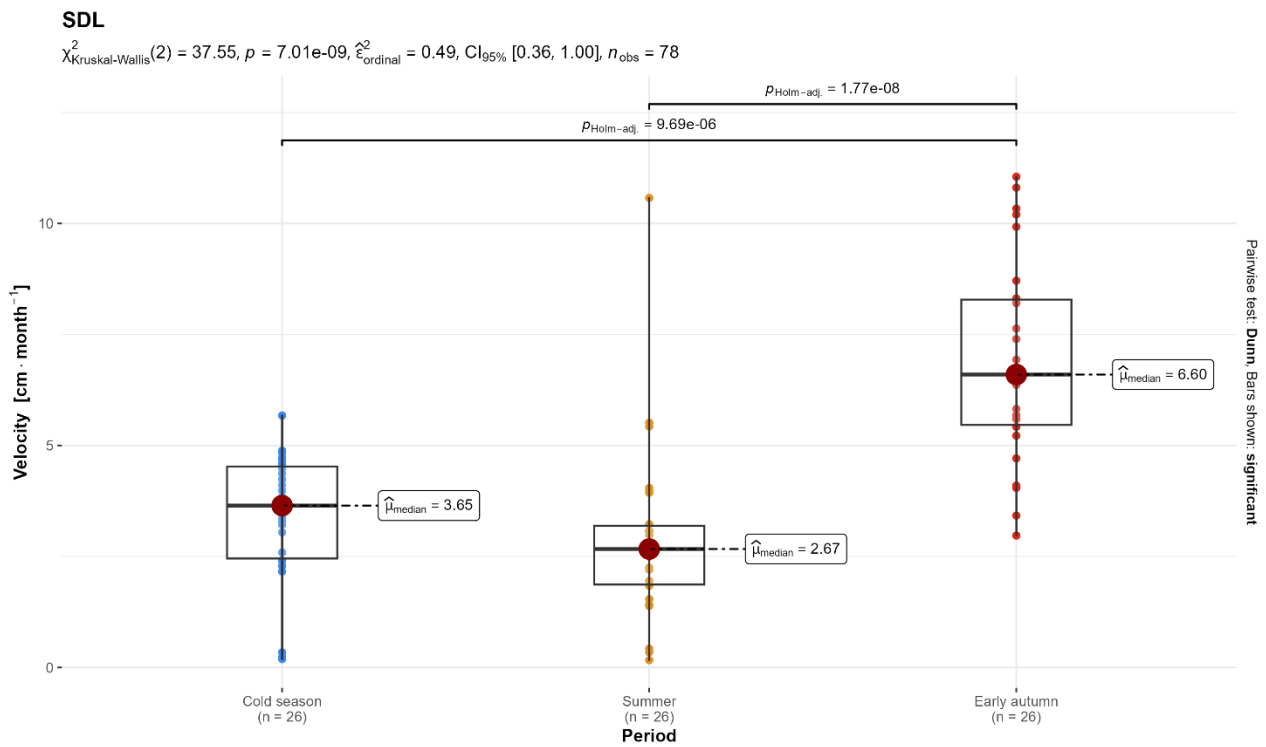
Figure 34: Statistical test on possible seasonal velocity differences for the reference points of Stabbio di Largario (SDL).

PB

$\chi^2_{\text{Kruskal-Wallis}}(2) = 5.30$, $p = 0.07$, $\hat{\epsilon}^2_{\text{ordinal}} = 0.09$, $\text{CI}_{95\%}$ [0.03, 1.00], $n_{\text{obs}} = 63$
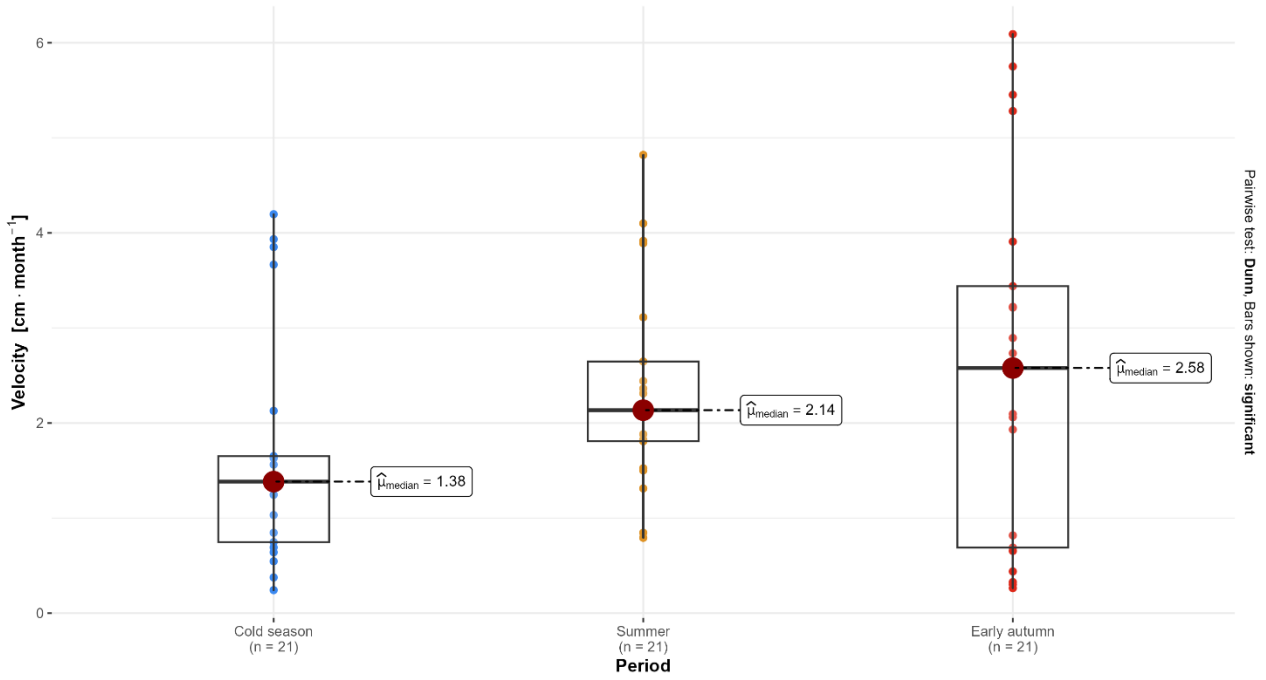
Figure 35: Statistical test on possible seasonal velocity differences for the reference points of Piancabella (PB).

MP

$\chi^2_{\text{Kruskal-Wallis}}(2) = 16.14$, $p = 3.12\text{e-}04$, $\hat{\epsilon}^2_{\text{ordinal}} = 0.34$, $\text{CI}_{95\%}$ [0.18, 1.00], $n_{\text{obs}} = 48$
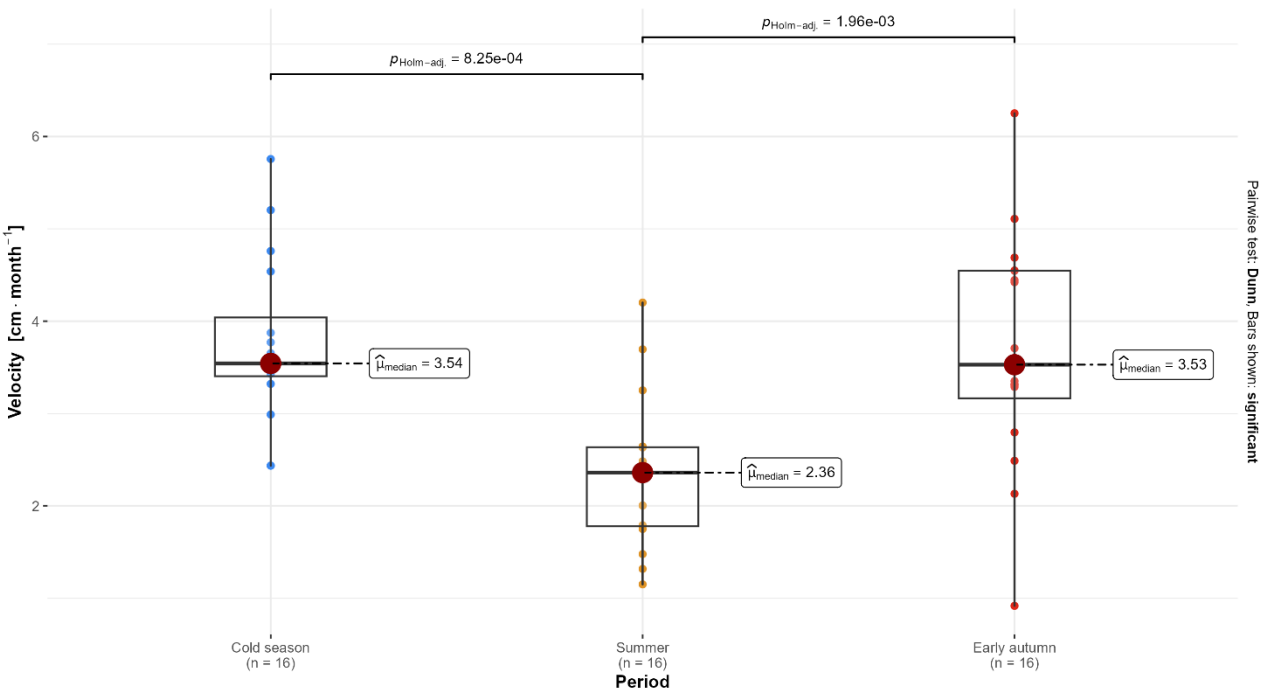
Figure 36: Statistical test on possible seasonal velocity differences for the reference points of Monte Prosa (MP).

GA

$\chi^2_{\text{Kruskal-Wallis}}(2) = 27.71$, $p = 9.60e\text{-}07$, $\hat{\varepsilon}^2_{\text{ordinal}} = 0.33$, $\text{CI}_{95\%}$ [0.25, 1.00], $n_{\text{obs}} = 84$
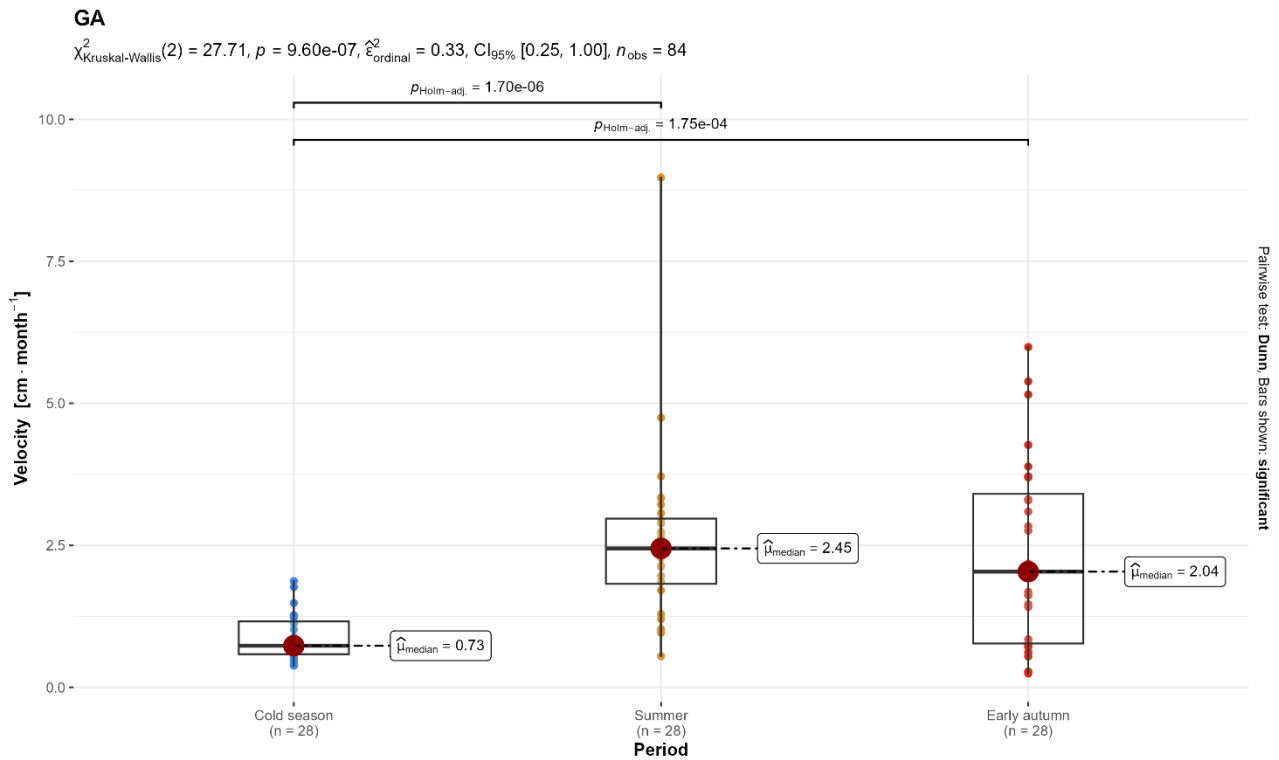
Figure 37: Statistical test on possible seasonal velocity differences for the reference points of Ganoni di schenadüi (GA).

The differences in seasonal velocities between the four rock glaciers were also calculated to see whether there was a regular pattern or whether they behaved differently from each other throughout the year (Figure 38 - Figure 39 - Figure 40). The cold season shows a clear difference between the rock glaciers of Stabbio di Largario and Monte Prosa and those of Piancabella and Ganoni di Schenadüi (see p-values in the graph). The median cold season velocities of the first two are just over 3.5 cm·month⁻¹, while those of the latter are 1.38 and 0.73 cm·month⁻¹, respectively. In contrast, summer shows no difference in velocities between the rock glaciers, with median values ranging from about 2 to 2.5 cm·month⁻¹. The last period, early autumn, shows a clear difference in velocity between Stabbio di Largario and the other three sites. In contrast, among the latter the differences visible in the graph are not statistically significant.

Cold season

$\chi^2_{\text{Kruskal-Wallis}}(3) = 39.91$, $p = 1.12\text{e-}08$, $\hat{\epsilon}^2_{\text{ordinal}} = 0.44$, $\text{CI}_{95\%}$ [0.32, 1.00], $n_{\text{obs}} = 91$
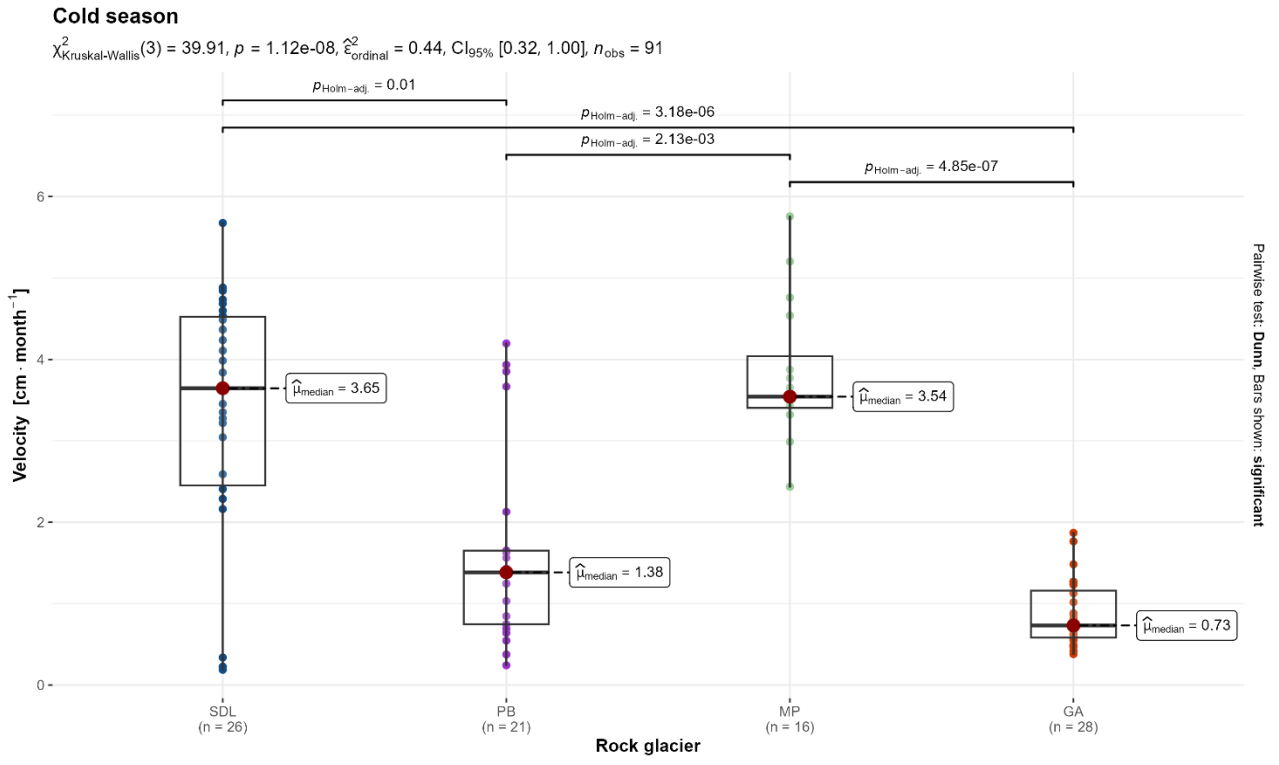
Figure 38: Statistical test to check for cold season velocity differences between rock glaciers.

Summer

$\chi^2_{\text{Kruskal-Wallis}}(3) = 1.86$, $p = 0.60$, $\hat{\epsilon}^2_{\text{ordinal}} = 0.02$, $\text{CI}_{95\%}$ [5.21e-03, 1.00], $n_{\text{obs}} = 91$
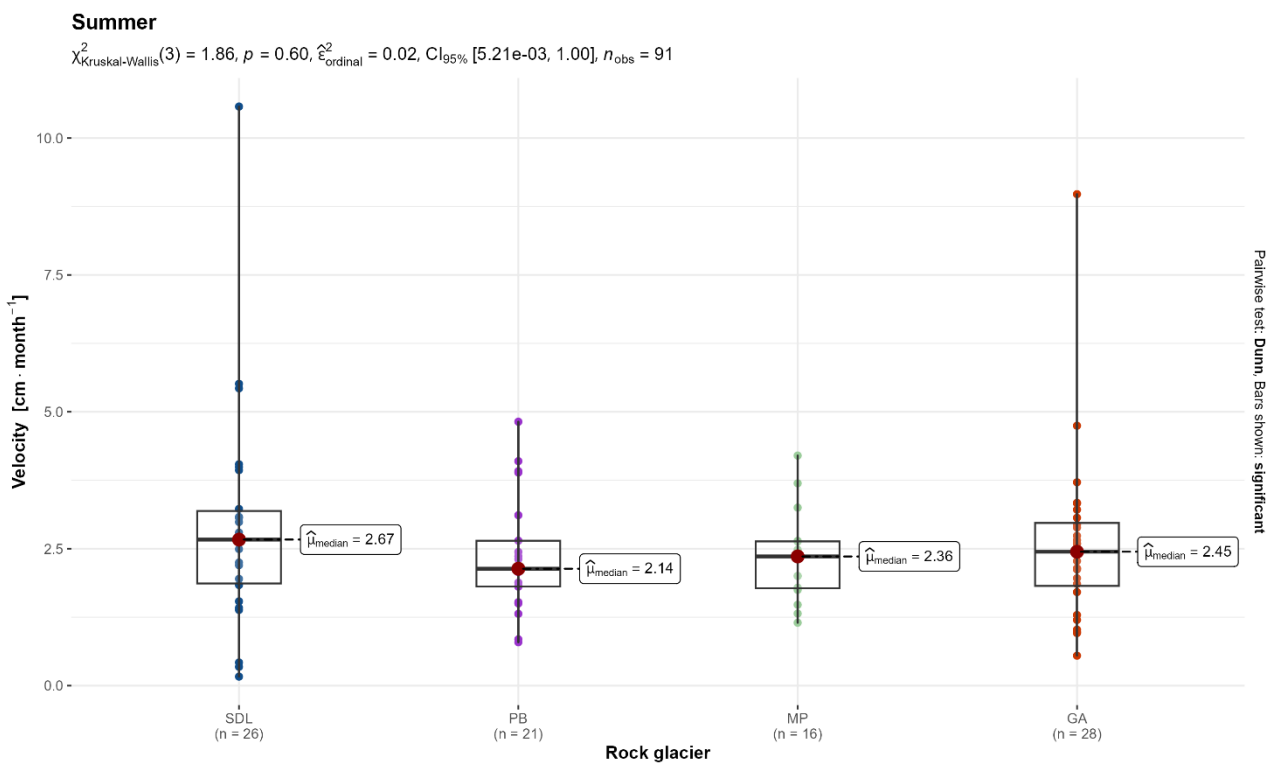
Figure 39: Statistical test to check for summer velocity differences between rock.

Early autumn

$\chi^2_{\text{Kruskal-Wallis}}(3) = 46.13$, $p = 5.33\text{e-}10$, $\hat{\epsilon}^2_{\text{ordinal}} = 0.51$, $\text{CI}_{95\%}$ [0.41, 1.00], $n_{\text{obs}} = 91$
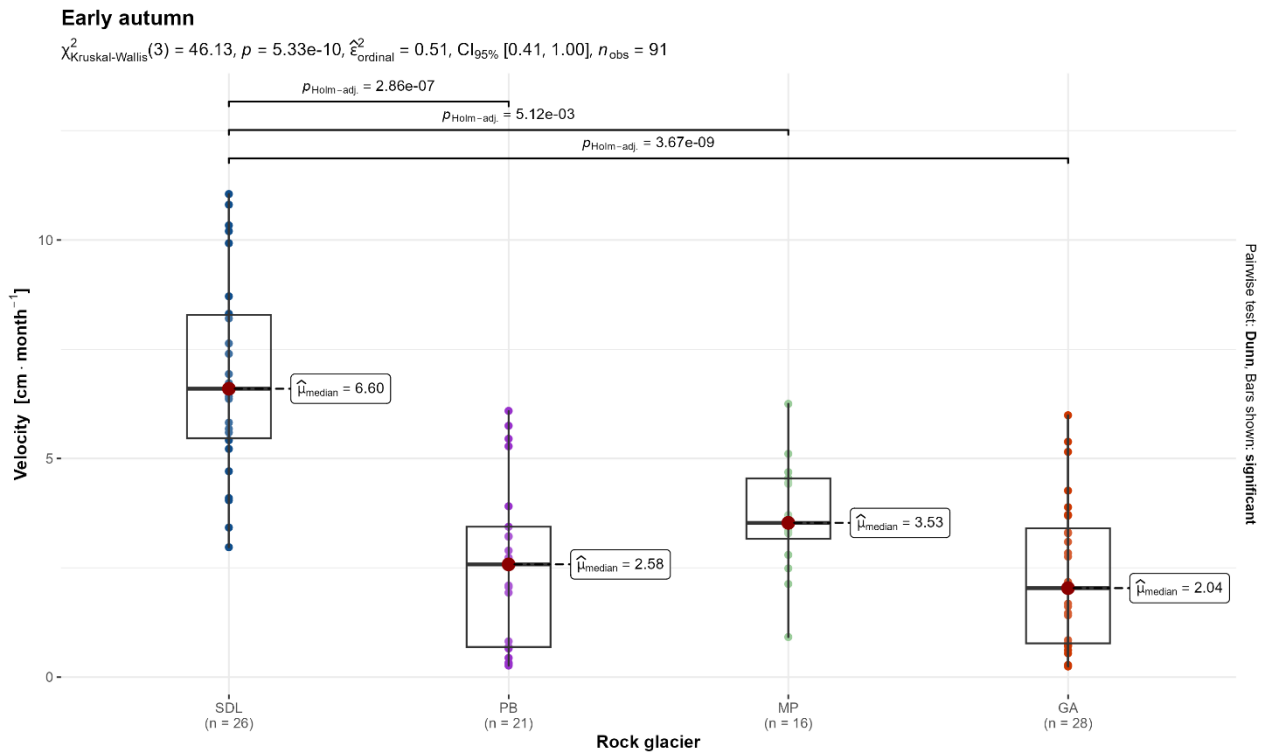
Figure 40: Statistical test to check for early autumn velocity differences (normalized in cm·month⁻¹) between rock

4.4   dGNSS vs UAV-derived horizontal velocities

4.4.1 Inter-annual comparison

This chapter deals with comparing point measurements performed using GNSS and measurements derived from the products of UAVs, i.e. orthomosaics. By comparing the image feature tracking method performed using the CIAS software on the orthomosaics produced in 2016 and 2023 with the dGNSS measurements taken in those years, it can be seen that the values obtained by the two methods are highly correlated (Figure 41). The differences between the two methods vary between -18 cm per year and 6 centimetres per year, with most values between -3 and 3 centimetres per year. The determination value R^2 of 0.98 indicates an almost perfect correlation between the two methods over the seven-year period between 2016 and 2023. The slope of the straight line indicates that for slower points, the image feature tracking method produces results with slightly lower speeds than those measured by GNSS. On the contrary, the generally faster points show slightly higher values.
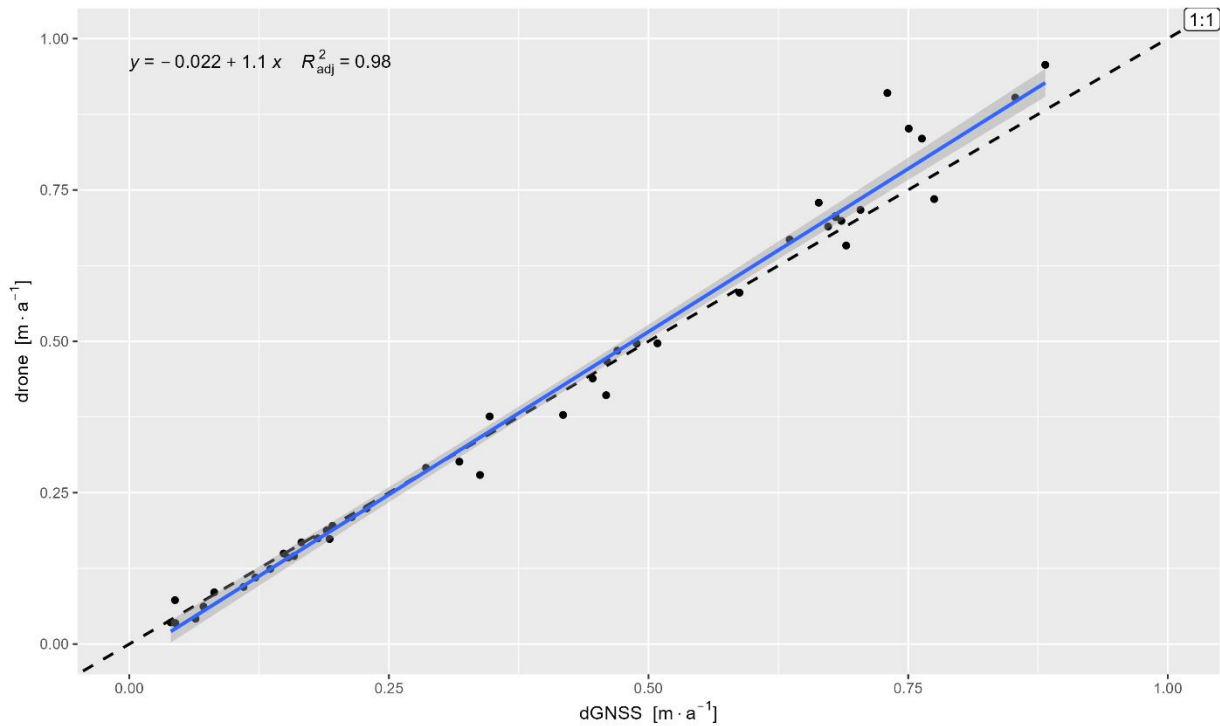
Figure 41: Comparison between Drone-based and dGNSS measured displacements from 2016 to 2023 for the reference points of Stabbio di Largario and Piancabella rock glaciers together.

Considering the same type of analysis but performed individually on the two rock glaciers, it can be seen that the result is slightly different (Figure 42). The rock glacier of Stabbio di Largario appears to have small variations between dGNSS and drone measurements, especially with regard to points with medium-high velocities. The determination value R^2 equal to 0.98, however, confirms that the two methods return very similar values. As far as the Piancabella rock glacier is concerned, it can be seen that the results obtained using the drone even better represent those obtained using dGNSS. The points lie almost perfectly along the bisector. The value of the slope of the straight line, which is equal to 1, as well as the value of the coefficient of determination, which is also equal to 1, confirm the agreement between the two methods.

SDL

$$y = -0.17 + 1.1\,x \quad R^2_{adj} = 0.98$$

drone $[m \cdot a^{-1}]$

dGNSS $[m \cdot a^{-1}]$

PB

$$y = -0.091 + 1\,x \quad R^2_{adj} = 1$$

drone $[m \cdot a^{-1}]$
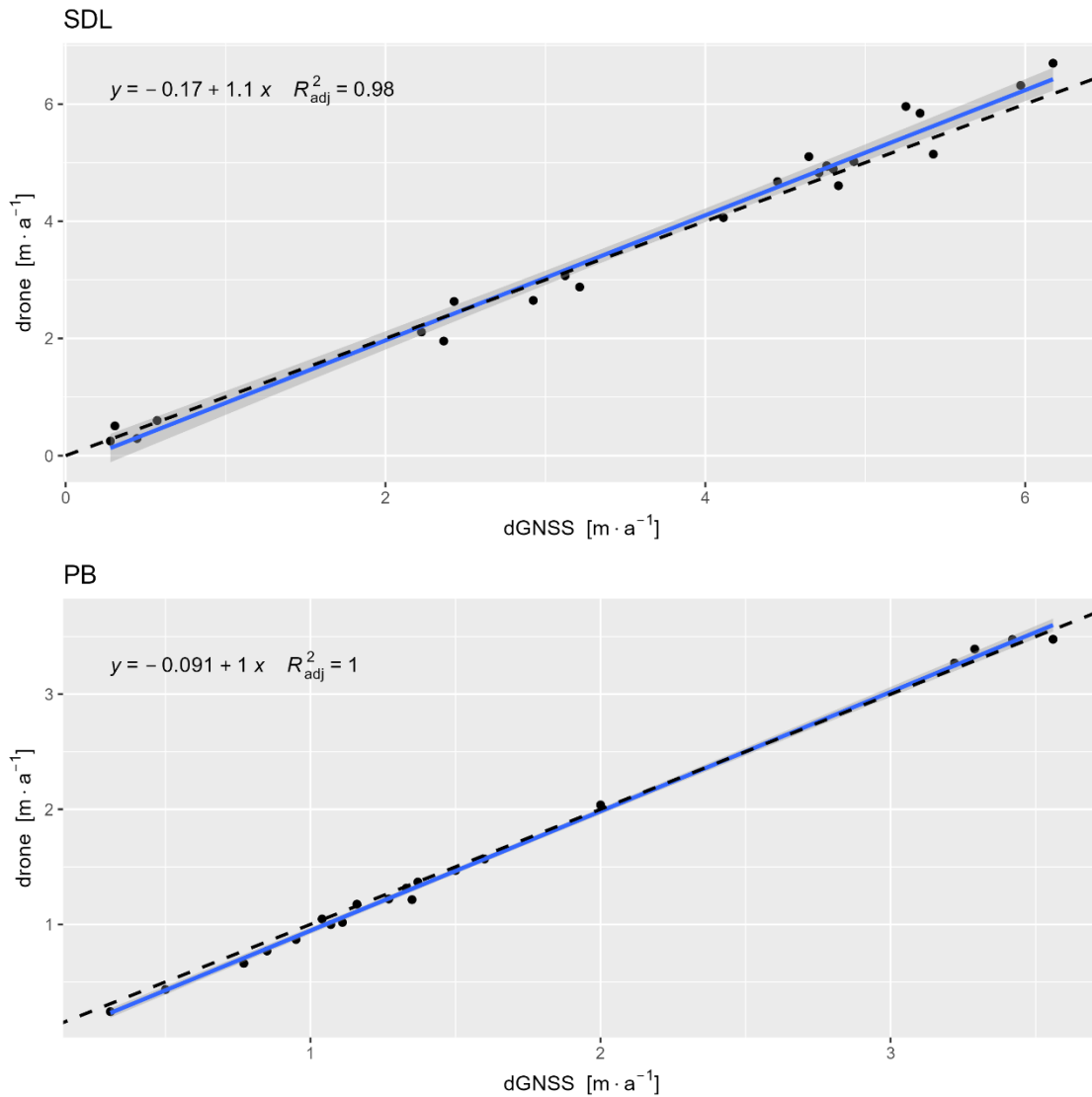
dGNSS $[m \cdot a^{-1}]$

Figure 42: Comparison between Drone-based and dGNSS measured displacements from 2016 to 2023 for the reference points of Stabbio di Largario (SDL) and Piancabella (PB) rock glaciers.

Although there are minor differences between individual cases, given the R^2 determination values very close to 1, it can be confirmed that over a 7-year time span, the measurements made using drone-produced orthomosaics mirror those made in the field using dGNSS equipment.

4.4.2 Intra-annual comparison

After confirming the strong correlation between measurements obtained by drone orthomosaics (using CIAS software) and dGNSS measurements over a 7-year period, the aim was to determine whether similar results could also be obtained over shorter periods. In this case, the two methods were compared over three periods: summer, early autumn and the entire warm season. This was done for all the reference points of the four study sites (Figure 43).
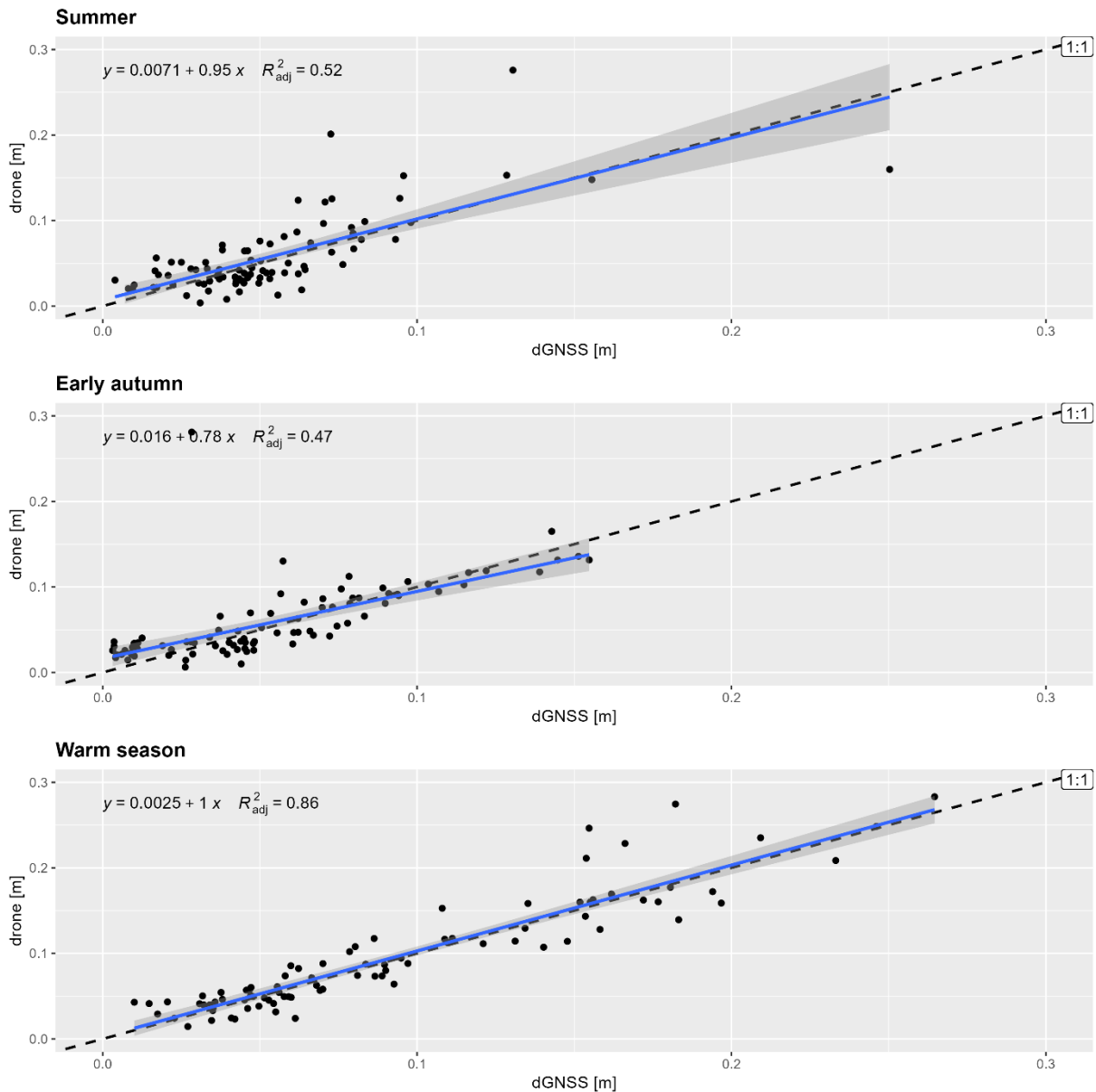
Figure 43: Comparison between drone-based and dGNSS measured displacements of summer , early autumn and warm season for the reference points of all rock glaciers together.

The first graph, representing the period between the first and second survey, shows that there is a direct positive correlation between the two variables, with a slope of the line of 0.95. However, the value of R^2 equal to 0.52 indicates that the values obtained by the CIAS software only partially match those obtained by dGNSS. The same trend is also clearly visible during the early autumn, between the second and third survey. The two methods have a positive correlation but with highly variable data and an R^2 value equal to 0.47. This indicates that the difference between the two methods is slightly greater in the early autumn than in the previous period, but they are still comparable.

Combining both periods, and thus comparing the two methods over the entire summer (between the first and third survey in 2023), the correlation between the two methods clearly improves, with the slope of the

60

straight line equal to 1 and an R^2 value of 0.86. This value indicates a very good correlation between the measurements obtained through the two methods.

Based on the result of Figure 43, and considering the one between 2016 and 2023 (Figure 41), it seems evident that for these rock glaciers, over a short period (approximately under two months), the comparison between the two measurement methods leads to less good results in terms of correlation. This indicates that there are sometimes important differences between the one and the other. As the time elapsed between the two surveys increases, the correlation increases considerably until it is almost perfect over the 7 years since the previous drone survey.

4.5   Evaluation of UAV-derived displacement accuracy (based on CIAS)

Table 7 and Table 8 show the accuracy values for horizontal displacements as well as thickness changes. These values confirm the high quality of the photogrammetric products as well as their coregistration. LoD of the horizontal displacements is 2 cm for all four rock glaciers and for all three periods: summer, early autumn and warm season. As expected, for 2016-2023, LoD is slightly higher, probably due to the lower quality of the older orthophotos. The standard deviations derived through CIAS analysis on the stable terrain are very similar if not identical, which means the almost complete absence of anisotropy in the resulting displacement uncertainties. Regarding the LoDs of the thickness changes, we see that they are certainly higher than the horizontal ones and lie between 6 cm at Piancabella and around 12 cm at Monte Prosa. These differences are mainly due to the different recording errors (RMSE on the stable ground after the ICP) incorporated into the LoD calculation using the M3C2 algorithm. This means that the LoD values tend to be large and therefore conservative, as confirmed by Lague *et al*. (2013). Again, as could be expected, the LoD value between 2016 and 2023 is higher, i.e. by 31 cm. The main reason for this is the lower density of the point cloud in 2016, as well as the different types of drones and procedures in the creation of the photogrammetric products.

Table 7: Assessment of the horizontal displacement accuracy of orthoimage pairs over stable terrain.

	n° stable points	x-shift (cm)	y-shift (cm)	σ_x (cm)	σ_y (cm)	LoD (cm)
SDL 1-2	59	-1	-2	5	3	2
SDL 2-3	50	1	3	3	3	2
SDL 1-3	49	0	1	4	4	2
SDL 16-23	14	1	-3	10	13	4
PB 1-2	47	0	0	2	1	2
PB 2-3	50	0	0	2	1	2
PB 1-3	48	0	0	2	1	2
PB 16-23	48	2	1	29	19	5

	n° stable points	x-shift (cm)	y-shift (cm)	σ_x (cm)	σ_y (cm)	LoD (cm)
MP 1-2	50	-1	2	2	2	2
MP 2-3	42	-2	2	2	3	2
MP 1-3	48	1	0	3	2	2
GA 1-2	47	1	1	2	2	2
GA 2-3	44	-1	0	3	2	2
GA 1-3	48	0	1	2	2	2

Table 8: Assessment of the M3C2 displacement accuracy of point cloud pairs over stable terrain. MP and GA have no LoD between 2016 and 2023 because drone surveys were not conducted in 2016

	LoD Summer (cm)	LoD Early autumn (cm)	LoD Warm season (cm)	LoD 2016 - 2023 (cm)
SDL	7.6	6.8	7	31
PB	6.1	6.1	6.3	31
MP	11.5	11.8	11.6	-
GA	11	9.6	11	-

4.6 Inter-annual horizontal velocities through image correlation

This chapter presents the results of the horizontal velocities obtained using the image feature tracking algorithm with the CIAS software on the orthomosaics produced in 2023 with that of 2016 for the rock glaciers of Stabbio di Largario and Piancabella. This will make it possible to understand and quantify kinematic trends at these two sites over the past seven years and compare them with those observed during the summer 2023.

Stabbio di Largario

The period between 2016 and 2023 shows velocities ranging from a few centimetres per year to about one metre in the fastest areas (Figure 44). The slower areas are mainly found in the upper part of the rock glacier, where the terrain morphology is less steep, as well as in the more marginal areas, such as the eastern margin. The area between the two lobes, where the two lobes diverge, also shows velocities that do not exceed one decimetre per year. Unlike the other parts of the front, the lower part of the underlying front shows a coherent flow with very low velocities. This is synonymous with the relative stability of that area. In general, there is an increase in velocity as one moves down the rock glacier, and especially in the central part, velocities tend to be higher than in the margins. The front of the small west lobe (located longitudinally roughly in the centre of the rock glacier) shows slightly greater displacements than the surrounding area, between 20 and 30 cm·a^{-1}. The same displacements are found moving further west on the central body at approximately the

same height. Within a few tens of metres, there are major changes in velocity, with values ranging from 5-10 cm·a⁻¹ to around 30-40 cm·a⁻¹, especially in the area of the longitudinal crevasse in the centre. The steep area between the divergence zone connecting the central part to the west lobe is devoid of arrows as the terrain, being very steep, must have undergone major changes. The software was not able to calculate any displacement or wrong displacements were calculated and, therefore, eliminated. Only the lower part of the lobe, near the front, appears to have had a homogeneous and consistent movement over the last seven years, with velocity displacements of around 60-80 cm·a⁻¹. On the other hand, the east lobe was found to have had more or less consistent movement along its entire length, with values near the front being higher than the west lobe, i.e. between approximately 80 and 110 cm·a⁻¹. It is interesting to note that in much of the east front, as well as the west front, no values are present. This is synonymous with great instability, which is very visible with the presence of small channels and levees at the base of the front caused by the sliding/collapse of parts of the front. The same, although to a lesser extent, is also visible on the western margin. It should be noted that in the upper-west part of the rock glacier, there is an area where the directions of the vectors point towards the rock face. This is a depression that was probably caused by the presence of a glacier during the Little Ice Age (LIA) (Scapozza *et al*., 2014a).
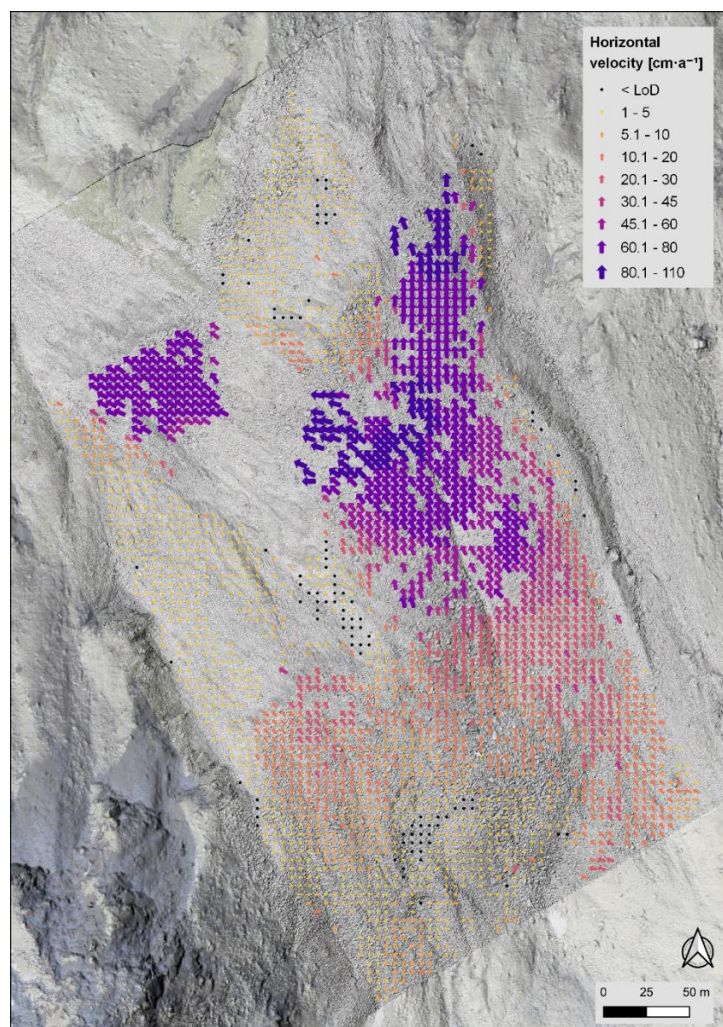
Figure 44: Horizontal velocities of the Stabbio di Largario rock glacier from 2016 to 2023 measured using CIAS software.

Piancabella

The Piancabella rock glacier shows great spatial heterogeneity in its velocity from 2016 to 2023 (Figure 45). The slowest parts are the eastern part of the lobe as well as the central western margin. The first part turns out to have velocities below the LoD. However, the adjacent parts of the lobe are rather slow, with maximum values of around 1-4 cm·a^{-1}. In that area, some vegetation indicates a substantial stability of the rock glacier. The central part of the western margin also shows displacement values of less than 4 cm·a^{-1}. The upper part of the rock glacier shows velocities varying between 10-17 cm·a^{-1} up to circumscribed areas with 25-34 cm·a^{-1}. Looking in detail, one can see that the slightly higher velocities in the upper part correspond to small lobes developed above the main body. Interestingly, a large part of the central sector flows with rather homogenous velocities of around 17-25 cm·a^{-1}. However, moving northwards, within a few tens of metres, there is a rapid change to very homogeneous velocities of 45-60 cm·a^{-1}, while moving north-eastwards, these velocities tend to decrease just as rapidly until they reach values close to 0. It is evident that there is an area where the measured velocities clearly outweigh all other values.
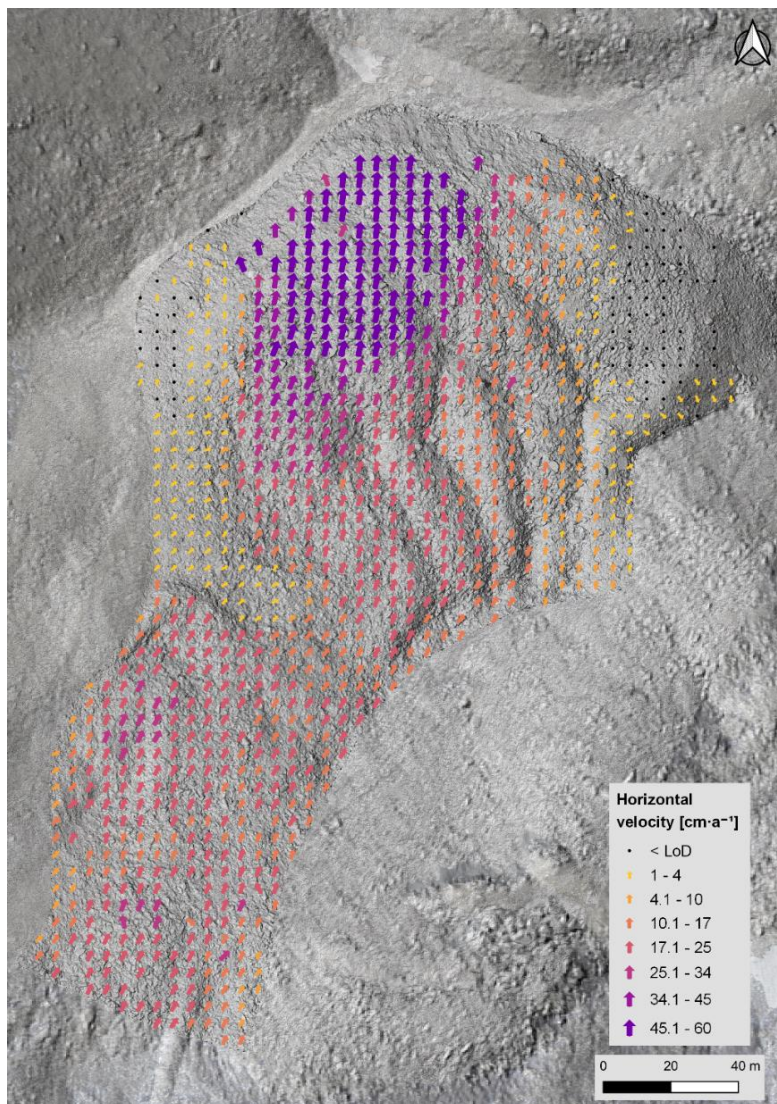
Figure 45: Horizontal velocities of the Piancabella rock glacier from 2016 to 2023 measured using CIAS software.

4.7 Inter-annual thickness changes and volume balances

In this chapter, the results of the thickness changes, in the form of 3D displacements, will be shown. They were obtained using the CloudCompare software and the M3C2 algorithm on the point clouds produced in 2023 and in 2016 for the Stabbio di Largario and Piancabella rock glaciers. In addition, an approximate volume balance was calculated from these values, which should be taken with great caution given the complexity of these geomorphological forms and their relative movement. In fact, over long timescales and especially in the part of the front, apparent volume gain could result from the latter advancing downstream, thus from the occupation of what was previously air by the rock glacier. On the other hand, apparent volume loss could result from the significant horizontal movement along a steep slope.

Stabbio di Largario

Figure 46 shows the M3C2 displacements, which essentially illustrate the thickness changes between the point clouds obtained in 2016 and early autumn 2023. It shows how most of the surface has subsided. The values range from -5 to -10 cm·a⁻¹ to over -30 cm·a⁻¹. It must be emphasised that many of them lie between about -5 and -15 cm·a⁻¹. There are also several areas where displacements are below the LoD of 4.5 cm·a⁻¹. For example, there appears to be a demarcated zone in the upper part where no significant thickness changes have occurred. The same can be said of much of the eastern margin and a small part of the east lobe. The most significant thickness loss values are near the front, especially in the east lobe, where they even exceed 30 cm·a⁻¹. This confirms what was already hypothesised in the description of Figure 44, i.e., a partial collapse of that part of the front, which caused a significant loss of material. Material that then descended further downstream, creating furrows and levees. The areas where thickness has increased are mainly at the foot of steeper parts and are mainly areas of accumulation of material that has slipped from those areas. An interesting area, however, is the one between the two lobes, where velocities already showed very low values over the 7 years. In that area, there seems to be a slight upward trend of about 5-10 cm·a⁻¹ (between 20-50 cm). The most significant uplift is seen at the foot of the western face and is caused by the deposition of eroded material. These thickness changes result in a net volume change of about 24'000 m³, resulting from a loss of about 31'000 m³ and a gain of about 7'000 m³.
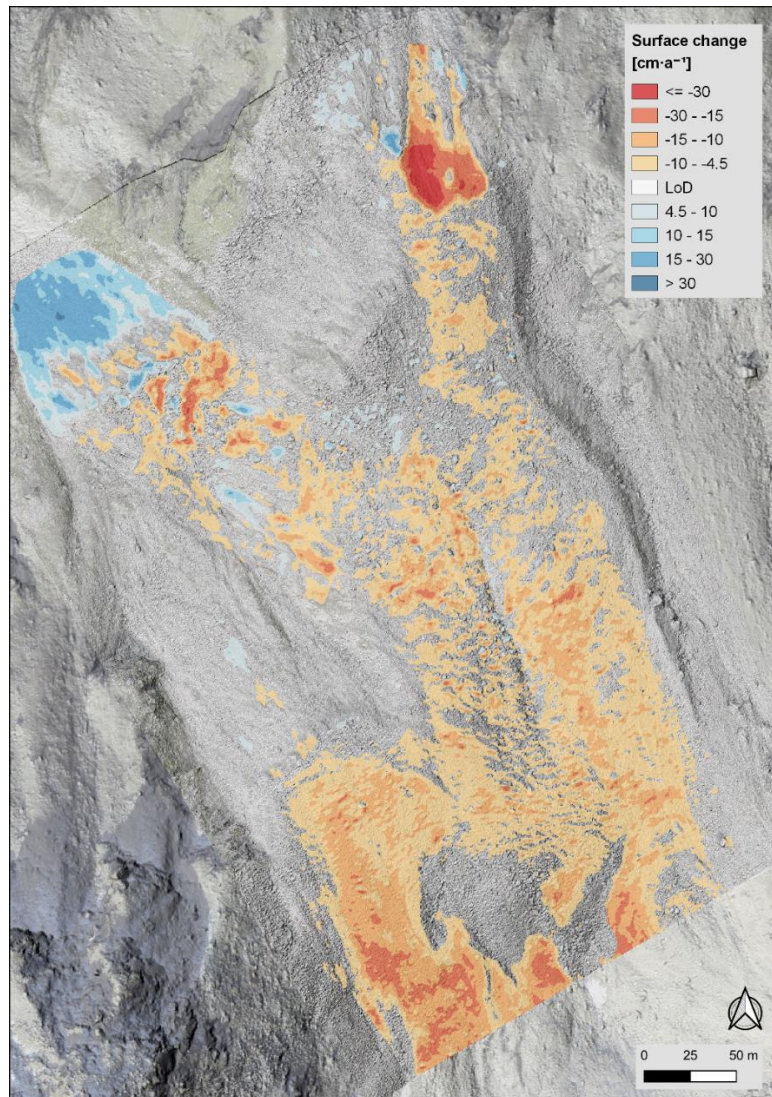
Figure 46: Thickness changes of the Stabbio di Largario rock glacier from 2016 to 2023 measured using the M3C2 algorithm.

Piancabella

The changes in the thickness of the Piancabella rock glacier between 2016 and 2023 are quite marked (Figure 47), especially in the central and northern parts of the front. In the central part, it can be seen that there is generally a loss in thickness of between -5 and -10 cm·a⁻¹. There is, however, a circumscribed zone, some 30 metres long, where the thickness loss values are decidedly higher and even exceed -20 cm·a⁻¹. In contrast, the northern part of the front shows an apparent increase in thickness, ranging from about 5 cm·a⁻¹ to more than 20 cm·a⁻¹. The values calculated for the upper part and the lateral margins are below the LoD of 4.5 cm·a⁻¹, so it cannot be said that there has been any change in thickness in those areas. The same applies to the eastern part of the lobe, near the front, where, as with the horizontal movements, vertical movements are also absent over the 7 years. Looking in more detail at the spatial patterns of the coloured areas, it appears that these follow the direction of the ridges and furrows. In fact, in a couple of places, a slight increase in

66

thickness can be seen at the front of the transverse ridges, while negative changes are predominantly found at the back of these ridges. This indicates the advance of the rock glacier especially in those areas.

Analysing these surface changes in detail through the approximate calculation of volume changes, it can be seen that the volume gain and loss are pretty similar over the 7 years, i.e. 2'100 m^3 and 3'000 m^3. This results in a net volume change of approximately -850 m^3.
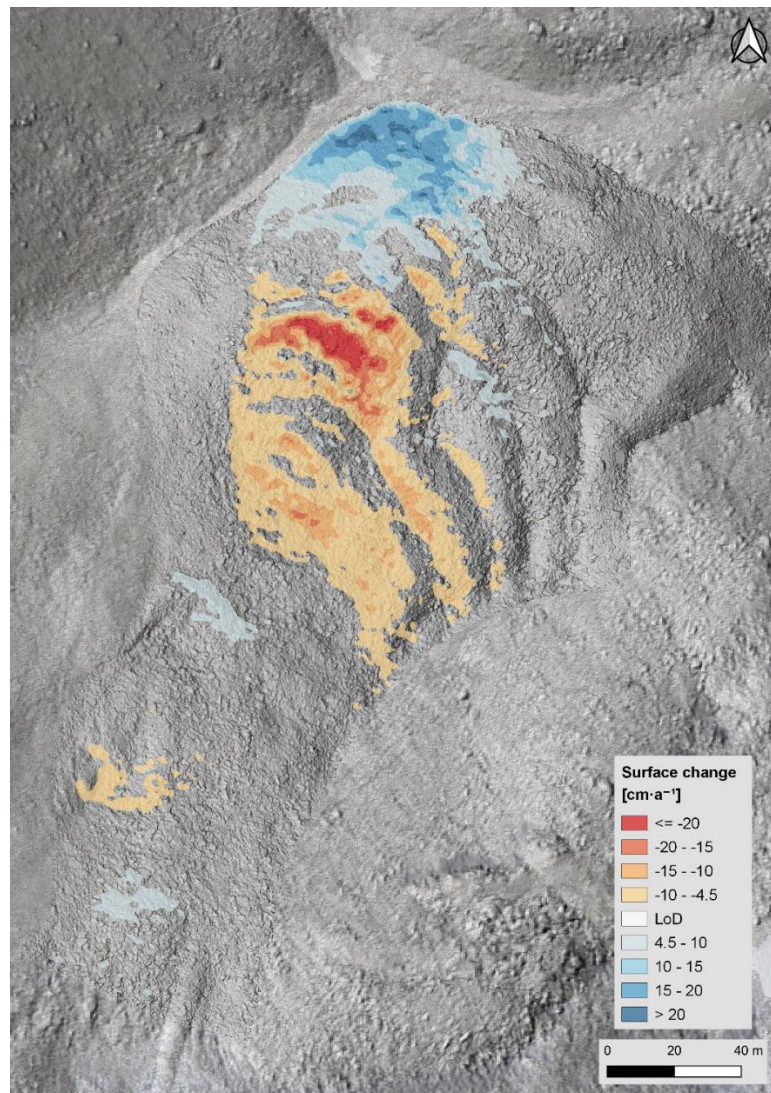
Figure 47: Thickness changes of the Piancabella rock glacier from 2016 to 2023 measured using the M3C2 algorithm.

4.8 Intra-annual horizontal velocities through image correlation

This chapter shows the results obtained through the image feature tracking algorithm performed by the CIAS software between the orthophotos created in the 2023 summer season for all four rock glaciers. In order to compare the results obtained for summer and early autumn, the displacements of the two periods were normalised, thus obtaining velocities expressed in cm·month^{-1}. The first figure of each rock glacier shows the horizontal velocities between the first and second drone surveys, i.e. between late June/early July and late

August. The second figure shows the horizontal velocities between the second and third drone survey, namely between late August and beginning/middle October. The displacements in the third figure have not been normalised, and therefore, it gives an idea of what the displacement rates were throughout the warm season. The fact that an intermediate survey was carried out around mid-summer made it possible to observe the sometimes important differences between the first and the second part of the summer.

Stabbio di Largario

In Figure 48, it can be clearly seen that this rock glacier has two distinct lobes in the lower part, as well as a third, smaller lobe located in the western part of the central area. The latter is characterised by the presence of a longitudinal furrow about a hundred metres long. The flow directions, which in the rooting zone and up to the central part are similar, split just near the end of the crevasse and the beginning of the two lobes, showing an interesting diffluence. In the rooting zone, the highest values are found in the part closest to the rock face, where the gradient is greatest. In that area, velocities also exceed 10 cm·month^{-1}. In the area with no displacement vectors at the end of June, there was still the presence of snow, as there is a basin (where a small glacier/snowfield was present during the LIA), and the displacements could not be calculated. Instead, the central part of the rock glacier shows rather little displacements, in many cases with very low velocities, approximately 1-2 cm·month^{-1}, with even several values below the LoD. However, some interesting areas show higher velocities than the surrounding area. This is, for example, the western part of the central area, where the third lobe is present, which shows velocities of up to 10 cm·month^{-1}. In addition, two small areas to the west and east of the crevasse also show rather high velocities between 4 and 10 cm·month^{-1}. The most interesting parts are the two lobes, east and west. The west one reaches velocities of up to 14 cm·month^{-1}, especially in the very steep part that connects it to the central part of the body. On the other hand, the front of the lobe shows smaller but more regular values over the entire area, ranging from 4-7 cm·month^{-1}, with slightly higher values near the front. The eastern lobe, on the other hand, shows a progressive increase in velocities as it approaches the front as well as from the margins towards the centre. It goes from 2-4 cm·month^{-1} to gradually reaching values of 7-10 cm·month^{-1} and even higher near the front. When comparing the two orthomosaics, it is interesting to note that the western part of the front has partially collapsed during between July and August, with the material being carried further downstream. For this reason, the displacement vectors are not present. The same applies to the western lobe, where various material was carried downstream and where snow persisted at the end of June (thus it was impossible to calculate displacements).
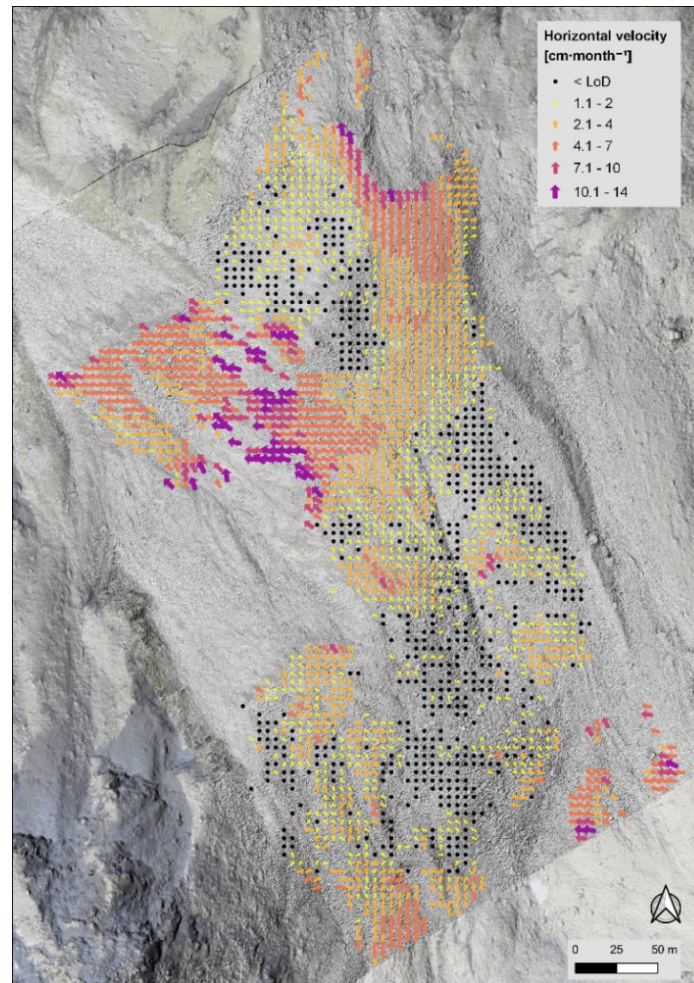
Figure 48: Horizontal velocities of the Stabbio di Largario rock glacier from 21.06.2023 to 31.08.2023 measured using CIAS software.

The second period (Figure 49), between 31 August and 12 October 2023, shows more homogenous velocities across the rock glacier, although important differences remain. Also in this case, the upper part of the rooting zone shows some rather high values. In the central part, the same areas described in Figure 48 are still slightly faster, with values of around 7-10 cm·month^{-1}. It is interesting to note that in the central part, at the beginning of the longitudinal furrow, the rock glacier shows velocities between 4 and 10 cm·month^{-1}, whereas in the previous period, the movement had been almost zero. As in the previous case, the two lobes show the highest velocities. This time, however, the east front shows more vectors with values around 10 to 14 cm·month^{-1} in the front area, while the west front shows values between 2 and 10 cm·month^{-1}. The steep part connecting the central part to the west lobe front remains very fast, with a good portion showing values of around 10-14 cm·month^{-1}.

Looking at the entire summer period (Figure 50), from 21 June to 12 October, one can see very clearly the consistency of the shifts and the most interesting areas seen above. The small lobe to the west of the central zone shows greater displacements, with values between about 15 and 25 cm. The same can be said for the two areas east and west of the longitudinal furrow, which show greater values than the surrounding areas.

The two lobes experienced the most significant displacements, up to about 50 cm. The western one has experienced the greatest displacements especially at the junction between the front and the central part, where the terrain is very steep. The eastern one, especially near the front, where the partial collapse and thus the removal of material could have caused an acceleration.
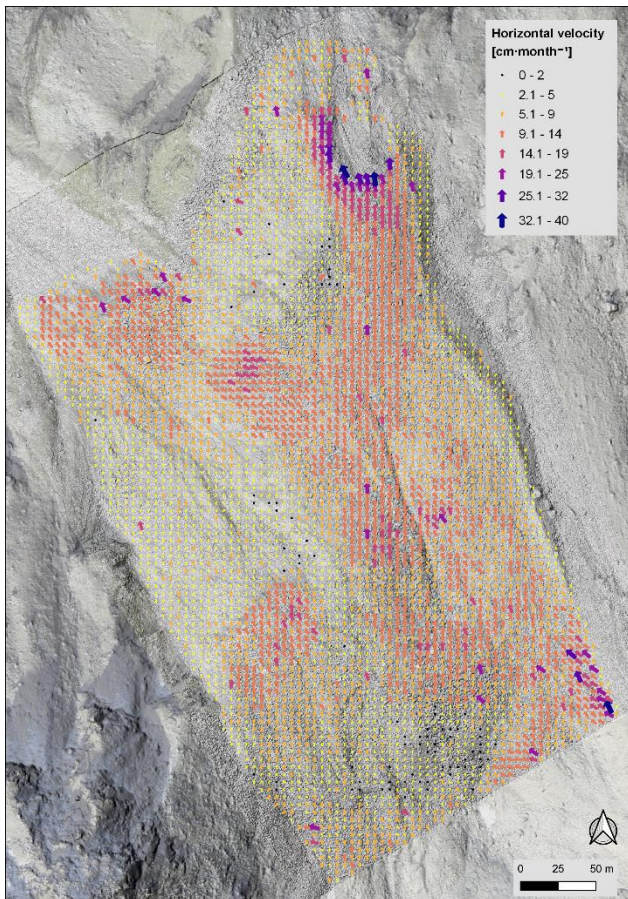
Figure 49: Horizontal velocities of the Stabbio di Largario rock glacier from 31.08.2023 to 12.10.2023 measured using CIAS software.
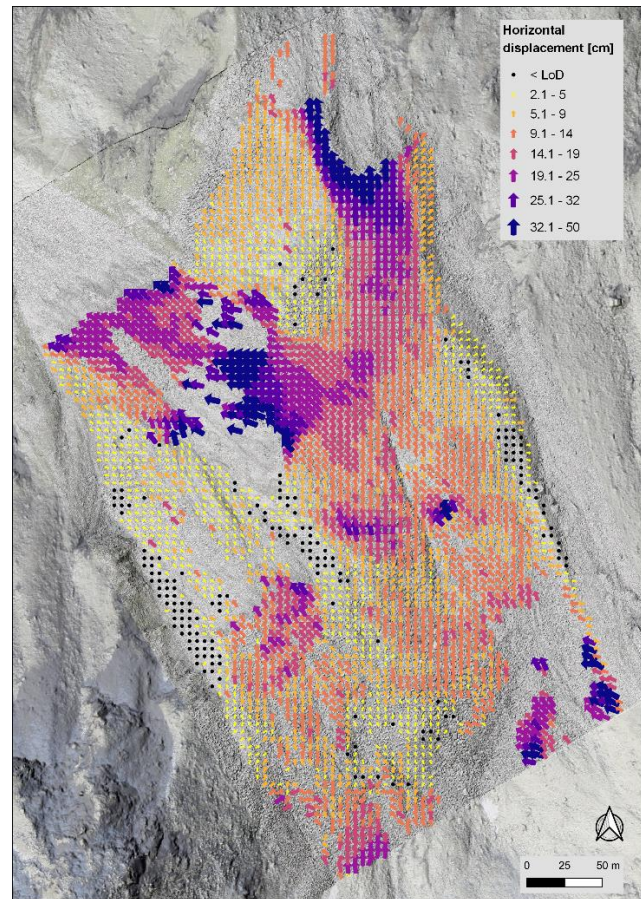
Figure 50: Total horizontal displacements of the Stabbio di Largario rock glacier from 21.06.2023 to 12.10.2023 measured using CIAS software.

Piancabella

Figure 51 shows the horizontal velocities of the Piancabella rock glacier between the end of June and August 2023, more precisely between 26 June and 24 August. Unlike Stabbio di Largario, this rock glacier shows several ridges and furrows, especially in the eastern part. The first part of the summer shows relatively low velocities (between 1 and 8 cm·month⁻¹), with many values below LoD. This means that many areas have not moved. This is the case in the rooting zone, the central part up to the eastern part of the front. Where displacements have been observed, the velocities do not exceed 2 cm·month⁻¹. The most interesting area is the northwest of the front, with significantly higher velocities and maximum values between 6 and 8 cm·month⁻¹ and 20 cm, and the entire area above 4 cm·month⁻¹.
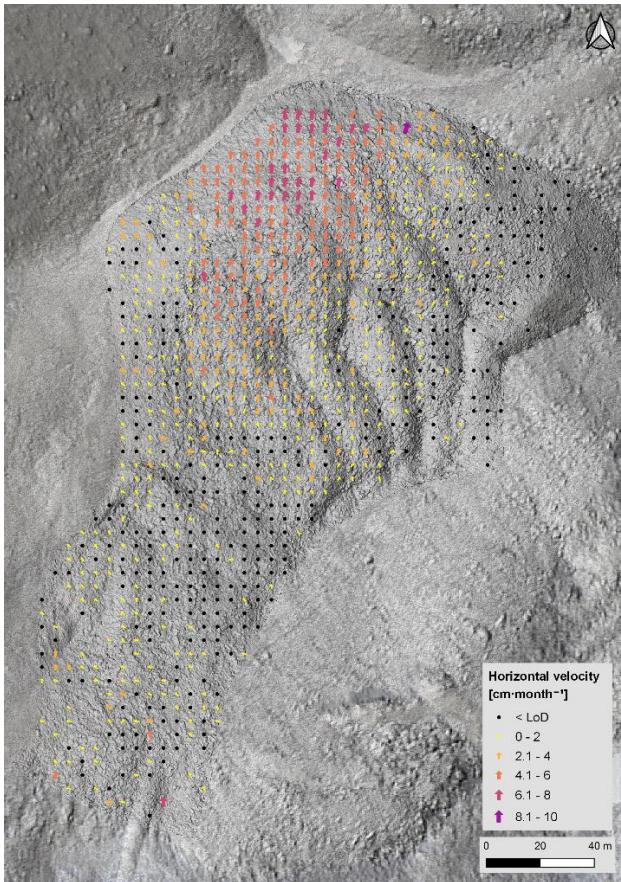
Figure 51: Horizontal velocities of the Piancabella rock glacier from 26.06.2023 to 24.08.2023 measured using CIAS software
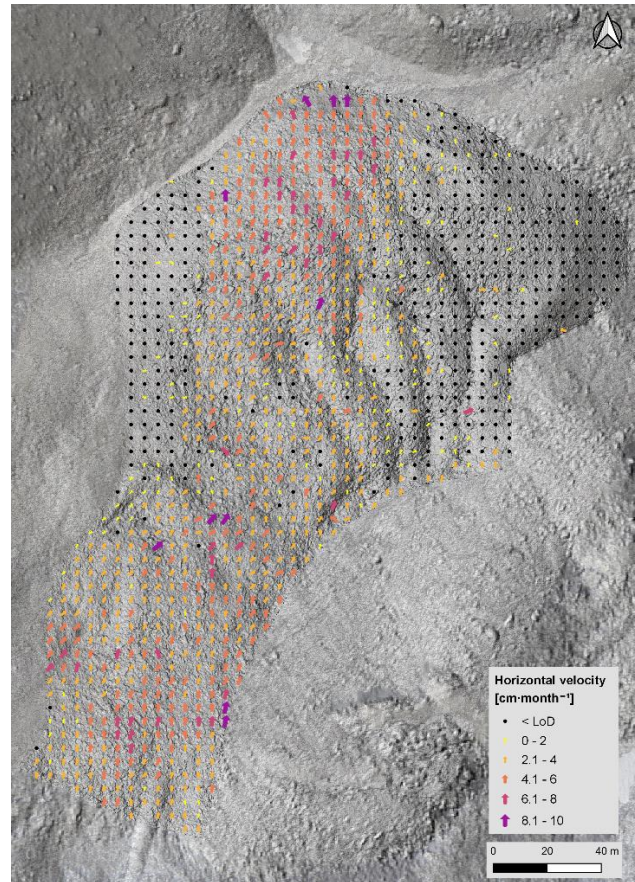
Figure 52: Horizontal velocities of the Piancabella rock glacier from 24.08.2023 to 05.10.2023 measured using CIAS software.

In the second period between 24 August and 5 October 2023 (Figure 52), the velocities measured in the fastest part of the lobe remained similar to those of the previous period. However, the velocities of the rooting zone and the central part increased significantly, with values averaging between 2 and 6 cm·month⁻¹. The western and eastern parts of the lobe, which were already almost stable in the previous period, did not show any significant movement. This could be the reason for the formation of ridges and furrows in the central part of the lobe. Figure 52 shows that there appears to be a central band that exhibits significantly higher velocities than the outermost edges.

The warm season from 26 June to 5 October 2023 confirms the trend seen in the two separate periods, i.e. greater displacements in the western part of the front of around 25 cm to values around 30 cm (Figure 53). In the rest of the rocky foreland, displacements are between 2 and 15 cm, with values below the LoD in the eastern part of the front and the western lateral margin in the central part. Comparing Figure 53 with Figure 45, which represents the displacements between 2016-2023, it can be stated that the areas with greater or lesser displacements match almost perfectly.
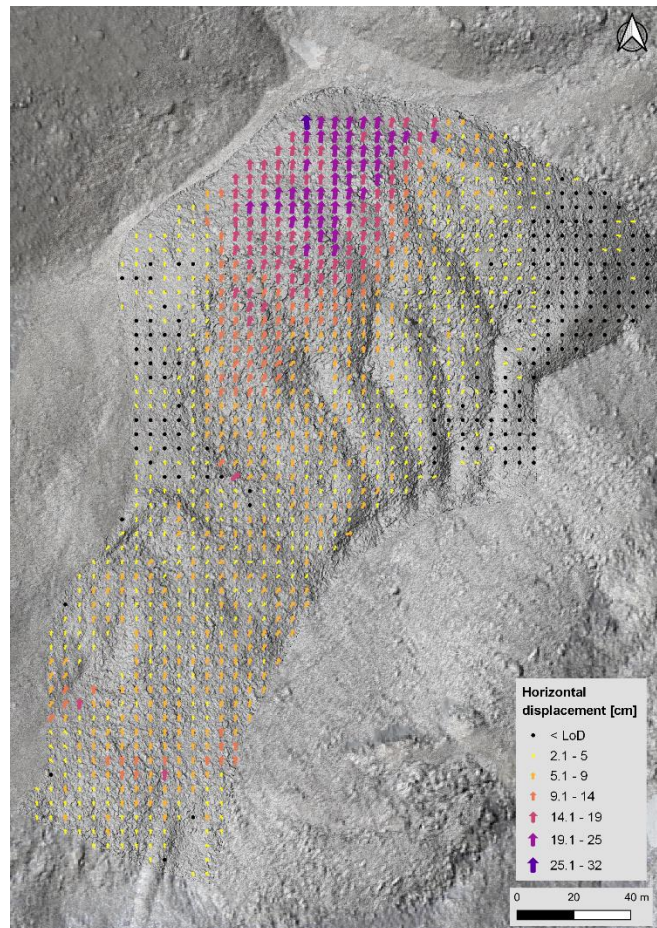
Figure 53: Total horizontal displacements of the Piancabella rock glacier from 26.06.2023 to 05.10.2023 measured using CIAS software.

Monte Prosa

Between the first and second survey, the rock glacier of Monte Prosa exhibits velocities between approximately 1 and 10 cm·month⁻¹ (Figure 54). Displacements are greatest in the rooting zone, as well as in the central part of the body near a longitudinal furrow and in the lower part before reaching the front. The lateral margins, especially the western ones, show rather low values, between 1-2 cm·month⁻¹, and several values below the LoD.

The period between 25 August and 3 October 2023 shows very similar velocities to the previous period (summer), with the fastest area still being the root, with values up to about 10 cm·month⁻¹ (Figure 55). The western edge has no vectors, as they were removed due to a random error resulting in contrary arrow directions. In general, the velocities recorded during this period do not show any clear patterns except for the upper part, somewhat like in the previous case.

Looking at the displacements over the summer season (Figure 56), between 10 July and 3 October (84 days), the trend of higher velocities in the rooting zone (up to 50-60 cm displacement) is confirmed, as well as in

the central part along the entire rock glacier (up to 20-25 cm). As already seen, especially in the first part of the summer, it is interesting to note that in the central part, there are a couple of circumscribed regions with slightly greater displacements than in the surrounding areas. It is also noticeable that the western margin tends to be slower, especially in the central part.
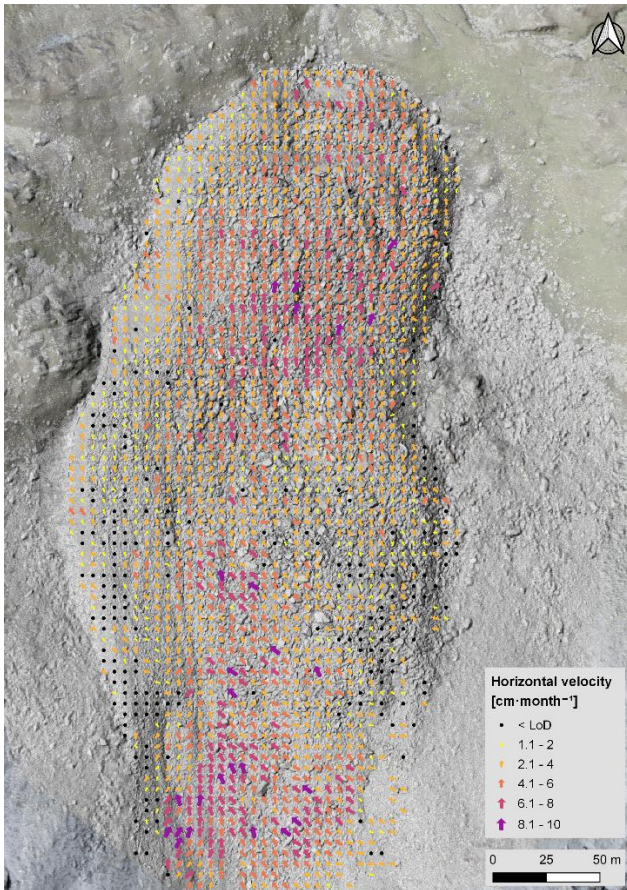
Figure 54: Horizontal velocities of the Monte Prosa rock glacier from 10.07.2023 to 25.08.2023 measured using CIAS software.
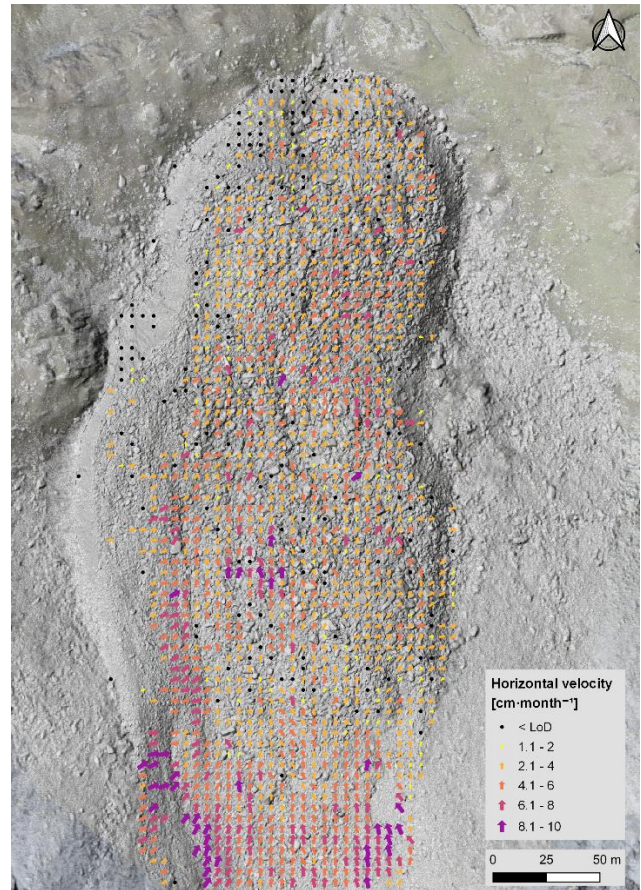
Figure 55: Horizontal velocities of the Monte Prosa rock glacier from 25.08.2023 to 03.10.2023 measured using CIAS software.
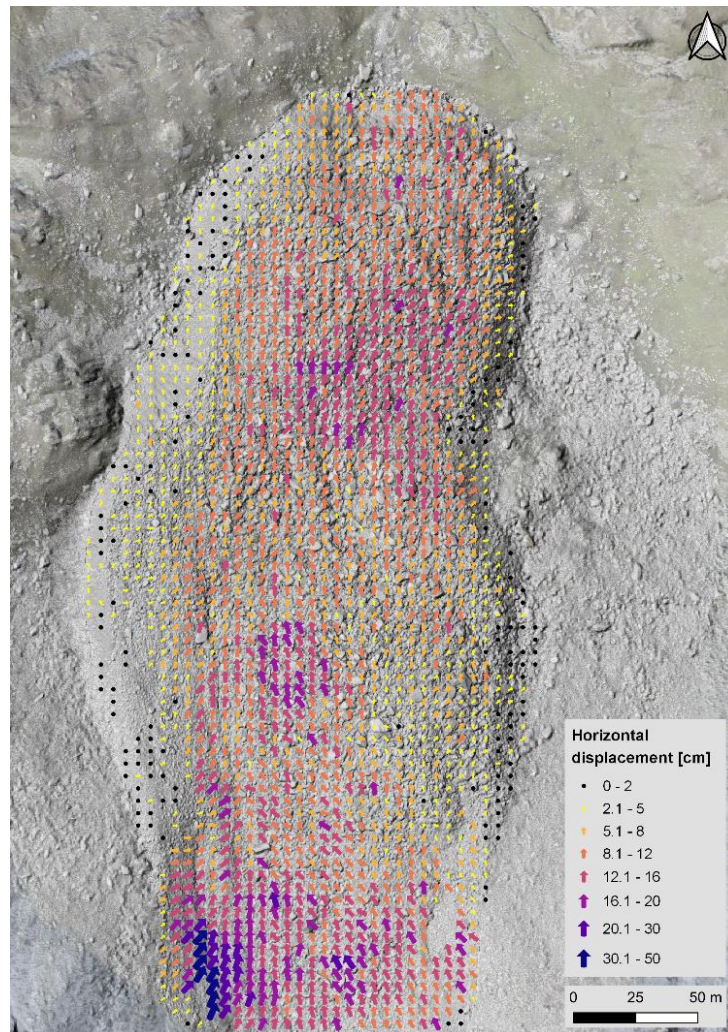
Figure 56: Total horizontal displacements of the Monte Prosa rock glacier from 10.07.2023 to 03.10.2023 measured using CIAS software.

Ganoni di Schenadüi

During the warm season, this rock glacier shows a very interesting trend. The period between 11 July and 1 September 2023 (51 days) shows large differences in velocity, with values between 1 and about 20 cm·month⁻¹. In the west margin in the central part and in the east lobe, the measured displacements remained below the LoD value (Figure 57). In the central part of the west lobe, velocities were also low, ranging between 1 and 4 cm·month⁻¹. On the other hand, it is interesting to note that in the lower part of the rooting zone and in the central part, there is an area with significantly greater displacements than the surrounding area, with velocities of around 8-10 cm·month⁻¹. The upper part of the rooting zone is also very fast, around 10-14 cm·month⁻¹, with values of up to 20 cm·month⁻¹. The mobile part of the eastern lobe, for the most part, shows velocities between 1 and 4 cm·month⁻¹.

The early autumn, i.e. from 1 September to 10 October, shows a decrease in the speed of the west lobe and an increase in that of the east lobe (Figure 58). In the front area, the central and left parts of the west lobe

are almost stationary, as is the entire western margin, with values often below LoD or only a few cm·month⁻¹. On the other hand, the right part of the west lobe shows almost unchanged velocities. Above all, the part of the east lobe front increases its speed, with values up to about 6-8 cm·month⁻¹. The central area, which previously differed significantly due to high velocities, shows slightly lower values (around 4-8 cm·month⁻¹), in line with the velocities of the entire central part. Again, the rooting zone records the highest velocities, in line with the previous period, between 10-20 cm·month⁻¹.

Looking at the entire summer period from 11 July to 10 October 2023, it can be seen that the fastest part was the rooting zone, with total displacement values of up to 50 cm (Figure 59). However, the central zone of the rock glacier was also relatively fast, with values of up to 25 cm. It can be seen that especially the front part of the east lobe has moved more than that of the west lobe. In addition, the right side of the west lobe was slightly faster than the left, with values of 5-9 cm and 2-5 cm, respectively. Together with the left part of the west lobe, the upper part of the east lobe was also slower, with most displacements between 2 and 5 cm.
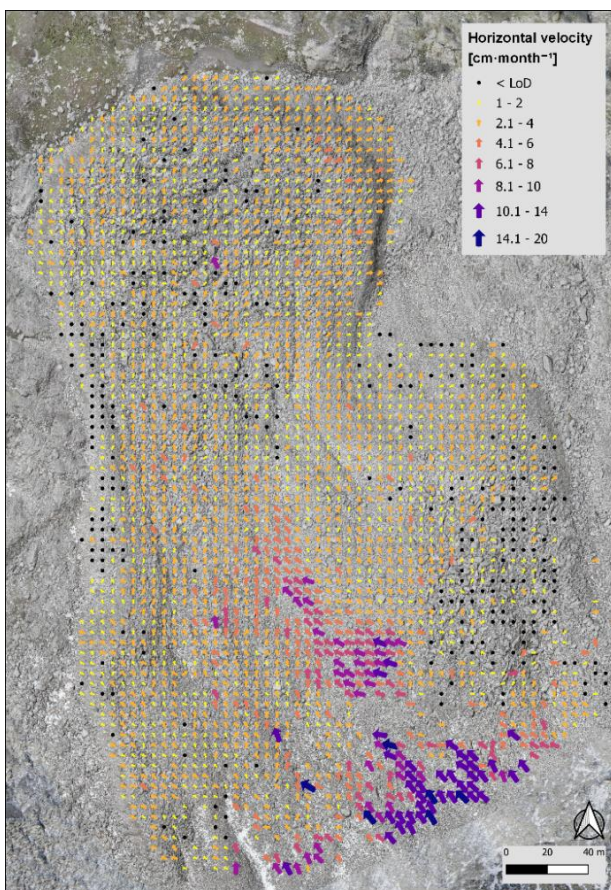
Figure 57: Horizontal velocities of the Ganoni di Schenadüi rock glacier from 11.07.2023 to 01.09.2023 measured using CIAS software.
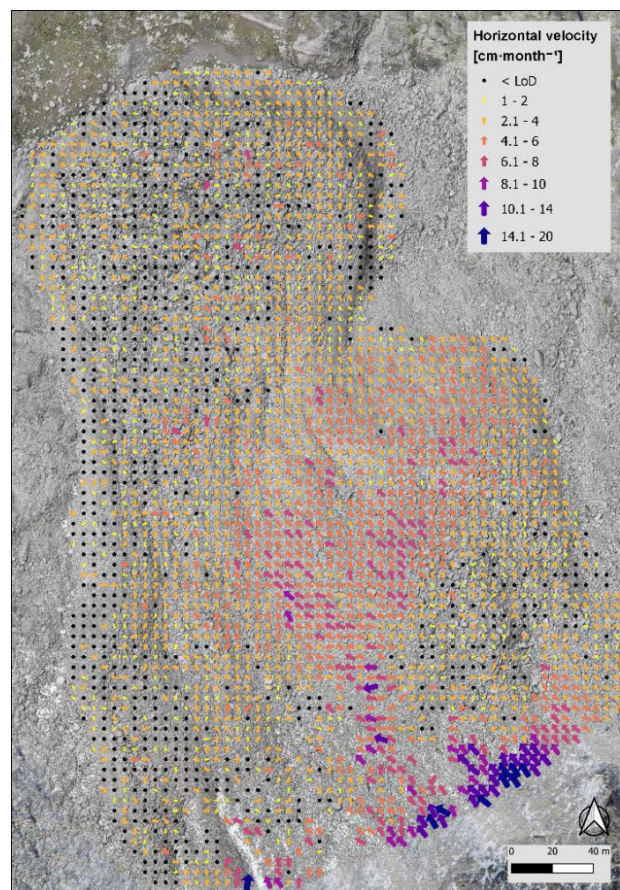
Figure 58: Horizontal velocities of the Ganoni di Schenadüi rock glacier from 01.09.2023 to 10.10.2023 measured using CIAS software.
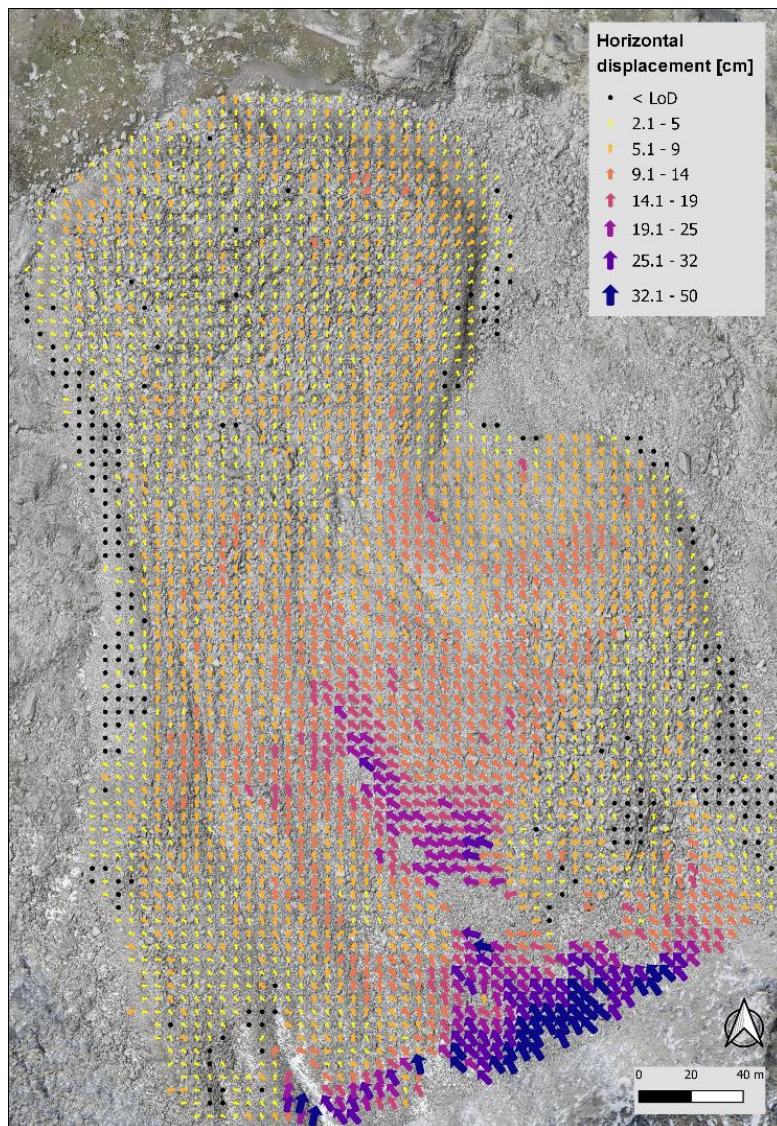
Figure 59: Total horizontal displacements of the Ganoni di Schenadüi rock glacier from 11.07.2023 to 10.10.2023 measured using CIAS software.

4.9   Intra-annual thickness changes and volume balances (2023)

This chapter shows the results of the thickness changes obtained using the CloudCompare software (algorithm M3C2) on the point clouds produced in summer 2023 for the four rock glaciers. In addition, approximate volume balances of the four rock glaciers and for all the periods ware calculated from these values and summarized in *Table* 9.

Table 9: Approximation of the volume changes of the four rock glaciers during summer 2023 derived using the M3C2 algorithm in CloudCompare.

Stabbio di Largario

	Volume gain (m³)	Volume loss (m³)	Net volume (m³)
Summer	1200	-4'600	-3'400
Early Autumn	100	-500	-400
Warm season	1000	-6'600	-5'600

Piancabella

	Volume gain (m³)	Volume loss (m³)	Net volume (m³)
Summer	20	-22	-1
Early Autumn	20	-10	11
Warm season	80	-50	33

Monte Prosa

	Volume gain (m³)	Volume loss (m³)	Net volume (m³)
Summer	62	-978	-917
Early Autumn	57	-610	-553
Warm season	119	-2'547	-2'428

Ganoni di Schenadüi

	Gain volume (m³)	Loss volume (m³)	Mass balance (m³)
Summer	17 ± 3	-590 ± 163	-573 ± 166
Early Autumn	6 ± 1	-99 ± 29	-93 ± 31
Warm season	19 ± 4	-1'185 ± 295	-1'165 ± 299

Stabbio di Largario

During summer, several areas of the rock glacier Stabbio di Largario underwent significant changes in thickness (Figure 60). Starting from the rooting zone, it can be seen that in parts of its western side, the thickness decreased between 3-10 cm·month^{-1}. Apart from that rather circumscribed area, there were no other changes in the upper part (note that some areas covered with snow at the end of June have been removed from this calculation). Two rather pronounced orange/red areas can be seen towards the central part, one on the front of the small western lobe, the second a little further down on the western margin. The surface subsidence in these areas appears to be several tens of cm·month^{-1}. Slightly further downstream, a blue zone is present in both cases, with accumulations of more than 30-50 cm·month^{-1}. This suggests rapid erosion of those areas, with consequent transport and deposition of material in the area below. Also on the west side, more precisely on the front of the west lobe, as in the previous case, material was removed (about 50 cm·month^{-1}) in some places and deposited a little further downstream. The probably most interesting part is the east lobe front, where there were large changes in thickness over the first two months of the summer. A good portion of the right side of the front collapsed and, as In the previous case, carried material further downstream. The thickness loss at this point is the greatest in the entire rock glacier, with values exceeding one metre per month in some places. The material transported downstream has created furrows that are more than 1 m deep along the front.

The second part of the summer shows a quiet situation, in which, unlike the first period, no major events significantly changed the thickness of the rock glacier surface (Figure 61). The areas with small losses in thickness (between -7 and -20 cm·month^{-1}) are found in the eastern part of the rooting zone and in the small lobe to the west. The area that had previously been the one with the most changes in thickness is still unstable, with erosion upstream and accumulation a little further downstream, albeit with much lower values.

Figure 62, which shows the sum of the two intra-seasonal periods, clearly emphasises the abovementioned areas. However, it can be seen that over the entire surface of the rock glacier, especially in its upper part and rooting zone, there is a slight tendency towards a decrease in thickness, between 7 and 20 cm. Again, for interpretation, it is important to know that the strange shapes visible in the upper part can be traced back to the polygons representing the snow patches present in the early summer, which were removed to calculate thickness changes.
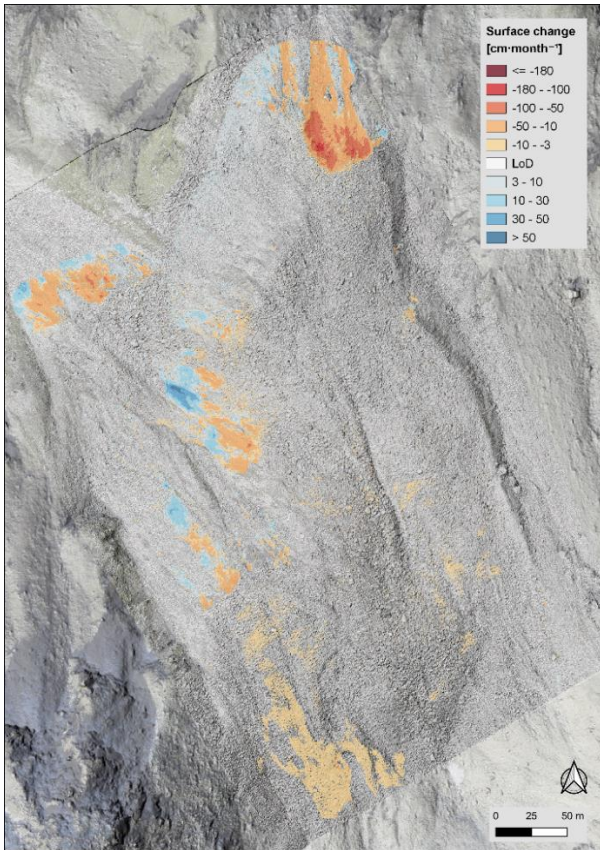
Figure 60: Thickness changes of the Stabbio di Largario rock glacier from 21.06.2023 to 31.08.2023 measured using the M3C2 algorithm.
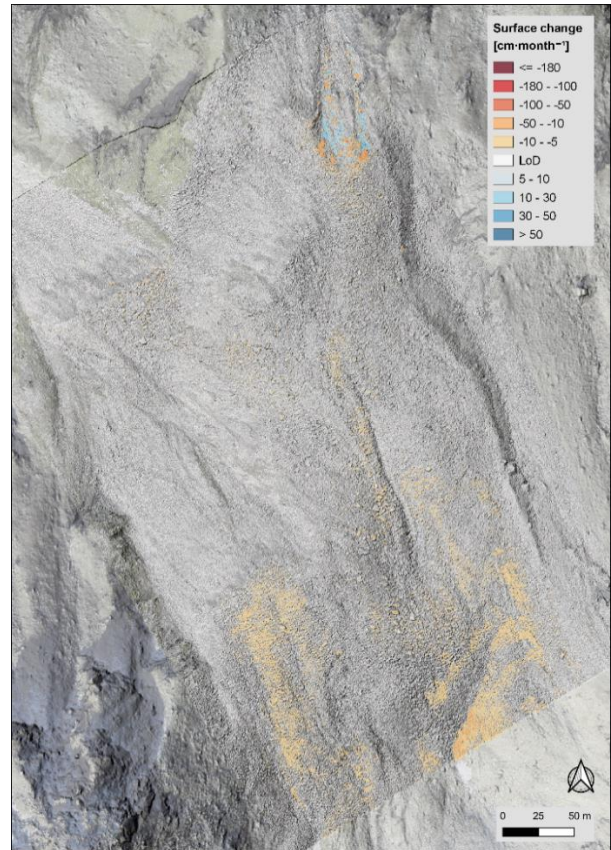
Figure 61: Thickness changes of the Stabbio di Largario rock glacier from 31.08.2023 to 12.10.2023 measured using the M3C2 algorithm.
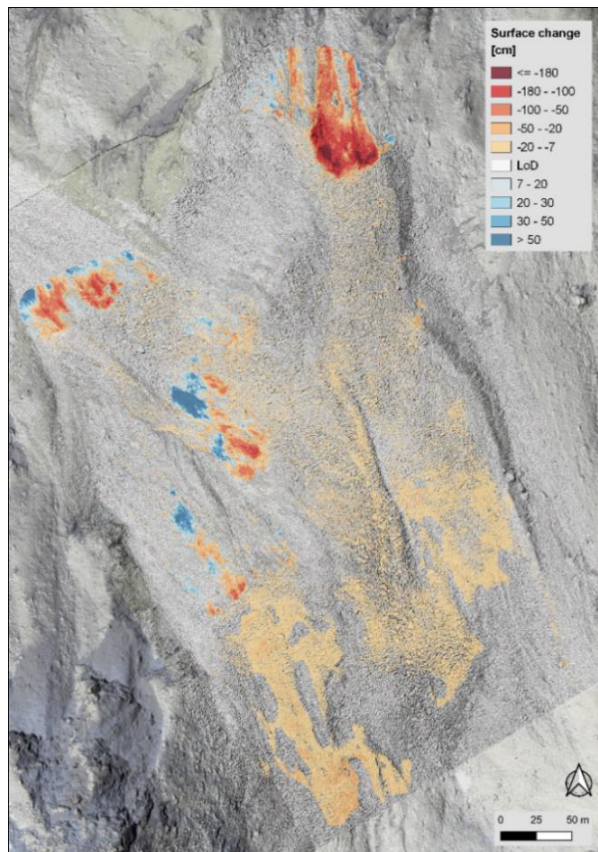
Figure 62: Thickness changes of the SDL rock glacier from 21.06.2023 to 12.10.2023 measured using the M3C2 algorithm.

Piancabella

In contrast to the rock glacier of Stabbio di Largario, the vertical displacements of Piancabella were similar throughout the summer. Starting with the first period, i.e. between 26 June and 24 August, it can be seen that thickness changes are practically absent (Figure 63). The only three points with significant changes are on the front and refer to minor episodes of collapse, with the material detached and deposited a few metres further down. In the second period (Figure 64), the situation does not change; practically all the calculated values are below the LoD, i.e., below 3 cm·month^{-1}.

Adding up the two periods gives the result of Figure 64, where, although still very limited, a couple of interesting areas can be glimpsed, with significant changes over the summer period between 26 June and 5 October. These are the same zones already seen in the calculation of vertical shifts between 2016 and 2023, namely the northern part of the front and an area of the central part of the lobe. In the former, there are increases in thickness of around 10 cm; in the latter, there is a decrease in thickness of around 10 cm.
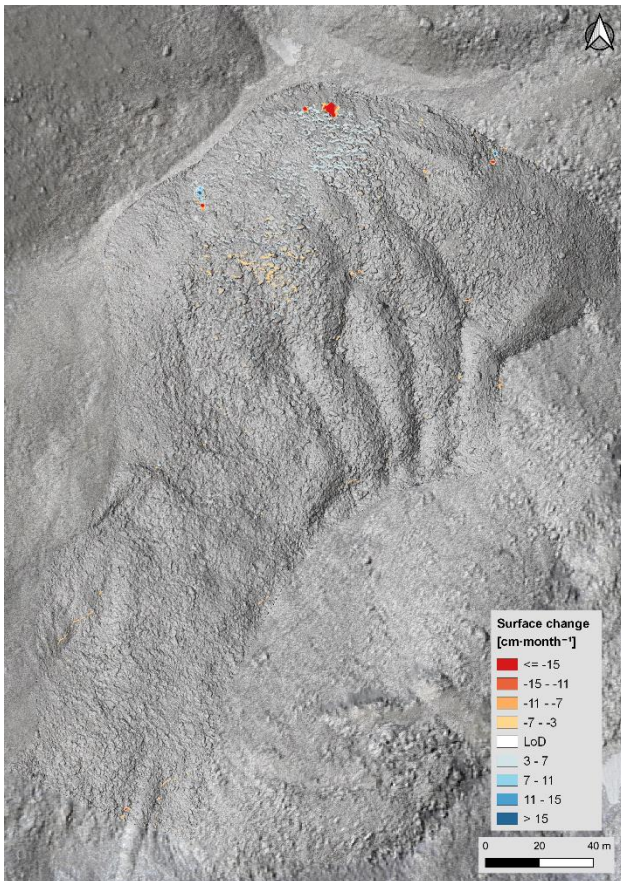
Figure 63: Thickness changes of the Piancabella rock glacier from 26.06.2023 to 24.08.2023 measured using the M3C2 algorithm.
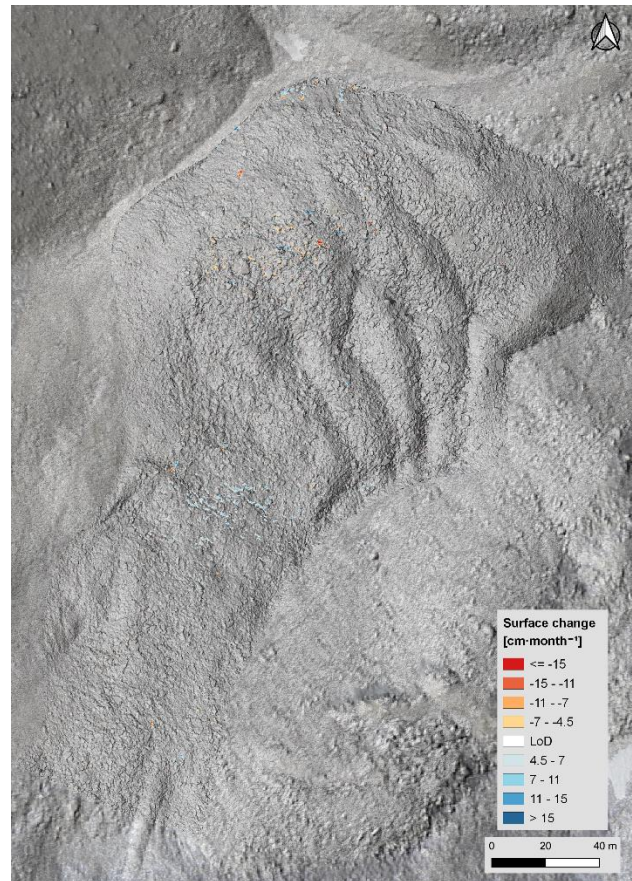
Figure 64: Thickness changes of the Piancabella rock glacier from 24.08.2023 to 05.10.2023 measured using the M3C2 algorithm.
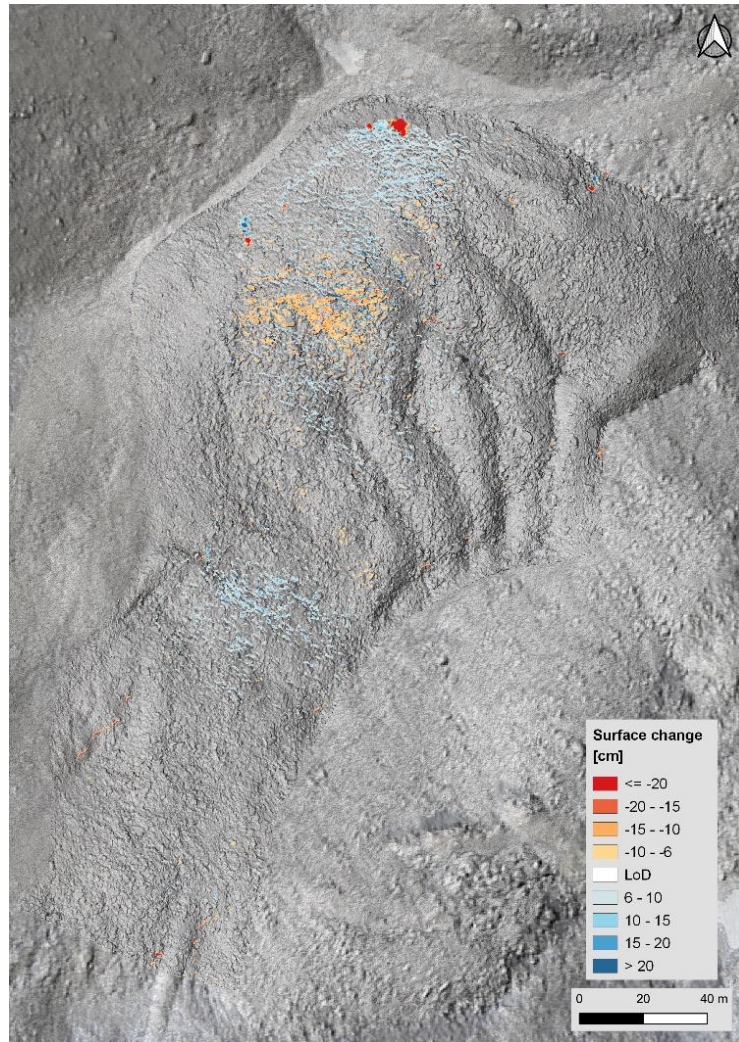
Figure 65: Thickness changes of the Piancabella rock glacier from 26.06.2023 to 05.10.2023 measured using the M3C2 algorithm.

Monte Prosa

The Monte Prosa rock glacier represents a very interesting case regarding the changes in thickness that occurred in the summer of 2023. In the 45 days between the first and second survey, the thickness of the front, as well as the central part of the rock glacier, remained unchanged (Figure 66). The only area with significant changes in thickness was the upper and rooting zone. Observing in more detail, it can be seen that in a small area near a topographic concavity, the thinning of the surface was greater than in the rest of the area, with values even exceeding -20 cm·month⁻¹.

The following period also showed similar behaviour in the same areas but with a smaller reduction in thickness, to around -16 and -20 cm·month⁻¹ (Figure 67).

The entire summer showed, as before, a very pronounced zone of thickness decrease, with values up to about -50 cm, which continues along the right side of the concavity until it reaches the central part of the rock glacier (Figure 68). Interestingly, there were hardly any significant changes in thickness below the middle of

the body during the three summer months. The only changes were those visible through the red and blue patches on the front, caused by the fall of a few boulders during the summer. This result, therefore, shows a clear difference between the middle and lower parts of the rock glacier, which are essentially stable in terms of vertical displacements, in comparison to the upper part and the rooting zone, which are much more dynamic with changes in thickness up to about -50 cm in the centre of the concavity that extends from the rooting zone to the middle part of the body. These thickness changes led to probable volume changes visible in , with a net volume over the entire summer of about -2'400 m^3.
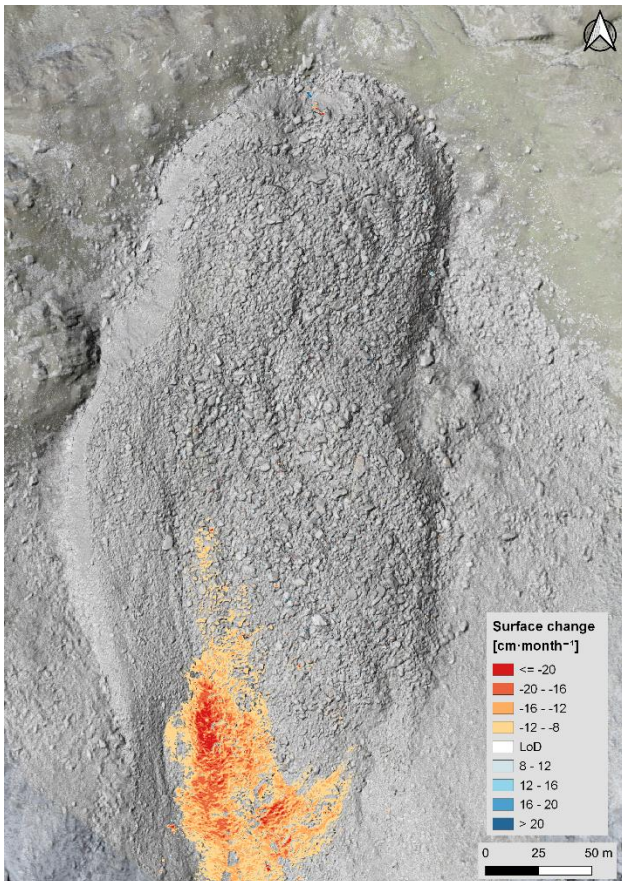
Figure 66: Thickness changes of the Monte Prosa rock glacier from 10.07.2023 to 25.08.2023 measured using the M3C2 algorithm.
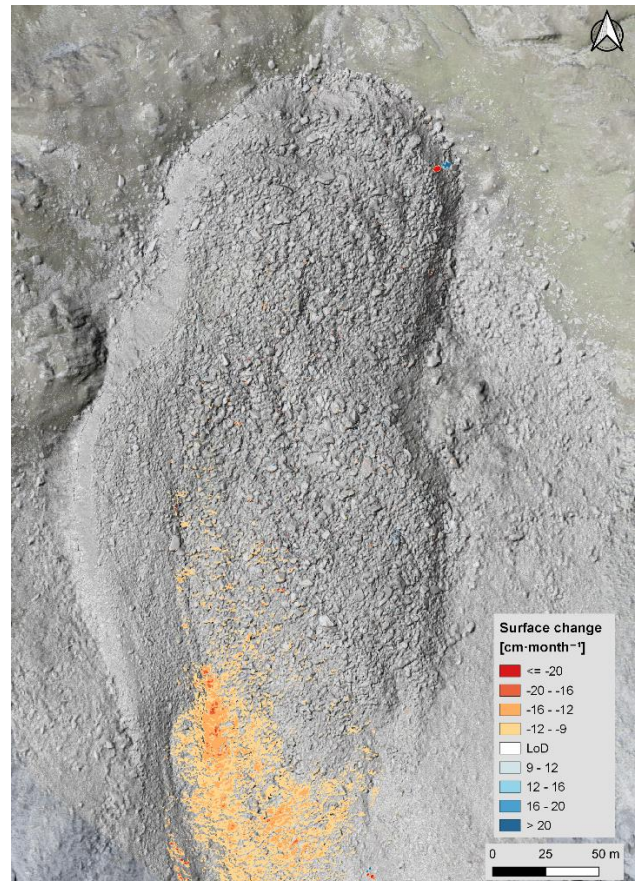
Figure 67: Thickness changes of the Monte Prosa rock glacier from 25.08.2023 to 03.10.2023 measured using the M3C2 algorithm.
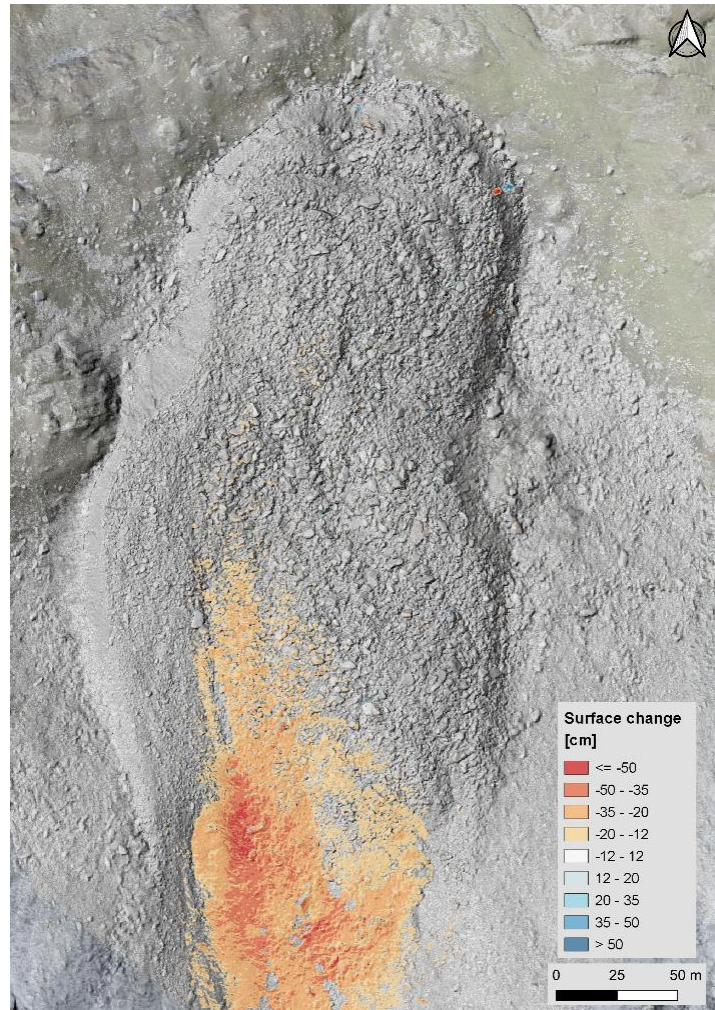
Figure 68: Thickness changes of the Monte Prosa rock glacier from 10.07.2023 to 03.10.2023 measured using the M3C2 algorithm.

Ganoni di Schenadüi

The behaviour of the Ganoni di Schenadüi rock glacier in Schenadüi is partly reminiscent of the behaviour of the Monte Prosa rock glacier in terms of thickness change. In the first part of the season, the greatest changes seemed to occur, especially in the rooting zone and the upper part, with reductions in thickness of between -7.5 and -16 cm·month^{-1} (Figure 69). There were no substantial changes in the lower part. The only exception is the fall of a boulder on the west side of the front, clearly visible through the two red and blue spots. In the upper part, the areas that were covered by snow during the first survey were removed.

The period between the beginning of September and mid-October shows a stable situation (Figure 70), where only a tiny portion of the upper part shows a decrease in thickness between 6-12 cm·month^{-1}.
Figure 71, representing the period between the first and the third survey shows what has already been stated above, with a thinning of 25 and 40 cm in the rooting zone, which continues in a small portion of the central part with values of up to approximately -25 cm.
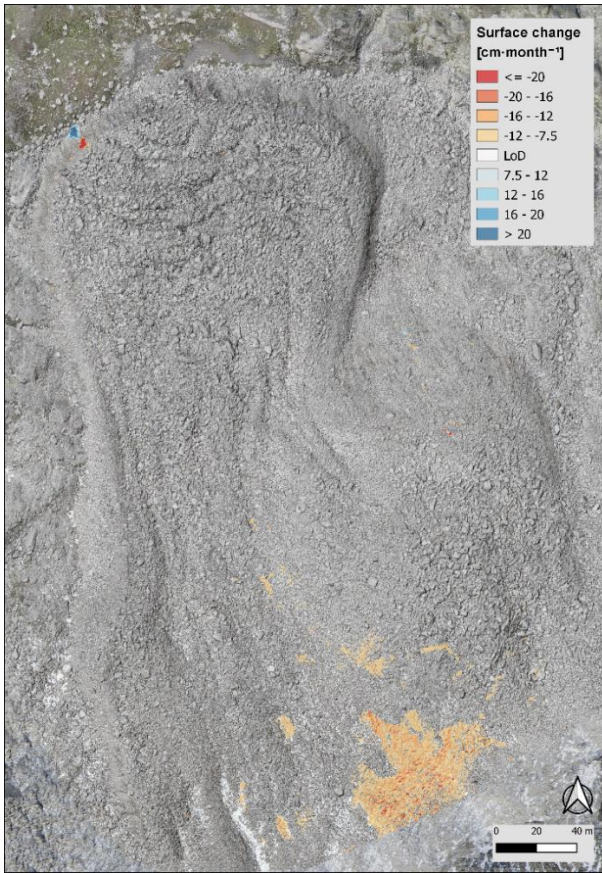
Figure 69: Thickness changes of the Ganoni di Schenadüi rock glacier from 11.07.2023 to 01.09.2023 measured using the M3C2 algorithm.
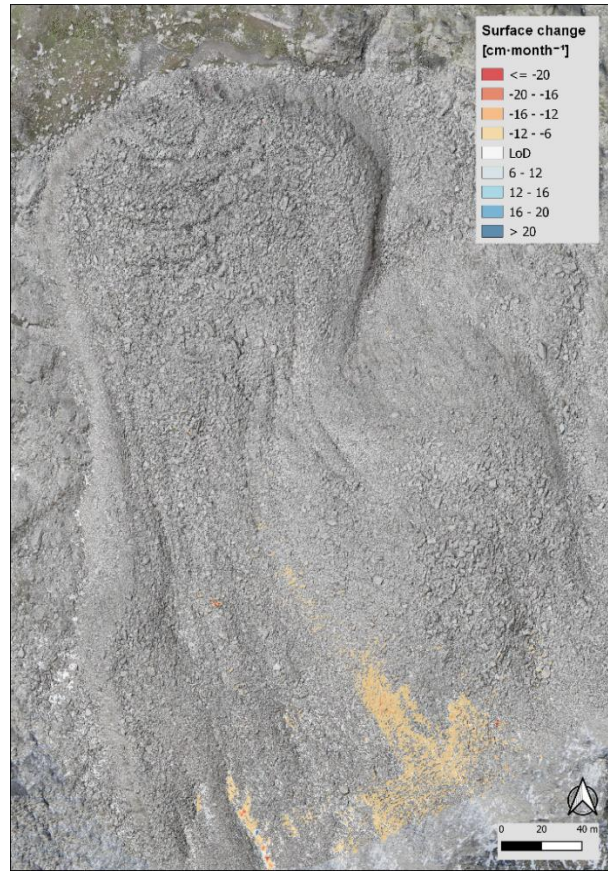
Figure 70: Thickness changes of the Ganoni di Schenadüi rock glacier from 01.09.2023 to 10.10.2023 measured using the M3C2 algorithm.
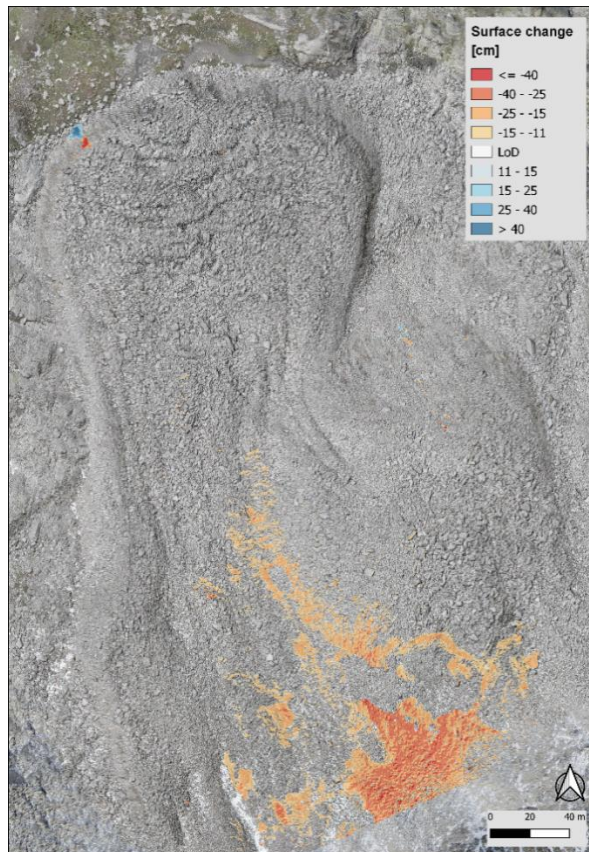
Figure 71: Thickness changes of the GA rock glacier from 11.07.2023 to 10.10.2023 measured using the M3C2 algorithm.

84

5 Discussion

5.1 Inter-annual kinematics

In recent decades, a large number of studies have analysed and monitored the kinematics of many rock glaciers scattered throughout the Alps (Scapozza *et al.*, 2014a; Cusicanqui *et al.*, 2021; Kaufmann *et al.*, 2021; Gärtner-Roer *et al.*, 2022; Kellerer-Pirklbauer *et al.*, 2024). The results showed that, since the early 1990s, there has been a significant acceleration in the horizontal velocities of active rock glaciers on the European continent (Haberkorn *et al.*, 2021; Roer *et al.*, 2008). Such acceleration has also been documented for the rock glacier Stabbio di Largario (Scapozza et al., 2014a). This long-term change in kinematics was mainly caused by two factors: environmental changes (such as temperature increase) that led to a degradation of the permafrost (Ikeda, 2004; Kellerer-Pirklbauer *et al.*, 2024) and an increase in the amount of water from precipitation, snowmelt and ground ice (Roer *et al.*, 2008). As already seen, these factors are directly linked to the two known processes that lead to the deformation of rock glaciers. The first is shearing, which occurs mainly at depth in the so-called shear horizon, while the second is the plastic deformation within the body of the rock glacier due to the viscosity of the material (permafrost ice) of which it is partially composed. As Harbor (1997) argued, the shearing process is influenced by the supply of water as well as its pressure, which controls the frictional resistance in the shear horizon. On the other hand, the plastic deformation that occurs within the body depends mainly on the mechanical characteristics of the ice contained within it. An increase in temperature can cause important changes in viscosity and hardness and the shear and crush resistance of polycrystalline ice (Arenson & Springman, 2005). This can lead to an acceleration of the rock glacier. The theory that the shearing process is mainly controlled by water input is also confirmed by stratigraphic data from a borehole of the Ritigraben rock glacier in a study by Kenner *et al.* (2017) in which it is shown that the shear horizon is located in a very wet transition zone between the frozen body of the rock glacier and the unfrozen part below, containing different water horizons. The authors, therefore, hypothesise that it is a partially water-saturated continuum between the ice-rich permafrost and the ice-free rock debris. The climate change-induced increase in temperature not only warms the permafrost body but is also responsible for the increasingly late freezing of the active layer in the early winter as well as increasingly early snowmelt in the spring period (Haberkorn *et al.*, 2021), thereby increasing the period in which water can reach the shear horizon. The long-term acceleration observed in recent decades, however, seems to be due not so much to the amount of water entering the system but rather to the efficiency with which water manages to reach the shear horizon (base flow) rather than running off along the permafrost table (quick flow) (Haberkorn *et al.*, 2021; Kenner *et al.*, 2017; Kenner *et al.*, 2019). The flow of water is controlled by the development of channels within the rock glacier. The fact that permafrost is approaching 0°C is synonymous with greater ice plasticity,

but it also means the development of more runoff channels towards the shear horizon. This could increase base flow at the expense of quick flow (Kenner *et al.*, 2019).

As already reported in several reports on permafrost in the Ticino Alps (Scapozza *et al.*, 2020, 2018), the relationship between velocity of rock glaciers and MAGST trend is also very clear, reflecting atmospheric temperature variations, but also snow cover variations such as thickness and duration, ground surface characteristics and subsurface heat transfer processes. This relationship was very well observed during the positive MAGST temperature anomalies recorded in 2015, 2019 and 2020, which led to an increase in the horizontal velocity of all monitored rock glaciers in those years.

The effect of water, as well as the warming of the land surface, also seems to influence the properties of ice and debris mixtures. In fact, it was noted that 2015 and 2019, in addition to being very warm, were the two years with the largest water stock of the entire decade (Scapozza *et al.*, 2020). However, given the complexity of the mechanisms and the absence of information on the internal composition of Ticino's rock glaciers, it is difficult to draw conclusions.

The two rapid decelerations observed following the velocity peaks of 2015 and 2019-2020, which continued into 2023, would appear to be due to falling ground surface temperatures during those periods (Kellerer-pirklbauer *et al.*, 2024). The cause of this decrease is the low autumn and winter precipitation, which allowed the soil to cool down significantly compared to years with abundant precipitation. Hanson and Hoelzle (2004) and Luetschg *et al.* (2008) argue that, depending on the roughness of the surface, a snow cover of at least 0.6-0.8 m is required to thermally isolate the active layer from the atmosphere. Looking at winter 2022-2023 (Figure 22), for example, we see that the snow cover was practically absent until the beginning of December and then settled right around 0.5-0.6 m. Only in late winter and for a short-time period did the coverage increase slightly, which was too late to allow good insulation from the atmosphere.

However, it seems clear that the increase in the temperature of the permafrost body has as a consequence not only the alteration of the rheology of the ice but also a change in the ratio of debris to ice, where the latter sees a decrease in its volume to make room for air and water in liquid form (Scapozza *et al.*, 2015). The changes within the rock glacier body cause a spatially heterogeneous alteration of viscosity as the effects of ice melt are not uniform but vary depending on the amount of ice as well as the slope of the rock glacier (Arenson & Springman, 2005; Müller *et al.*, 2016).

5.2 Intra-annual horizontal velocity variations

5.2.1 General trend

The results from GNSS measurements clearly show variations in horizontal velocities depending on the time of the year. Such seasonal differences have already been observed in several studies and show an acceleration in summer, with peak speeds reached between autumn and early winter, as well as a deceleration leading to a minimum speed in late spring (Delaloye *et al.*, 2010; Wirz *et al.*, 2016). It has also been shown how the seasonal velocity signal, depending on the rock glacier, can show a time lag of up to several months with respect to peak air and ground temperatures. This is because the temperature signal needs time to propagate within the permafrost cover (Haeberli *et al.*, 2006; Kääb *et al.*, 2007). However, confirming what has already been discussed above, Cicoira *et al.* (2019b) and Wirz *et al.* (2016) showed that the sole influence of temperature through heat conduction on rheology cannot explain the seasonal and inter-annual changes observed in reality. They indicate that the short- to mid-term velocity changes of rock glacier flow can only be explained by the advection of surface water into the glacier and its interaction over pore-water pressure with the creep rheology. Furthermore, Kenner *et al.* (2020) showed how the acceleration of the rock glacier they studied during the spring period occurred when the ground surface temperatures were still decreasing. In addition, they saw how the snow water equivalent in spring showed no significant effect on the magnitude of the acceleration, while the sum of summer precipitation had a barely considerable influence on the movements of the rock glacier. This would confirm the theory of the importance of the amount of water that reaches the shear horizon, thus the importance of base flow, as opposed to quick flow.

Seasonal velocity fluctuations can be high, up to and exceeding 50% of the annual average (Delaloye *et al.*, 2010). The results of this thesis show that warm season velocities are indeed higher than annual ones. The values for the reference points of all four rock glaciers over the entire summer are roughly between +30% and +50% of the annual velocities. However, taking summer and early autumn individually, it is interesting to note how these velocities differ. In fact, during the summer, the median value of the horizontal velocities is +70% compared to the annual value. However, the large standard deviation indicates a large difference between the values. Taking the median value of +22%, the result still shows the higher speeds of the summer compared to the annual ones. The early autumn period, which reflects the September and early October movements, shows an increase in horizontal velocity compared to the previous period, with a median value of +75%. What has been discussed is also confirmed by the statistical tests on the differences in velocity between the different periods (Chapter 4.3), in which a significant difference was found between summer and early autumn. This is in line with other studies (Wirz *et al.*, 2016; Kenner *et al.*, 2017; Ulrich *et al.*, 2021), which have shown a clear seasonal pattern in the horizontal velocities, with the peak reached between August and January, i.e. in the period between the second and third survey until late winter. The cold season, with

the average value of the seasonal to annual velocity ratio of -3%, suggests a slight decrease in velocity during this period. However, it must be carefully evaluated, considering it is a nine-month period, i.e. between the measurements in September 2022 and those at the end of June/beginning of July 2023. Following what has already been discussed, what is observed is, therefore, an average between the usually high-velocity values in the autumn and early winter months and the lower values measured in late spring, before the onset of snowmelt. However, it is remarkable the fact that there is no significant difference between cold season and summer velocities, although there is an apparent trend of increasing speed.

What is noticeable when looking at the deviation between the seasonal and annual velocity ratios (Figure 32) is how the standard deviations are clearly more significant at the points where the velocities are lower. This is undoubtedly due to the fact that the measured movements are normalised over the entire year. This means that even just 1 cm of error (about the instrument's accuracy) in the measurement of the coordinates can lead to significant deviations when comparing the velocities over the whole year. The points particularly affected by this 'problem' are those that move below about 10 cm annually. As one moves towards greater movements, the ratio deviation also decreases almost exponentially.

5.2.2 Within and between rock glaciers

Seasonal fluctuations do not always occur simultaneously for all rock glaciers (Delaloye *et al*., 2010). The results of this thesis also confirm this point. Observing the summer period, the velocities of Stabbio di Largario are below the annual ones. Comparing this period with the cold season, however, there is no statistically significant difference, although there does appear to be a slight slowing trend in summer. The substantial increase in velocity measured in early autumn suggests a general seasonal increase in velocity that is progressive and delayed in time, as also observed in the case of the Muragl rock glacier (Delaloye *et al*., 2010). Interestingly, the two lobes show different seasonal contributions. The fact that the west lobe shows a lower contribution during the early autumn and a higher one during the cold season would suggest a slower reaction than the other lobe. In fact, the latter sees a threefold increase in early autumn speed compared to the previous period, while the west lobe only doubles. Possible causes could be the different ice content, the slope of the bedrock, or the fact that the west lobe is almost separated from the rest of the body, with a very uniform sliding movement rather than creeping, interpretable as a translational slide over a shear horizon (like a debris slide *sensu* Varnes, 1978), containing ice. Without the help of geophysical information, however, it is difficult to interpret these differences. In general, despite the slightly lower altitude compared to the other three sites, this could be a rock glacier still containing a good amount of ice, with an underdeveloped drainage system, where meltwater flows mainly on the surface and, therefore, does not lead to a sudden increase in velocity.

In contrast to Stabbio di Largario, Ganoni di Schenadüi has been showing seasonal velocities well above annual velocities since summer, with practically all values above 0% up to about +400%. The almost threefold and fourfold increase in mean summer velocity (east and west lobes respectively) compared to the cold season indicates a probable connection between surface velocity and snowmelt phase, as already observed for other rock glaciers such as Becs-de-Bosson and Gemmi/Furggentälti (Krummenacher, *et al*., 2008; Perruchoud & Delaloye, 2007). Although there is a slight downward trend in early autumn, the difference between the two summer periods is not statistically significant. The difference between the two lobes is again quite marked. Cold season speeds are higher in the main (western) lobe. However, in the two summer periods, the eastern one seems to be more active. These differences confirm how microtopography and internal thermal conditions can affect the kinematics of an individual rock glacier in different ways (Jorgenson et al., 2010). Overall, this very seasonal behaviour indicates that this rock glacier reacts importantly as a result of water input due to snow melt. This means that most likely, the main processes influencing the velocities of this rock glacier occur primarily at the surface and not at depth, effectively excluding permafrost temperature as a predominant direct factor (Kenner *et al*., 2019). Following the reasoning of Cicoira *et al*. (2021), the fact that water flow has such a significant influence on the velocities of this rock glacier would suggest high structural heterogeneity, preferential flow paths and an increase in interstitial water content. Considering the time between snowmelt from 21 May to 4 June (recorded by the GST loggers), and taking into account the survey carried out on 11 July, the velocities had likely already increased during June and therefore a large part of that month's contribution was incorporated into the 'cold' period. If this were the case, this would indicate a further imbalance of movements over the year, with winter movement virtually absent, at the expense of a large (proportionally) late spring and summer movement. There would also be the possibility of a delayed snowmelt reaction of a few weeks. This could be due to the time needed for water to reach the basal zone of the rock glacier or the time required for the seasonal ice formed deeper in the permafrost table zone to melt.

In the case of Monte Prosa, the speed seems to be much more constant over time than in the others. Indeed, what is surprising is how the cold season contribution to the total displacement is almost 80%, roughly 15-20% more compared to the other sites. In summer, it is interesting to note that snowmelt does not seem to create the conditions for a marked increase in surface velocity. On the contrary, the speed in summer is significantly lower than in the cold season, a fact that has also been observed in other cases (Lambiel *et al*., 2005). The following period sees an increase in velocities, which can nevertheless be compared to cold season velocities. Despite the increased precipitation in the second summer period, given the lack of response to the water supply from the snowmelt in the previous period, it is very likely that this acceleration (delayed in time) is a response to the increase in temperature. What was observed during the summer of 2023 seems to confirm what the study by Mari *et al*. (2012) reported, in which a comparison was made between summer velocities of Monte Prosa and Ganoni di Schenadüi. Concerning the former, they noted that it shows relatively

small seasonal variations in velocity. In contrast, the latter shows well-defined seasonal variations with marked accelerations in the summer period, with higher velocities measured on the right side of the west lobe. Again, similar to Stabbio di Largario, Monte Prosa would appear to have a significantly delayed reaction in time, showing an increase in velocities only in the early autumn, and then probably peaking in the late autumn and winter. The low velocities in summer could result from the slow reaction of this rock glacier to external changes. This would suggest an internal condition that is still favourable to the presence of ice, with a rather homogenous structure and fewer preferential channels, which allow less water to penetrate it and reach the shear horizon.

Although Piancabella shows no significant difference in velocity between the three periods (Figure 35), it appears to have a rather similar trend to that of the western lobe of Ganoni di Schenadüi. Summer velocity tends to increase, with substantial stability in the warm season. Again, the effect of increased rainfall during early autumn would appear not to lead to increased velocities.

If in the cold season and summer the speeds of Stabbio di Largario and Monte Prosa are comparable, in early autumn that of the former is almost double. This difference could be attributed to the difference in GST between the two rock glaciers. However, Piancabella and Ganoni di Schenadüi also show lower velocities in that period, without their GST being significantly lower. This difference could therefore be due to different response times caused by the different geometries and internal thermal conditions.

The fact that differences in the seasonal contributions to the total are quite marked both within the same rock glacier and between different rock glaciers indicates the great complexity of these geomorphological forms related to high mountain permafrost. What has been observed would thus seem to indicate a complex interaction between external climatic factors, especially snow cover and its duration, as well as temperature, with local factors related to the individual rock glacier, such as microtopography and the thermal state of the permafrost, which may first favour the development of surface deformation mechanisms and then influence deeper processes, such as the development of channels that bring water down to the shear horizon. These factors and their interactions appear to determine both the seasonal course of rock glacier kinematics and its inter-annual trend, which is smoother over time (Buchli *et al*., 2018; Ulrich *et al*., 2021).

5.3   Spatialisation of information

Displacement vector maps produced by orthophotos and CIAS software help to spatialise the information measured by dGNSS, so that a global view of movements across the entire surface of rock glaciers can be obtained, thus aiding interpretation and discussion of the possible causes of such movements. This product also makes it possible to understand whether the position of the dGNSS measurement points is representative of surface movement. Thanks to the surveys carried out during the summer of 2023, several

interesting movements could be observed for all four rock glaciers. As seen above, the speed of these movements can vary greatly depending on the time of year. In addition, it was noted that within each rock glacier, there are large differences in speed, even within a few tens of metres.

What was measured for Stabbio di Largario by dGNSS is also found in the CIAS products, with more spatial information. As already discussed, horizontal velocities appear to increase in the latter part of the summer. However, the maps show that this increase occurs mainly in the middle and upper parts of the rock glacier, where, in the first two months of summer, many values are below LoD. The same does not apply to the parts very close to the front. In fact, their velocities are similar to those of the second period. Interestingly, the only area in which the velocity decreased significantly during the early autumn is the steep area joining the central part from the western lobe. Looking at the entire summer period, the consistent movement can be seen very clearly, and high-speed zones can be seen next to much slower zones. For example, the central part shows two high-speed zones to the east and west of the longitudinal crevasse. The latter is especially limited in terms of area, yet the differences in speed are remarkable. Another interesting zone is the one between the two lobes. There is a substantial shift from 20-25 cm summer displacements to displacements below 5 cm, if not below LoD within 30-40 m. These very low displacements are probably due to the dynamics in that area. This is, in fact, a point where there is a diffluence between the east and west lobes. It could be that this diffluence somehow balances the displacements on either side, resulting in minimal movements. Another possible factor could be a particular conformation of the bedrock, which could slow down its advance in that area. The general increase in movements during the early autumn, especially in the middle and upper part, seems to confirm that this rock glacier is less affected by snowmelt than others and, therefore, reacts more slowly over time.

Piancabella, excluding its rooting zone, rather than showing great temporal differences in velocity, shows great spatial variability. Interestingly, its central zone, near the front, has significantly higher velocities than all the other zones. Furthermore, the transition from fast zones to relatively slow or almost stationary zones appears to take place over a period of only a few metres, about 10-15. It seems evident that the high speed of the central/frontal part of the rock glacier, as well as the substantial stalling of the lower part of the lobe (to the east) cause the formation of ridges and furrows in the central part. The fact that there a fast and a slow part means that these ridges and furrows are not perpendicular to the flow but tend to elongate and take a more longitudinal direction. The greater displacements of the upper part during the early autumn could be due to both the late reaction to the temperature increase as well as the increased water supply from precipitation.

The CIAS result for Monte Prosa once again confirms what has already been reported by Mari *et al*. (2012), with greater velocities in the central part of the rock glacier. In this case, too, for example when observing the western lateral margins, the transition from almost no summer displacements to displacements of 10-20 cm

happens within a few tens of metres. Although the differences in velocity within the rock glacier are smaller than in the other two, the three areas with higher velocities show that uneven internal thermal conditions probably exist.

The low summer velocities measured on the west lobe of Ganoni di Schenadüi are mainly attributable to the lobe's slope, which is rather low. It ends in a flat area, which is not conducive to downstream movement. However, there seems to be a slight difference between the west and east sides of the lobe, with the latter being slightly faster, as also reported by Mari *et al.* (2012). The most interesting part, however, is the central part, which shows greater displacements than the surrounding area. This is the beginning of an area with a rather marked slope, which could cause the observed increase in speed. It is difficult to understand why neighbouring areas with similar or steeper slopes do not show equal velocities. The most widely accepted interpretation is that several factors overlap, which may favour increased velocities in one area of the rock glacier over another. For example, in the case of Ganoni di Schenadüi, the fastest zone is located at the beginning of a depression, and therefore, it is possible that the flow of meltwater as well as rainwater is concentrated there. This factor, combined with that of the slope and likely favourable internal thermal conditions, could result in a higher velocity. However, looking at the entire rock glacier, especially its main lobe, as well as the two margins, one can see that the velocities are very low, if not below LoD. This could suggest a possible transition to an inactive state. However, thanks to the historical series of dGNSS measurements, the above cannot be stated, as in 2017 and 2018, the velocities were, on average, lower than those measured in 2023.

From a general perspective, the rapid reaction and acceleration of a rock glacier during the snow melt period or following heavy precipitation events is probably due to the greater amount of water reaching the shear horizon (Kenner *et al.*, 2017). This could be the case for the Ganoni di Schenadüi rock glacier. This increase in water at depth could be due to the gradual increase in ground temperature measured in recent decades and consequently to permafrost degradation. Temperatures close to 0°C do not allow water to refreeze, and consequently, percolating water adds energy and contributes to ice melt. These conditions are optimal for forming taliks in the form of runoff channels, which promote the passage of water from the surface to the base (Kenner *et al.*, 2017).

Other rock glaciers, such as Stabbio di Largario and Monte Prosa, react less abruptly, suggesting a lower water supply in the shear horizon zone. This could mean that the thermal conditions of the ice within these two rock glaciers are less favourable for the development of channels within their bodies. Despite the similar water supply (normalised over 1 month) between the two summer periods for Stabbio di Largario and the larger one for Monte Prosa, as well as an apparent decrease in GST (not statistically significant) during the second part, both rock glaciers showed a significant increase in their velocity. This would confirm the delayed

reaction in time of these two rock glaciers, which would not appear to be directly related to changes in water supply but rather to the time it takes for heat to penetrate into the ground.

As recently argued by Bast *et al.* (2024), the lowering of the water content within rock glaciers is crucial for their deceleration in the short term. What has been observed in Southern Swiss Alps would seem to confirm this, with a deceleration in the last two years caused by two winters with little snow and below-average precipitation. Due to the snow-poor winter of 2022-2023, and thus a significant cooling of the ground surface, the recorded summer heat peaks had a more limited impact on the surface velocities of these rock glaciers. The general warming of the ground surface, and consequently that of the permafrost, is having and will have an impact on the rheological properties of the material of rock glaciers, which will see a change in the energy and mass balance (Cicoira, 2020). Rock glaciers approaching 0°C will experience major structural changes due to higher temperatures, increased water content, increased creep rates and the onset of degradation. Hydro-mechanical processes are therefore likely to become more important than thermal mechanisms and will take greater control over short-term changes in rock glacier kinematics (Cicoira, 2020).

5.4 Intra-annual thickness (and volume) changes

Seasonally, there can also be short-term velocity peaks/thickness changes (episodes of a few seconds/hours), which are often related to overturns or boulder slides, thus mainly linked to the active layer of the rock glacier (Wirz *et al.*, 2014). These types of displacements have been recorded on all four rock glaciers, with some boulders falling or sliding in the foreland area, where the stability of the boulders is lower due to the change in slope. They are visible by observing the figures representing the changes in thickness (Figure 62 - Figure 65 - Figure 68 - Figure 71). In the case of Ganoni di Schenadüi, Monte Prosa and Piancabella, these are mainly rockfall events, i.e. caused by the fall of one or a few boulders without any other particular changes in the surrounding area (Kummert *et al.*, 2018). These events thus modify, albeit slightly, the shape of the rock glacier. However, there can be more important erosional events that significantly change the surface and its thickness. In this sense, the most important event was that occurred on the front of the east lobe of Stabbio di Largario between the end of June and the end of August (Figure 60). A large amount of material (approx. 2'000 m^3), mainly from the active layer, slipped and ended up further downstream. This is visible by observing the changes in thickness and the graph representing the profiles plotted along the digital terrain models (Figure 73). As already observed in other rock glaciers with fast movements and steep fronts (Buchli *et al.*, 2018; Kummert *et al.*, 2018), this would be a seasonal failure, a mix between a widespread superficial flow and a concentrated flow (Kummert *et al.*, 2018). The former has been associated with low-flow water circulation at the surface or in the first few decimetres of the rock glacier front and downstream debris slope, sometimes causing small linear erosional events such as rill washes and small mudflows. These surface flow

events have been identified in the presence of a wet surface due to snowmelt or precipitation. The second process, on the other hand, is characterised by much more pronounced linear erosion, linked to a greater water input and incision, and mobilises up to several hundred cubic metres of material. In their study, Kummert *et al*. (2018) always identified the presence of water sources during concentrated flow events. Widespread superficial flow events were typically linked to rainfall events and happened less frequently between July and October than during snowmelt. In the summer and autumn, concentrated flow events were uncommon and required frequent or severe rainfall. In the case of Stabbio di Largario, the lack of webcams near the front does not allow to reliably confirm the cause of what was observed. However, it can be assumed an event caused by heavy rainfall at the end of August, a few days before the second survey. Observing the values measured at nearby weather stations, approximately 190 mm of rain fell over four days, with the peak rainfall on 27 August (101 mm). Marcer *et al*. (2020) also identified the infiltration of meteoric water as an important preparatory and triggering factor for frontal instabilities. Therefore, it is highly probable that this was the triggering event, as other areas of the rock glacier also underwent rather significant changes, albeit to a lesser extent. These events can be explained as high-frequency signals superimposed on a more regular velocity pattern, which better represents the real movement of the rock glacier or part of it (Cicoira *et al*., 2019).
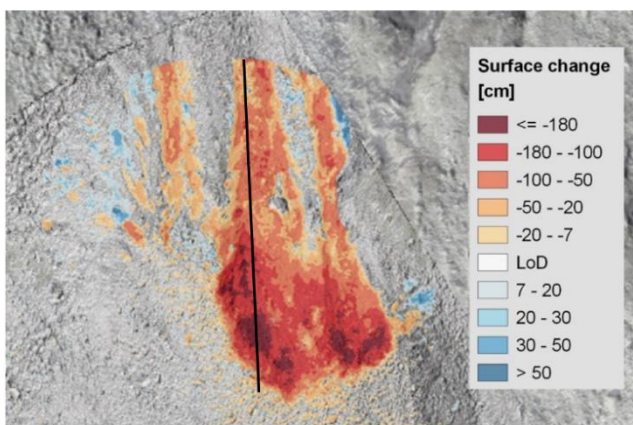
Figure 72: Collapsed area oft he Stabbio di Largario east front. The black line represents the location of the profiles visible in figure 73.
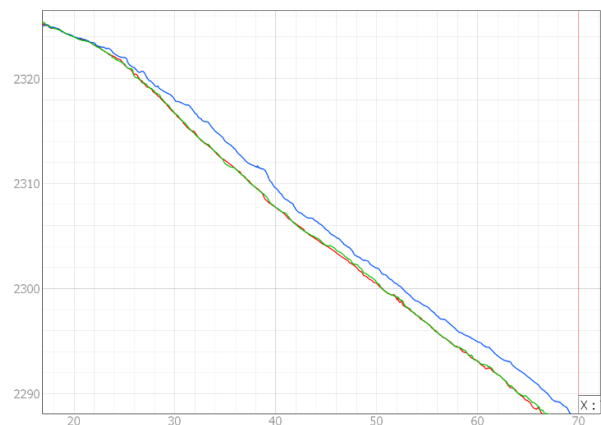
Figure 73: Height profiles along the eastern front of Stabbio di Largario rock glacier. X-axis: profile length (m). Y-axis: terrain elevation (m). Blue: first survey (21.06.2023). Red: second survey (31.08.2023). Green: third survey (12.10.2023).

Other thickness changes, however, linked to different processes, occurred in particular on the Monte Prosa rock glacier. It can be seen that in the upper part of the rock glacier, in the rooting zone, there was an area along a longitudinal furrow with a lowering of the surface by up to 50-60 cm over 3 months, between the beginning of July and the beginning of October (Figure 74).
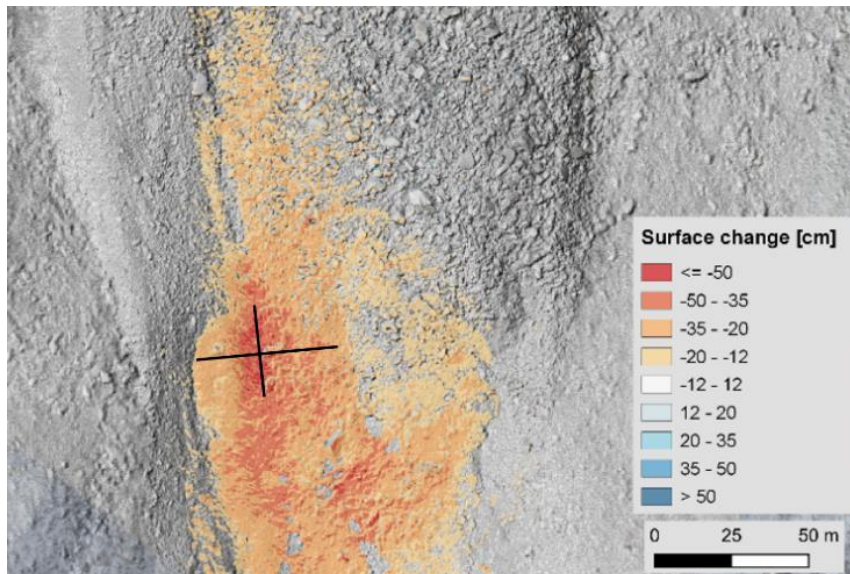
Figure 74: Subsidence area of the Monte Prosa rok glacier. The two black lines represent the profiles visible in figures 75 and 76.

Theoretically, subsidence could result from ice melt, reduced ice and sediment input, acceleration of the entire landform, or most likely a combination of these factors (Müller *et al*., 2016), but the understanding of the processes and models linking them to external forces is still rather limited (Scherler *et al*., 2014). Generally, the theory of ice-melt-related subsidence seems to find consensus (Haeberli *et al.,* 2024; Harris *et al*., 2001; Ikeda & Matsuoka, 2002; Kääb *et al*., 1997). As already discussed in other studies (Müller *et al*., 2016; Ulrich *et al*., 2021), given the prevalence of surface subsidence compared to the downward movement of the rock glacier during a short period, it is very likely that a real thaw settlement is taking place . In favour of the permafrost degradation theory, Del Siro *et al*. (2023b) showed how, generally, during the summer period, the springs emerging from the rock glacier increase their electrical conductivity as well as their ion concentration and are enriched in isotopes of ^{18}O. This physicochemical change of water would justify the probable melting of the ice within the rock glacier. However, observing the difference between the first and second part of the summer, it would seem that the lowering of the surface is more pronounced in the first part when the effect of temperature should not yet affect the inner ice so markedly. This gives rise to a second possible process that could play a role, namely a deformation due to overloading in the region affected by this subsidence (Kenner *et al*., 2017).
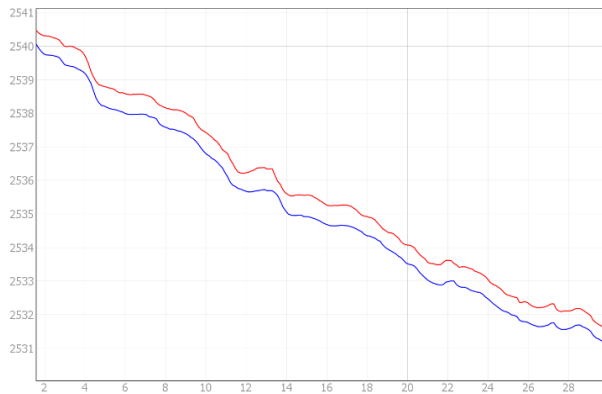
Figure 75: Longitudinal height profile along the subsidence area of Monte Prosa rock glacier. X-axis: profile length (m). Y-axis: Terrain elevation (m). Red: first survey (10.07.2023). Blue: third survey (03.10.2023).
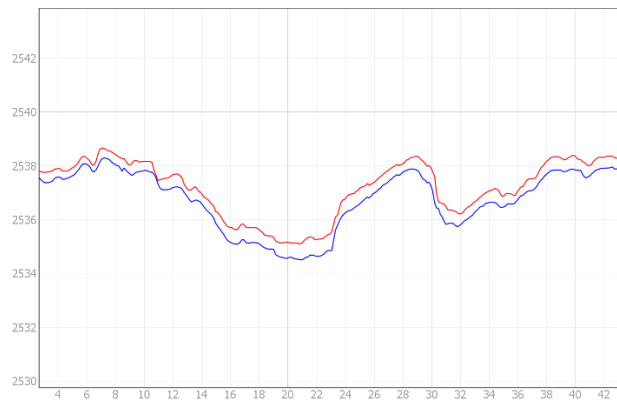
Figure 76: Transversal height profile along the subsidence area of Monte Prosa rock glacier. X-axis: profile length (m). Y-axis: Terrain elevation (m). Red: first survey (10.07.2023). Blue: third survey (03.10.2023).

To better understand these phenomena, one must return to the definition of a rock glacier and its components. The rock boulders of the lower part of the rock glacier carapace, which includes the active layer, are also present below the permafrost table and are firmly frozen within the creeping mass (Haeberli *et al.*, 2023). Generally, temperatures below the permafrost table are below 0°, causing these boulders to be firmly anchored to the ground and also transmitting the movement of the perennially frozen mass to the surface. However, the interlocking effect between rock components at the surface is weakened by extending flow with tensile stresses where movement speeds increase along the flow direction, particularly in steep root zones of rock glacier flow. This process frequently results in partially diffuse surface structures or longitudinal rather than transverse ridge-and-furrow structures (Haeberli *et al.*, 2023).

The surface heating seen above causes an increase in the thickness of the active layer, as it is thermally defined, which adapts to near-equilibrium conditions (Haeberli *et al.*, 2023; Noetzli & Pellet, 2022). This temperature increase above 0°C in the underlying frozen mixture of ice and rock causes the release of debris, which results in the thickening of the active layer (Harris *et al.*, 2001). The resulting subsidence is caused by thaw settlement due to the melting of excess ice within the frozen debris (Figure 77). In other words, it is due to the melting of ice that occupies a space within the subsurface ice matter greater than the naturally available pore space (Bollmann *et al.*, 2015; Haeberli *et al.*, 2023). This coupling process seems to be among the main reasons for the relatively low subsidence rates measured over the past decades (Gärtner-Roer *et al.*, 2022). The increased thermal protection of permafrost due to the thickening of the active layer together with the effects of the latent heat required to melt the ice means that the degradation of ice-rich permafrost due to climate change occurs very slowly (Haeberli *et al.*, 2023). In addition, increasing the thickness of the active layer enhances air circulation and consequently allows greater cooling of the ground surface through air convection (Wicky & Hauck, 2020, 2017).
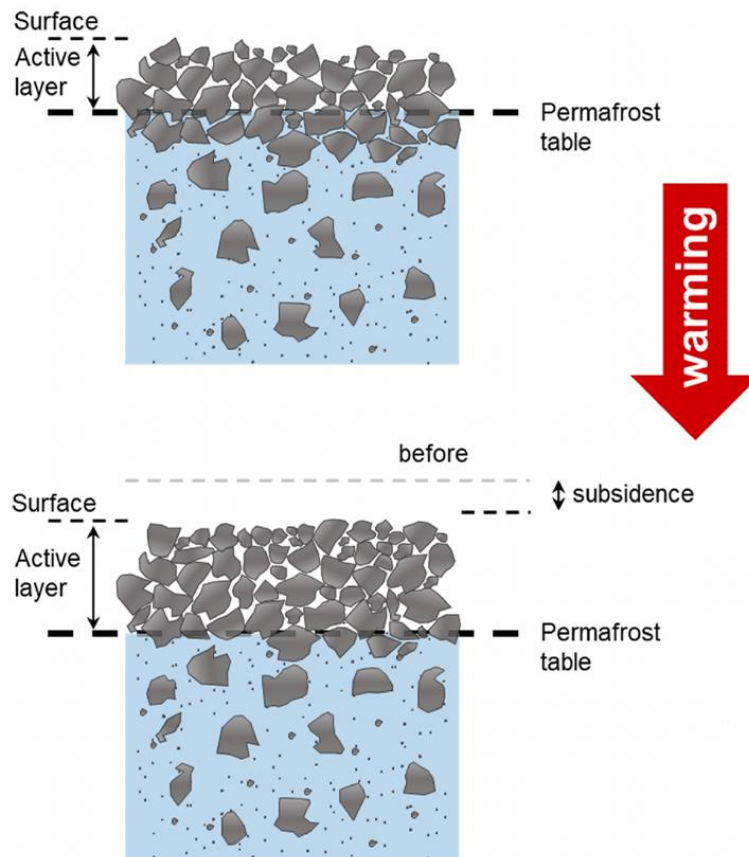
Figure 77: Ice-debris coupling and adjustment to warming effect for perennially frozen debris supersaturated in ice. Adapted from Haeberli et al. (2023).

Negative thickness changes, such as those measured almost exclusively in the upper/rooting zone on Monte Prosa, have already been observed in the past for other rock glaciers (Cusicanqui *et al*., 2021; Fleischer *et al*., 2021; Gärtner-Roer *et al*., 2022; Kääb *et al*., 1998; Kaufmann *et al*., 2021). Kenner *et al*. (2017) gave a possible interpretation for this phenomenon, essentially dividing the rock glacier into two parts: the rooting zone and the remaining part of the rock glacier. In the rooting zone, they argue that the prevailing type of deformation is the plastic one. This internal deformation of the viscous material corresponds to a power-law fluid influenced by gravity. Deformation increases near the surface, resulting in subsidence in the overburden zones. In the lower part, due to the thinning of the mobile layer, the surface plastic deformation decreases, and the dominant process becomes basal deformation (Figure 78). In the case of Monte Prosa, this process could indeed be the case since the subsidence zone is located at the beginning of the longitudinal furrows, where the material load appears to be greater than in neighbouring areas (see horizontal displacement vectors).
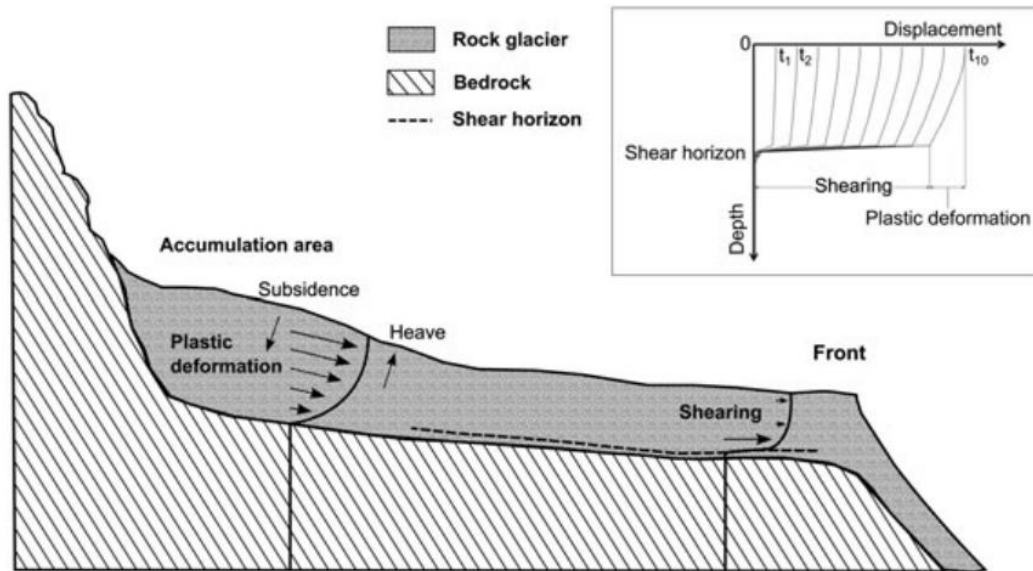
Figure 78: Schematic diagram of an idealised deformation profile (Kenner *et al.*, 2017).

This mechanism, combined with the subsidence explained by Haeberli *et al*. (2023), could be behind the thickness changes seen in the rooting zone of Monte Prosa and perhaps also in part of Ganoni di Schenadüi. This suggests that the upper part of these two glaciers is rich in ice, a fact confirmed during the early July survey carried out on the Monte Prosa, where seasonal ice was seen between boulders in the subsidence zone. The somewhat surprising fact is that in the most affected area of Monte Prosa, the surface subsidence reached up to 50-60 cm (equivalent to about -2'400 m³) in a little less than three months, a very short period. By checking the relevant literature, such a rate of susbidence not directly caused by direct erosion has never been observed.

In favour of the above is the Piancabella rock glacier, which shows no apparent signs of subsidence in the rooting zone, both in the warm period of 2023 and during the seven years from 2016 to 2023. In addition, the horizontal velocities recorded in those zones tend to be low, averaging around 20 cm·a⁻¹. These two pieces of information indicate that the rooting zone and the upper part of Piancabella undergo minimal plastic deformation due to the likely lower presence of ice in the permafrost and the limited material load. In contrast to the other three rock glaciers, the Piancabella rock glacier does not have a steep rock face behind it. Bearzot *et al*. (2022) obtained a similar result, i.e. almost no subsidence at the upper part of the Gran Sometta rock glacier, and this is due to the absence of subsurface ice as measured by Electrical Resistivity Tomography (ERT) profiles. The same could also be the case at Stabbio di Largario, in a well-defined area of the western part of the rooting zone. No significant subsurface subsidence was also seen over a 7-year period. As for Bearzot *et al*. (2022), this could be attributable to very little or no permafrost occurrence due to the presence of a small glacier during the LIA, which probably provided for the degradation of the former permafrost.

The lowering of the surface visible at Piancabella between the first and third survey and more markedly between 2016 and 2023 would appear to be caused by a different process from that described above for Monte Prosa, namely a 3-dimensional effect of extensional and compressional flow (Kääb *et al.*, 1997). In the front area, in fact, a raising of the surface can be seen. This would appear to be caused by the front approach to a counter-slope area. At that point, the surface tends to 'swell' because it cannot compensate for the relatively high velocities downstream with material transport. Considering that the velocities above the downslope zone are considerably slower, the amount of material transported there is likely to be less than that transported towards the front. Consequently, the rock glacier may react by lowering its surface to compensate for this lack of material. This mechanism would seem to be confirmed by the calculation of the net volume, which was only about -800 m^3 in seven years between 2016 and 2023 and almost zero in summer 2023.

These case studies clearly show how specific surface changes can be caused by complex and diverse processes that are not yet fully understood. The triggering factors are manifold, such as the thermal state of the permafrost, microtopography, liquid water intrusion, as well as the input of sediments that influence the load exerted on the rock glacier body (Müller *et al.*, 2016). In the case of Monte Prosa, but also for Ganoni di Schenadüi, there seems to be a general tendency for permafrost degradation in the upper part, accentuated precisely near the longitudinal furrows, where the topography is steeper and where the water supply during snowmelt and precipitation events is greater. The superposition of these factors, combined with the likely high amount of ice, could, therefore, be the cause of these subsidence rates, which are less visible on the Piancabella and Stabbio di Largario rock glaciers.

5.5 M3C2 vs. DoD

As already explained in the methods section, to estimate distance differences in the elevation of point clouds and thus to evaluate possible thickness changes, in this thesis it was opted for the use of the M3C2 algorithm. It should better represent thickness changes than a DoD, especially in more complex and steep surfaces such as those of a rock glacier, as it operates directly on the point cloud without meshing or gridding, reducing the uncertainty (Nourbakhshbeidokhti *et al.*, 2019; Bearzot *et al.* 2022). To assess how well this algorithm works, a DoD for Monte Prosa was created for comparison (Figure 79). What immediately strikes is the difference between the two LoDs of M3C2 and DoD, about 12 cm and 4 cm, respectively. This allowed to state that M3C2 tends to be more conservative (Lague *et al.*, 2013). Furthermore, the values obtained via DoD turned out to be slightly higher, probably due to the horizontal displacement component. The calculation of volume changes is a very complex issue in the case of rock glaciers, as there are multiple displacement components and the volume is occupied by rock, ice, water, air and other components. For this reason, the use of M3C2 should be more robust in these cases and, at the same time, allows to remain more conservative given the tendentially higher LoD value and the surface change values in the direction of the normals. This would also seem to be the case in this thesis. For example, for Monte Prosa, a net volume change via M3C2 of -2'400 m^3 was calculated for the entire summer period, while via DoD, it resulted in -4'100 m^3.
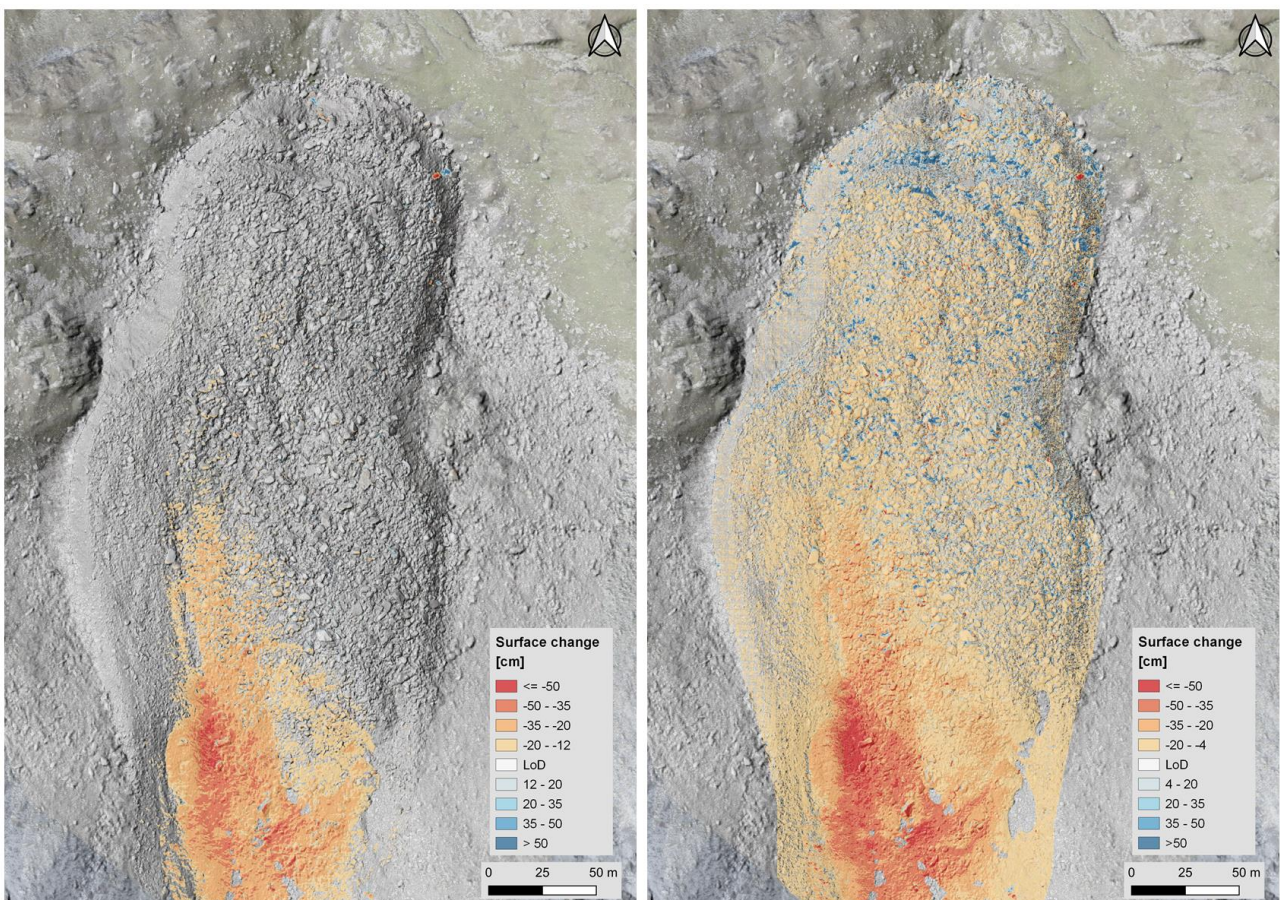
Figure 79: Comparison between thickness changes derived from the M3C2 (left) algorithm and from the DoD (right).

5.6   Advantages of using drones to monitor rock glacier kinematics

Large spatial differences can be seen when observing the horizontal and vertical displacements of the individual rock glaciers. In this respect, the drone was of great help, as it made possible to spatialise the point information obtained through dGNSS and to identify in all four rock glaciers areas with major changes, both in terms of horizontal and vertical displacements.
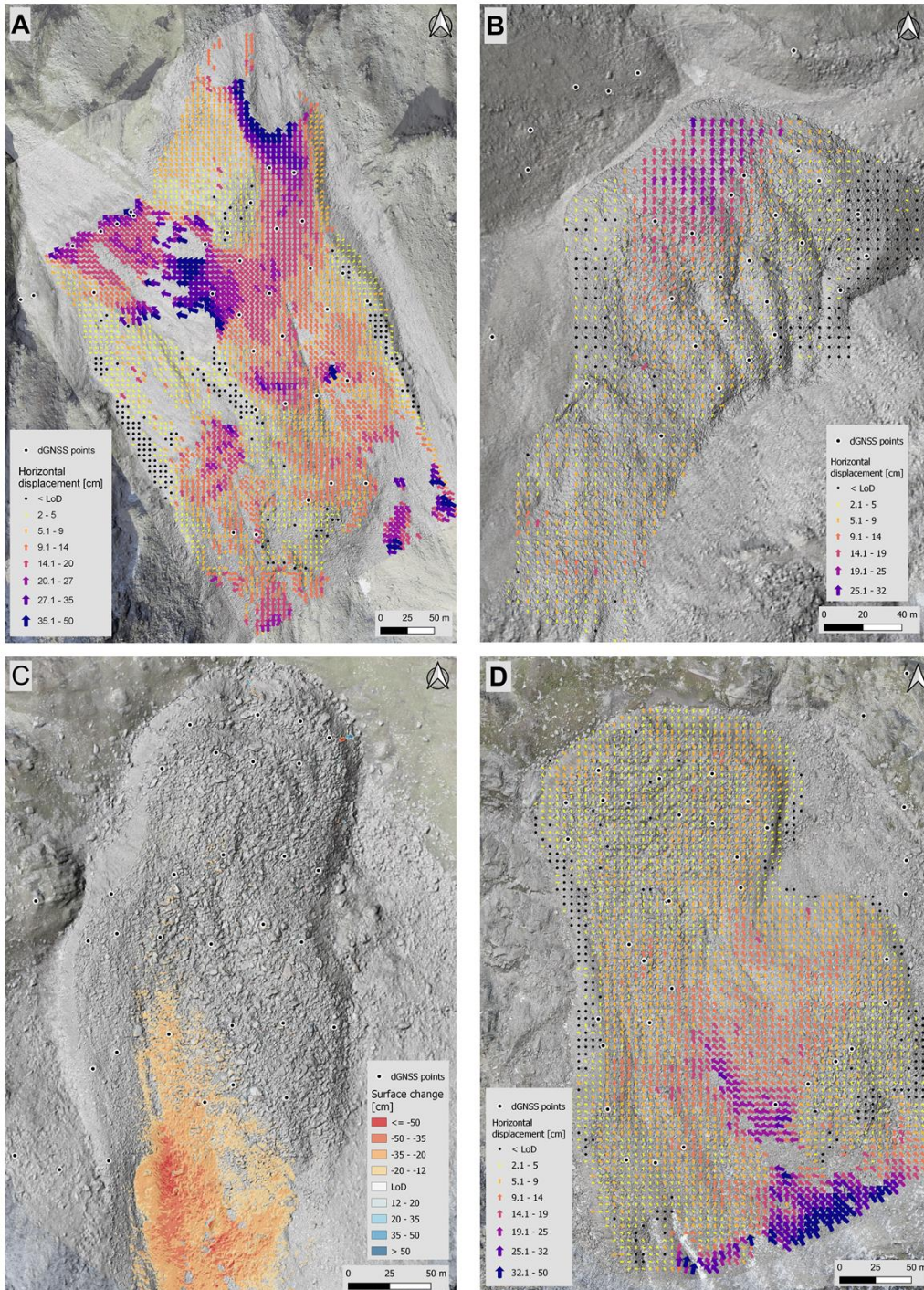
Figure 80: Position of the dGNSS measuring points on A) Stabbio di Largario B) Piancabella C) Monte Prosa D) Ganoni di Schenadüi.

Indeed, looking at Figure 80, it can be seen that the dGNSS points are generally well distributed over the entire area of the rock glacier. However, because they were generally placed on large boulders that should be accessible even with a few dm of snow, steep and most depressional areas, as well as rooting zones (which often have topographical concavities), are not represented. For example, in the case of Stabbio di Largario, the point measurements taken on the east lobe do not go as far as the front (also due to the impervious terrain). The points alone would not capture the gradual increase in velocity as the front approaches, just as they would not have captured the major erosion events between the end of June and the end of August. There is also a lack of points in the area between the central part and the western lobe due to the lack of large boulders caused by the steep slope and instability. Also, in the case of Piancabella, the points are generally well distributed, but in the area where the highest velocities were measured by the drone, the points are missing (because of the very steep terrain). For Monte Prosa, the part affected by the marked subsidence of the surface is not covered by dGNSS points. Here too, the drone was able to show a process that otherwise would not have been detected. The same can be said for the small area in the centre, where the horizontal velocities are slightly higher but no dGNSS points are present. Last but not least, at Ganoni di Schenadüi, like at Monte Prosa, the part of the rooting zone, which has the greatest displacements, is uncovered by points.

The differences observed between drone and GNSS are sometimes relatively high over short periods. These differences can be attributed to several factors:

1. The instrumental error related to the measurement method, both drone and dGNSS. Considering that LoD is around 2 cm with the product of photogrammetry and around 1 cm for that of dGNSS, the differences between the two methods, especially in the case of points with minimal displacements, could be very large. This also influences photogrammetric reconstruction.

2. The presence of shadows between boulders, which in some areas resulted in a significant degradation of the CIAS analysis (Vivero *et al*., 2022).

3. The Triangulated Irregular Network (TIN) interpolation method used on QGIS to calculate velocities is sensitive to possible errors in calculating vectors by CIAS and to areas without vectors, as they are deleted when being wrong. This resulted in values being under- or overestimated in some areas.

By increasing the period between the two surveys, there appears to be a marked improvement in the comparison between drone and dGNSS. The comparison over the entire period shows a good correlation between the two methods with an R-value^2 of 0.86. In a study carried out by Bearzot *et al*. (2022), over three consecutive years, the comparison between drone and dGNSS resulted in a coefficient of determination of 0.99, while Scapozza *et al*. (2018), over the two years between 2014 and 2016 obtained an R-value^2 of 0.98. Also, in the case of Stabbio di Largario and Piancabella, taking the displacements measured by drone and by dGNSS between 2016 and 2023, the value of R^2 is in line with previous studies, i.e. 0.98.

However, despite these differences in part due to the reasons explained above, it has been ascertained by many studies that the use of UAV-photogrammetry has great potential and makes an important contribution to a better understanding of the kinematics of rock glaciers and landslides (Dall'Asta *et al.*, 2015; Peternel *et al.*, 2022; Vivero *et al.*, 2021; Westoby *et al.*, 2012; Zhang *et al.*, 2019). This also occurs at the intra-seasonal level. Comparing the fastest zones of the 2016-2023 surveys with the intra-seasonal 2023 surveys shows that they coincide very well. However, the displacements measured using dGNSS remain extremely important, both to validate the displacements measured by photogrammetry and to continue the long-term monitoring of the rock glacier kinematics of Canton Ticino that began about fifteen years ago.

5.7   Limitations and methodological teaching

The main **limitations** encountered during the thesis are the following:

- There are no direct observations or information on the internal structure of these rock glaciers. Consequently, the hypothesis regarding kinematics discussed above cannot be confirmed.

- In terms of absolute values, the CIAS software is mainly accurate over the long term. In the short term, the values are strongly influenced by the quality of the photogrammetric product (even random errors of a few cm) and the variation of light and shadow conditions due to terrain roughness and weather conditions.

- The M3C2 algorithm overcomes the problem of loss of information when converting 3D data into a 2.5D representation. In general, it is more suitable for complex terrains. However, it still has limitations, with possible errors in the calculation of normals, which can affect the accuracy (Yang *et al.*, 2024).

- dGNSS measurements between September 2022 and June 2023 represent the movement of 8-9 months, including the autumn period, which, especially for Monte Prosa and Stabbio di Largario, could contribute a great deal in terms of movement. If within the warm season it is relatively easy to have data on kinematics, for the cold season it is extremely complicated due to the presence of snow and less favourable conditions. It is, therefore, very difficult to separate late autumn/early winter kinematics from late winter and spring kinematics.

- The use of six or seven CPs would have allowed a more robust indication of the quality of the reconstructions. However, only 10 GCPs were available

Methodological teachings

- In order to obtain quality photogrammetric products, planning accurate drone missions in advance is necessary. In this respect, the DroneHarmony software proved to be a good choice due to its ease of use. However, for Ganoni di Schenadüi and Monte Prosa, the drone flew too high compared to what had been planned while maintaining the same number of pictures. For this reason, we obtained more than 2000 images in some cases, which was the cause of the slow photogrammetric processing. The cause of the flights being too high was a higher take-off point than planned. The difference in altitude was not compensated for, so the drone flew at the planned height of 50 metres plus the difference in altitude between the planned and real take-off point. This means that if the starting point is changed, the plan must be changed (this can be done directly from the drone controller, although rather inconvenient due to the size of the screen).

- It would have been possible to fly higher, around 80 metres. The quality of the results would still have been very good, and by doing so, less time would have been needed for missions on the ground, less battery power consumed, and fewer photographs taken, which would also have reduced the time required to create point clouds and orthophotos. In this way, a larger area could have been considered, which would have been helpful to identify more stable areas, for example, for the coregistration of the point cloud or possibly that of the orthomosaics.

- As terrain models vary more in areas with very complex topography, to avoid geomorphic interpretation bias, we used additional oblique images as well as an overlap between photos greater than 5 (>80%) and during the creation of the terrain model a medium quality (Hendrickx *et al*., 2019).

- The PPK method alone without ground control points is less accurate than integrating GCPs (at least in those regions). To obtain accurate terrain models without major deformations and comparable with the reference points measured on the boulders, 7 GCPs were sufficient.

- CPs are essential to validate the absolute accuracy of the models, especially in mountainous areas , where satellite coverage is not always optimal.

- It is important during the photogrammetric process to "check" the point confidence calculation box before creating the dense point cloud. This allows at the end of the process to clean the point cloud and thus eliminate noise, keeping only points with very high confidence.

- It is always good to bring a power bank to recharge the tablet required for dGNSS measurements or the drone battery in case of problems.

6   Conclusion and future studies

Pressing climate change is having a major impact on high mountain environments. In such a context, with the rapid disappearance of glaciers and decreasing snowfall, studying Alpine permafrost, which visibly manifests itself in the form of rock glaciers, becomes extremely important. The hydrological potential of these complex geomorphological forms is now recognised and will become increasingly important in the future, but the reduced understanding of the processes and factors influencing their reactions makes it necessary to study them in greater depth. Globally, the relatively small number of studies on seasonal displacements has not yet made it possible to clearly break down short-term versus annual processes and exactly understand the influence of various external and internal factors. To this end, the main objective of this thesis was to calculate, analyse and better understand the intra-annual kinematics of four rock glaciers located in the Southern Swiss Alps using two techniques: dGNSS and UAV-photogrammetry. More precisely, the aim was to calculate the horizontal displacements as well as the thickness changes visible at the surface that occurred between September 2022 and October 2023, in order to better understand the seasonal kinematics of these rock glaciers and assess possible permafrost degradation. The results of this thesis allowed some interesting conclusions to be drawn.

From a **geomorphological** point of view:

- The four rock glaciers show a similar trend in their inter-annual kinematics between 2010 and 2023, which closely follows the MAGST trend. This means that, over a medium to long period, they react similarly to changing external factors such as temperature and water supply especially from snowmelt.

- On an intra-annual level, significant velocity differences were found depending on the rock glacier. In general, the average velocities recorded over the entire warm season were higher than those of the cold season (which includes late autumn 2022, winter 2022/2023 and spring 2023). Ganoni di Schenadüi proved to be reactive and experienced a rapid increase in its speed following snowmelt during summer. In contrast, Monte Prosa (and partly Stabbio di Largario) saw a decrease in velocities during that period. For the latter, there was a marked increase in velocities during the second part of the summer, synonymous with a delayed reaction of at least 2-3 months. Monte Prosa, on the other hand, showed late-summer velocities in line with cold season velocities, synonymous with an even more delayed reaction in time and likely rather limited annual variations in kinematics.

- At the intra-annual level, significant displacement differences were found between the four rock glaciers. Stabbio di Largario and Monte Prosa showed similar cold season velocities and significantly higher than the other two. In summer, no significant differences were found. In the early autumn, only Stabbio di Largario was significantly faster than the other three sites. Given the geographical proximity, these different reactions could indicate different internal thermal states. The rapid responses of Ganoni di Schenadüi in summer could indicate a permafrost temperature probably closer to zero degrees, favouring the development of channels carrying water towards the shear horizon. With the gradual degradation of permafrost, on an intra-annual level, hydro-mechanical processes may become increasingly more important than thermal ones (Cicoira, 2020).

- The measured displacements are not evenly distributed over the surface of the four rock glaciers. Speeds can change from zero to several decimetres per month within a few tens of metres. The cause is probably the microtopography and the difference in ice quantity, along with the structure of the rock glacier itself.

- The spatialisation of kinematic information using photogrammetry made it possible to identify interesting surface movements, probably related to different processes, which also gave insight into the possible internal conditions of these rock glaciers. The most pronounced surface movements, recorded in the rooting zone (where dGNSS measurement points are missing) of Monte Prosa and partially Ganoni di Schenadüi, suggest a probable great amount of ice, which in turn suggests a process of surface deformation. On the contrary, given the limited displacements in the rooting zone of Piancabella and Stabbio di Largario, less ice and therefore less surface deformation in that area are assumed. The result of the M3C2-alorithm on Monte Prosa showed significant subsidence in the upper part, which could result from the melting of the ice contained just below the permafrost table and, therefore, from permafrost degradation but also from the deformation caused by the overloading of material in that area. Stabbio di Largario also showed changes in thickness, especially in the area of the east lobe front. The loss of thickness exceeded 2 metres in some places, leading to a material loss at around 2000 m^3. The probable cause was the heavy rainfall at the end of August, a few days before the second survey. This would suggest an erosion event lasting a few minutes to a few hours.

From a **methodological** point of view:

- The integration of dGNSS measurements and photogrammetry using the DJI Mavic 3E drone proved to be very interesting for the purposes of spatialising the information obtained through point measurements alone. However, the latter remains fundamental for continuing the historical series that began about 15 years ago in Canton Ticino and for having reference points measured on the ground and used in the photogrammetric process to georeference the point cloud, digital terrain models as well as orthomosaics.

- The software used in this study, including Agisoft Metashape photogrammetric software, CIAS (image feature tracking algorithm) and CloudCompare (M3C2 algorithm), has proven to be not only suitable but also highly reliable. These tools played a crucial role in identifying areas of both horizontal movement and thickness changes, which would have been undetectable through dGNSS points alone. Their reliability and effectiveness underline their value in future studies of this nature.

- The comparison between displacements obtained using dGNSS and those obtained using the CIAS software on orthomosaics showed a direct relationship between the concordance of the two results and the distance elapsed between the surveys. In other words, the greater the time between surveys, the greater the concordance between the two methods and vice versa. This is because, over a very short period of time and given the relatively low displacement rates, the result is more influenced by instrumental errors (e.g. related to satellite coverage), as well as uncertainties related to photogrammetric reconstruction, shadows present in the orthomosaics (which disturb the feature tracking process) and the interpolation method used to extract the velocity values obtained by CIAS at the exact point measured by dGNSS.

Future studies

The presence of changes in horizontal displacements and thickness during the two summer periods and variations between seasonal velocities measured by dGNSS shows that their drivers vary seasonally (e.g. Ulrich *et al*., 2021). In the case of the four rock glaciers studied in this thesis, by increasing the frequency of seasonal or intra-seasonal surveys, as well as by expanding the spatial information through the use of drone and photogrammetry, it was possible to capture interesting surface processes. However, surface information alone (dGNSS + drone) does not provide a complete view of the structure of the rock glaciers and the internal conditions of the permafrost. In the future, to better understand the annual and intra-annual kinematics of these rock glaciers and to analyse the findings of this thesis in more detail, it will be necessary to continue research on these sites and to carry out further analyses that could include:

- Continue monitoring through photogrammetry. Alternatively, given the rather costly methodology in terms of time and resources, kinematics could be monitored through the use of other remote sensing techniques such as interferometry (InSAR). Despite some limitations, this technique provides accurate data without the need of in-situ measurements.

- Developing more efficient algorithms that can help to understand kinematic changes even better, and thus calculate with greater precision and a higher degree of reliability horizontal displacements, but especially vertical ones, on which many open questions still remain today. Geodetic measurements form the basis of models and simulations that predict changes in creep rates as the climate changes. The more reliable the measurements, the better these models will be.

- Continuing the physicochemical analyses of rock glacier sources, which were already undertaken by Chantal del Siro during her Master Thesis (Del Siro, 2021; Del Siro *et al*., 2023b) and are currently going on during her PhD. This has already allowed and will allow a clearer idea of the origin of the water in the springs (snow, seasonal ice, ice within the permafrost) at a very high temporal resolution. It will, therefore, be possible to understand if and when the ice melts and at what point in the season the degradation of the permafrost begins.

- Further hydrological measurements, such as tracing (planned by Del Siro for summer 2024), are needed to try to understand the time it takes for water to flow over, into, or at the base of rock glaciers. This could help to confirm or disprove hypotheses about internal ice conditions or at least give some indication of possible reaction times.

- Analysis of a fixed GPS antenna in Stabbio di Largario. This antenna has existed for several years and records movements at a very high temporal resolution (a few hours). It would be interesting to analyse these movements to assess possible movement patterns of this rock glacier over very short periods of time and relate them to, for example, extreme precipitation events or the period of snowmelt.

- Geophysical measurements would allow us to understand the internal composition of the rock glaciers and monitor their condition over time. Combined with geodetic measurements and physico-chemical and hydrological measurements of the sources, this would provide a much clearer picture of the processes that influence rock glaciers kinematics.

7 References

Abermann, J., Fischer, A., Lambrecht, A., & Geist, T. (2010). On the potential of very high-resolution repeat DEMs in glacial and periglacial environments. *Cryosphere*, *4*(1), 53–65. https://doi.org/10.5194/tc-4-53-2010

Arenson, L. U., & Springman, S. M. (2005). Mathematical descriptions for the behaviour of ice-rich frozen soils at temperatures close to 0 °C. *Canadian Geotechnical Journal*, *42*(2), 431–442. https://doi.org/10.1139/t04-109

Barsch, D. (1996). *Rockglaciers. Indicators for the present and former geoecology in high mountain environments* (Springer).

Bast, A., Kenner, R., & Phillips, M. (2024). *Short-term cooling , drying and deceleration of an ice-rich rock glacier*. 1–26.

Bearzot, F., Garzonio, R., Di Mauro, B., Colombo, R., Cremonese, E., Crosta, G. B., Delaloye, R., Hauck, C., Morra Di Cella, U., Pogliotti, P., Frattini, P., & Rossini, M. (2022). Kinematics of an Alpine rock glacier from multi-temporal UAV surveys and GNSS data. *Geomorphology*, *402*, 108116. https://doi.org/10.1016/j.geomorph.2022.108116

Beniston, M. (2006). Mountain weather and climate: A general overview and a focus on climatic change in the Alps. *Hydrobiologia*, *562*(1), 3–16. https://doi.org/10.1007/s10750-005-1802-0

Beniston, M., Farinotti, D., Stoffel, M., Andreassen, L. M., Coppola, E., Eckert, N., Fantini, A., Giacona, F., Hauck, C., Huss, M., Huwald, H., Lehning, M., López-Moreno, J. I., Magnusson, J., Marty, C., Morán-Tejéda, E., Morin, S., Naaim, M., Provenzale, A., … Vincent, C. (2018). The European mountain cryosphere: A review of its current state, trends, and future challenges. *Cryosphere*, *12*(2), 759–794. https://doi.org/10.5194/tc-12-759-2018

Bertone, A., Seppi, R., Callegari, M., Cuozzo, G., Dematteis, N., Krainer, K., Marin, C., Notarnicola, C., & Zucca, F. (2023). Unprecedented Observation of Hourly Rock Glacier Velocity With Ground-Based SAR. In *Geophysical Research Letters* (Vol. 50, Issue 9, pp. 1–10). https://doi.org/10.1029/2023GL102796

Bianconi, F., Beffa, F. A., Steiger, R. H., Günthert, A., Hasler, P., Baumer, A., & Huber, C. W. (2014). *Blatt 1252 Ambrì-Piotta. – Geol. Atlas Schweiz 1:25 000, Karte 138*.

Binggeli, V. (1965). DER BLOCKSTROM IM VAL CADLIMO. *Regio Basiliensis: Hefte Für Jurassische Und Oberrheinische Landeskunde*, *6*.

Bodin, X., Schoeneich, P., Deline, P., Ravanel, L., Magnin, F., Krysiecki, J.-M., & Echelard, T. (2015). Mountain permafrost and associated geomorphological processes: recent changes in the French Alps. *Journal of Alpine Research*, *103*(2). https://doi.org/10.4000/rga.2885

Bodin, X., Thibert, E., Sanchez, O., Rabatel, A., & Jaillet, S. (2018). Multi-Annual kinematics of an active rock glacier quantified from very high-resolution DEMs: An application-case in the French Alps. *Remote Sensing*, *10*(4), 1–14. https://doi.org/10.3390/rs10040547

Boeckli, L., Brenning, A., Gruber, S., & Noetzli, J. (2012). Permafrost distribution in the European Alps: Calculation and evaluation of an index map and summary statistics. *Cryosphere*, *6*(4), 807–820. https://doi.org/10.5194/tc-6-807-2012

Bollmann, E., Girstmair, A., Mitterer, S., Krainer, K., Sailer, R., & Stötter, J. (2015). A Rock Glacier Activity Index Based on Rock Glacier Thickness Changes and Displacement Rates Derived From Airborne Laser Scanning. *Permafrost and Periglacial Processes*, *26*(4), 347–359. https://doi.org/10.1002/ppp.1852

Bollmann, E., Klug, C., Sailer, R., Stötter, J., & Abermann, J. (2012). Quantifying Rockglacier Creep Using

Airborne Laser Scanning A Case Study from Two Rockglaciers in the Austrian Alps. *Tenth INternationa Conference on Permafrost*, *JUNE*, 1–7.

Brighenti, S., Tolotti, M., Bruno, M. C., Wharton, G., Pusch, M. T., & Bertoldi, W. (2019). Ecosystem shifts in Alpine streams under glacier retreat and rock glacier thaw: A review. *Science of the Total Environment*, *675*, 542–559. https://doi.org/10.1016/j.scitotenv.2019.04.221

Buchli, T., Kos, A., Limpach, P., Merz, K., Zhou, X., & Springman, S. M. (2018). Kinematic investigations on the Furggwanghorn Rock Glacier, Switzerland. *Permafrost and Periglacial Processes*, *29*(1), 3–20. https://doi.org/10.1002/ppp.1968

Chaix, A. (1923). Les coulées de blocs du Parc national suisse d'Engadine (Note préliminaire). *Le Globe. Revue Genevoise de Géographie*, *62*(1), 1–35. https://doi.org/10.3406/globe.1923.5609

Chakraborty, A. (2021). Mountains as vulnerable places: a global synthesis of changing mountain systems in the Anthropocene. *GeoJournal*, *86*(2), 585–604. https://doi.org/10.1007/s10708-019-10079-1

Chen, Y., & Medioni, G. (1991). Object Modeling by Registration of Multiple Range Images. *Proceedings - IEEE International Conference on Robotics and Automation*, 2724–2729. https://graphics.stanford.edu/~smr/ICP/comparison/chen-medioni-align-rob91.pdf

Cicoira, A. (2020). On the Dynamics of Rock Glaciers. In *Dissertation* (Issue June). https://doi.org/10.13140/RG.2.2.29726.56649

Cicoira, A., Beutel, J., Faillettaz, J., & Vieli, A. (2019). Water controls the seasonal rhythm of rock glacier flow. *Earth and Planetary Science Letters*, *528*. https://doi.org/10.1016/j.epsl.2019.115844

Cicoira, A., Marcer, M., Gärtner-Roer, I., Bodin, X., Arenson, L. U., & Vieli, A. (2021). A general theory of rock glacier creep based on in-situ and remote sensing observations. *Permafrost and Periglacial Processes*, *32*(1), 139–153. https://doi.org/10.1002/ppp.2090

Clapuyt, F., Vanacker, V., Schlunegger, F., & Van Oost, K. (2017). Unravelling earth flow dynamics with 3-D time series derived from UAV-SfM models. *Earth Surface Dynamics*, *5*(4), 791–806. https://doi.org/10.5194/esurf-5-791-2017

Cook, K. L. (2017). An evaluation of the effectiveness of low-cost UAVs and structure from motion for geomorphic change detection. *Geomorphology*, *278*, 195–208. https://doi.org/10.1016/j.geomorph.2016.11.009

Cusicanqui, D., Rabatel, A., Vincent, C., Bodin, X., Thibert, E., & Francou, B. (2021). Interpretation of Volume and Flux Changes of the Laurichard Rock Glacier Between 1952 and 2019, French Alps. *Journal of Geophysical Research: Earth Surface*, *126*(9). https://doi.org/10.1029/2021JF006161

Dall'Asta, E., Delaloye, R., Diotri, F., Forlani, G., Fornari, M., Di Cella, U. M., Pogliotti, P., Roncella, R., & Santise, M. (2015). Use of uas in a high mountain landscape: The case of gran sommetta rock glacier (AO). *International Archives of the Photogrammetry, Remote Sensing and Spatial Information Sciences - ISPRS Archives*, *40*(3W3), 391–397. https://doi.org/10.5194/isprsarchives-XL-3-W3-391-2015

Del Siro, C., Antognini, M., & Scapozza, C. (2023a). Il permafrost nelle Alpi Ticinesi (2019/2020, 2020/2021 e 2021/2022). Rapporto No. 6 del Gruppo Permafrost Ticino. *Bollettino Della Società Ticinese Di Scienze Naturali*, *111*, 27–39.

Del Siro, C., Scapozza, C., Perga, M. E., & Lambiel, C. (2023b). Investigating the origin of solutes in rock glacier springs in the Swiss Alps: A conceptual model. *Frontiers in Earth Science*, *11*, 1–20. https://doi.org/10.3389/feart.2023.1056305

Delaloye, R., Lambiel, C., & Gärtner-Roer, I. (2010). Overview of rock glacier kinematics research in the Swiss Alps: seasonal rhythm, interannual variations and trends over several decades. *Geographica Helvetica*,

65(2), 135–145. http://www.geogr-helv.net/65/135/2010/

Delaloye, R., Perruchoud, E., Bodin, X., Kääb, A., Kellerer-pirklbauer, A., Krainer, K., Lambiel, C., Roer, I., & Thibert, E. (2008). Recent Interannual Variations of Rock Glacier Creep in the European Alps Interannual Velocity Survey and Dataset. *Weather*, 343–348.

Deluigi, N., & Scapozza, C. (2020). Il permafrost nelle Alpi Ticinesi: ripartizione potenziale attuale e futura. *Bollettino Della Società Ticinese Di Scienze Naturali*, *108*, 19–31.

Dinkov, D. (2023). Accuracy assessment of high-resolution terrain data produced from UAV images georeferenced with on-board PPK positioning. *Journal of the Bulgarian Geographical Society*, *2023*(48), 43–53. https://doi.org/10.3897/jbgs.e89878

Dinno, A. (2015). Nonparametric pairwise multiple comparisons in independent groups using Dunn's test. *Stata Journal*, *15*(1), 292–300. https://doi.org/10.1177/1536867x1501500117

DJI. (n.d.). *DJI Mavic 3 Enterprise - Specs*. https://enterprise.dji.com/mavic-3-enterprise/specs

Dobiński, W. (2020). Permafrost active layer. *Earth-Science Reviews*, *208*. https://doi.org/10.1016/j.earscirev.2020.103301

Etzelmüller, B., Guglielmin, M., Hauck, C., Hilbich, C., Hoelzle, M., Isaksen, K., Noetzli, J., Oliva, M., & Ramos, M. (2020). Twenty years of European mountain permafrost dynamics-the PACE legacy. *Environmental Research Letters*, *15*. https://doi.org/10.1088/1748-9326/abae9d

Federal Office for the Environment FOEN. (2005). *Hinweiskarte der Permafrostverbreitung in der Schweiz*. https://map.geo.admin.ch/?zoom=4&bgLayer=ch.swisstopo.pixelkarte-grau&layers=ch.bafu.permafrost&layers_opacity=0.7&lang=de&topic=bafu&E=2702910.66&N=1138286.32

Federal Office of Topography swisstopo. (2022). *GeoCover V3*. https://map.geo.admin.ch/?topic=ech&lang=it&bgLayer=ch.swisstopo.pixelkarte-farbe&layers=ch.swisstopo.zeitreihen,ch.bfs.gebaeude_wohnungs_register,ch.bav.haltestellen-oev,ch.swisstopo.swisstlm3d-wanderwege,ch.swisstopo.geologie-geocover&layers_visibility=

Fey, C., & Krainer, K. (2020). Analyses of UAV and GNSS based flow velocity variations of the rock glacier Lazaun (Ötztal Alps, South Tyrol, Italy). *Geomorphology*, *365*. https://doi.org/10.1016/j.geomorph.2020.107261

Fleischer, F., Haas, F., Altmann, M., Rom, J., Knoflach, B., & Becht, M. (2023). Combination of historical and modern data to decipher the geomorphic evolution of the Innere Ölgruben rock glacier, Kaunertal, Austria, over almost a century (1922–2021). *Permafrost and Periglacial Processes*, *34*(1), 3–21. https://doi.org/10.1002/ppp.2178

Fleischer, F., Haas, F., Piermattei, L., Pfeiffer, M., Heckmann, T., Altmann, M., Rom, J., Stark, M., Wimmer, M. H., Pfeifer, N., & Becht, M. (2021). Multi-decadal (1953-2017) rock glacier kinematics analysed by high-resolution topographic data in the upper Kaunertal, Austria. *Cryosphere*, *15*(12), 5345–5369. https://doi.org/10.5194/tc-15-5345-2021

Gärtner-Roer, I., Brunner, N., Delaloye, R., Haeberli, W., Kaab, A., & Thee, P. (2022). Glacier-permafrost relations in a high-mountain environment: 5 decades of kinematic monitoring at the Gruben site, Swiss Alps. *Cryosphere*, *16*(5), 2083–2101. https://doi.org/10.5194/tc-16-2083-2022

GeoMax AG. (n.d.). *Zenith15 & 25 Pro Series*. https://geomax.gr/wp-content/uploads/2019/06/GNSS_Zenith15_Zenith25_Datasheet_ENUS_LR.pdf

Gienko, G. A., & Terry, J. P. (2014). Three-dimensional modeling of coastal boulders using multi-view image. *Earth Surf. Process. Landforms*, *39*, 853–864.

Gruber, S., & Haeberli, W. (2008). Mountain Permafrost. *Permafrost Soils*, 33–44. https://doi.org/10.1007/978-3-540-69371-0_3

Haberkorn, A., Kenner, R., Noetzli, J., & Phillips, M. (2021). Changes in Ground Temperature and Dynamics in Mountain Permafrost in the Swiss Alps. *Frontiers in Earth Science*, *9*(April), 1–21. https://doi.org/10.3389/feart.2021.626686

Haeberli, W. (1985). Creep of mountain permafrost: internal structure and flow of alpine rock glaciers. *Mitteilungen Der Versuchsanstalt Für Wasserbau, Hydrologie Und Glaziologie Der ETH Zürich*, *77*, 1–142.

Haeberli, W., Arenson, L. U., Wee, J., Hauck, C., & Mölg, N. (2023). *Discriminating viscous creep features (rock glaciers) in mountain permafrost from debris-covered glaciers – a commented test at the Gruben and Yerba Loca sites, Swiss Alps and Chilean Andes*. 1–22. https://doi.org/https://doi.org/10.5194/egusphere-2023-1191

Haeberli, W., Arenson, L. U., Wee, J., Hauck, C., & Mölg, N. (2024). Discriminating viscous creep features (rock glaciers) in mountain permafrost from debris-covered glaciers – a commented test at the Gruben and Yerba Loca sites, Swiss Alps and Chilean Andes. *The Cryosphere*, *18*, 1669–1683. https://doi.org/https://doi.org/10.5194/tc-18-1669-2024

Haeberli, W., & Beniston, M. (1998). Climate change and its impacts on glaciers and permafrost in the Alps. *Ambio*, *27*(4), 258–265.

Haeberli, W., Hallet, B., Arenson, L., Elcolin, R., Humlum, O., Kääb, A., Kaufmann, V., Ladanyi, B., Matsuoka, N., Springmann, S., & Vonder Mühll, D. (2006). Permafrost Creep and Rock Glacier Dynamics. *Permafrost and Periglacial Processes*, *17*, 189–214. https://doi.org/10.1002/ppp

Haeberli, W., & Hohmann, R. (2008). Climate, Glaciers and Permafrost in the Swiss Alps 2050: scenarios, consequences and recommendations. *9th International Conference on Permafrost*, 607–612. http://www.zora.uzh.ch/6025/

Haeberli, W., Schaub, Y., & Huggel, C. (2017). Increasing risks related to landslides from degrading permafrost into new lakes in de-glaciating mountain ranges. *Geomorphology*, *293*, 405–417. https://doi.org/10.1016/j.geomorph.2016.02.009

Hafner, S., Günthnert, A., Burckhardt, C. E., Steiger, R. H., Hansen, J. W., & Niggli, C. R. (1975). *Blatt 1251 Val Bedretto. – Geol. Atlas Schweiz 1:25000, Karte 68.*

Halla, C., Henrik Blöthe, J., Tapia Baldis, C., Trombotto Liaudat, D., Hilbich, C., Hauck, C., & Schrott, L. (2021). Ice content and interannual water storage changes of an active rock glacier in the dry Andes of Argentina. *Cryosphere*, *15*(2), 1187–1213. https://doi.org/10.5194/tc-15-1187-2021

Hanson, S., & Hoelzle, M. (2004). The thermal regime of the active layer at the Murtèl rock glacier based on data from 2002. *Permafrost and Periglacial Processes*, *15*(3), 273–282. https://doi.org/10.1002/ppp.499

Harbor, J. (1997). Influence of subglacial drainage conditions on the velocity distribution within a glacier cross section. *Geology*, *25*(8), 739–742. https://doi.org/10.1130/0091-7613(1997)025<0739:IOSDCO>2.3.CO;2

Harris, C., Davies, M. C. R., & Etzelmüller, B. (2001). The Assessment of Potential Geotechnical Hazards Associated with Mountain Permafrost in a Warming Global Climate Charles. *Permafrost and Periglacial Processes*, *12*(January), 145–156. https://doi.org/10.1002/ppp 376

Harris, C., Mühll, D. V., Isaksen, K., Haeberli, W., Sollid, J. L., King, L., Holmlund, P., Dramis, F., Guglielmin, M., & Palacios, D. (2003). Warming permafrost in European mountains. *Global and Planetary Change*, *39*(3–

4), 215–225. https://doi.org/10.1016/j.gloplacha.2003.04.001

Hayamizu, M., & Nakata, Y. (2021). Accuracy Assessment of Post-processing Kinematic Georeferencing Based on Real-time Kinematic Unmanned Aerial Vehicle and Structure-from-motion Photogrammetry: Topographic Measurements of a Riverbed in a Small Watershed with a Check Dam. *TechRxiv*. https://doi.org/10.36227/techrxiv.16987960.v1

Hendrickx, H., Vivero, S., De Cock, L., De Wit, B., De Maeyer, P., Lambiel, C., Delaloye, R., Nyssen, J., & Frankl, A. (2019). The reproducibility of SfM algorithms to produce detailed Digital Surface Models: the example of PhotoScan applied to a high-alpine rock glacier. *Remote Sensing Letters*, *10*(1), 11–20. https://doi.org/10.1080/2150704X.2018.1519641

Hoelzle, M., Wegmann, M., & Krummenacher, B. (1999). Miniature temperature dataloggers for mapping and monitoring of permafrost in high mountain areas: First experience from the Swiss Alps. *Permafrost and Periglacial Processes*, *10*(2), 113–124. https://doi.org/10.1002/(SICI)1099-1530(199904/06)10:2<113::AID-PPP317>3.0.CO;2-A

Iglhaut, J., Cabo, C., Puliti, S., Piermattei, L., O'Connor, J., & Rosette, J. (2019). Structure from Motion Photogrammetry in Forestry: a Review. *Current Forestry Reports*, *5*(3), 155–168. https://doi.org/10.1007/s40725-019-00094-3

Ikeda, A. (2004). Rock glacier dynamics near the lower limit of mountain permafrost in the swiss alps. In *Dissertation* (Issue January). papers2://publication/uuid/4968DE43-6C90-477D-ACB6-30CA695EECB3

Ikeda, A., & Matsuoka, N. (2002). Degradation of talus-derived rock glaciers in the upper engadin, Swiss alps. *Permafrost and Periglacial Processes*, *13*(2), 145–161. https://doi.org/10.1002/ppp.413

Immerzeel, W. W., Lutz, A. F., Andrade, M., Bahl, A., Biemans, H., Bolch, T., Hyde, S., Brumby, S., Davies, B. J., Elmore, A. C., Emmer, A., Feng, M., Fernández, A., Haritashya, U., Kargel, J. S., Koppes, M., Kraaijenbrink, P. D. A., Kulkarni, A. V., Mayewski, P. A., … Baillie, J. E. M. (2020). Importance and vulnerability of the world's water towers. *Nature*, *577*(7790), 364–369. https://doi.org/10.1038/s41586-019-1822-y

James, M. R., & Robson, S. (2012). Straightforward reconstruction of 3D surfaces and topography with a camera: Accuracy and geoscience application. *Journal of Geophysical Research: Earth Surface*, *117*(3), 1–17. https://doi.org/10.1029/2011JF002289

James, M. R., & Robson, S. (2014). Mitigating systematic error in topographic models derived from UAV and ground-based image networks. *Earth Surface Processes and Landforms*, *39*(10), 1413–1420. https://doi.org/10.1002/esp.3609

James, M. R., Robson, S., d'Oleire-Oltmanns, S., & Niethammer, U. (2017). Optimising UAV topographic surveys processed with structure-from-motion: Ground control quality, quantity and bundle adjustment. *Geomorphology*, *280*, 51–66. https://doi.org/10.1016/j.geomorph.2016.11.021

Jemai, M., Loghmari, M. A., & Naceur, M. S. (2023). A GNSS Measurement Study Based on RTK and PPK Methods. *2023 IEEE International Conference on Advanced Systems and Emergent Technologies (IC_ASET)*, 1–6. https://doi.org/10.1109/ic_aset58101.2023.10151238

Jiménez-Jiménez, S. I., Ojeda-Bustamante, W., Marcial-Pablo, M. D. J., & Enciso, J. (2021). Digital terrain models generated with low-cost UAV photogrammetry: Methodology and accuracy. *ISPRS International Journal of Geo-Information*, *10*(285). https://doi.org/10.3390/ijgi10050285

Jorgenson, M. T., Romanovsky, V., Harden, J., Shur, Y., O'Donnell, J., Schuur, E. A. G., Kanevskiy, M., & Marchenko, S. (2010). Resilience and vulnerability of permafrost to climate change. *Canadian Journal of Forest Research*, *40*(7), 1219–1236. https://doi.org/10.1139/X10-060

Kääb, A., Frauenfelder, R., & Roer, I. (2007). On the response of rockglacier creep to surface temperature

increase. *Global and Planetary Change*, *56*(1–2), 172–187. https://doi.org/10.1016/j.gloplacha.2006.07.005

Kääb, A., Gudmundsson, G. H., & Hoelzle, M. (1998). Surface deformation of creeping mountain permafrost. Photogrammetric investigations on rock glacier Murtèl, Swiss Alps. *Seventh International Conference on Permafrost, Yellowknife (Canada), Collection Nordicana No 55, 1998.*, *55*, 531–537. http://folk.uio.no/kaeaeb/publications/ipc98.pdf

Kääb, A., Haeberli, W., & Hilmar Gudmundsson, G. (1997). Analysing the creep of mountain permafrost using high precision aerial photogrammetry: 25 years of monitoring Gruben rock glacier, Swiss Alps. *Permafrost and Periglacial Processes*, *8*(4), 409–426. https://doi.org/10.1002/(SICI)1099-1530(199710/12)8:4<409::AID-PPP267>3.0.CO;2-C

Kääb, A., & Vollmer, M. (2000). Surface geometry, thickness changes and flow fields on creeping mountain permafrost: Automatic extraction by digital image analysis. *Permafrost and Periglacial Processes*, *11*(4), 315–326. https://doi.org/10.1002/1099-1530(200012)11:4<315::AID-PPP365>3.0.CO;2-J

Kaiser, S., Boike, J., Grosse, G., & Langer, M. (2022). The Potential of UAV Imagery for the Detection of Rapid Permafrost Degradation: Assessing the Impacts on Critical Arctic Infrastructure. *Remote Sensing*, *14*(23). https://doi.org/10.3390/rs14236107

Kaufmann, V., Kellerer-Pirklbauer, A., & Seier, G. (2021). Conventional and UAV-Based Aerial Surveys for Long-Term Monitoring (1954–2020) of a Highly Active Rock Glacier in Austria. *Frontiers in Remote Sensing*, *2*, 1–18. https://doi.org/10.3389/frsen.2021.732744

Kellerer-Pirklbauer, A., Bodin, X., Delaloye, R., Lambiel, C., Gärtner-Roer, I., Bonnefoy-Demongeot, M., Carturan, L., Damm, B., Eulenstein, J., Fischer, A., Hartl, L., Ikeda, A., Kaufmann, V., Krainer, K., Matsuoka, N., Di Cella, U. M., Noetzli, J., Seppi, R., Scapozza, C., … Zumiani, M. (2024). Acceleration and interannual variability of creep rates in mountain permafrost landforms (rock glacier velocities) in the European Alps in 1995 2022. *Environmental Research Letters*, *19*. https://doi.org/10.1088/1748-9326/ad25a4

Kellerer-pirklbauer, A., Bodin, X., Delaloye, R., Lambiel, C., Gärtner-roer, I., Bonnefoy-demongeot, M., Carturan, L., Damm, B., Eulenstein, J., Fischer, A., Hartl, L., Ikeda, A., Kaufmann, V., Krainer, K., Matsuoka, N., Morra Di Cella, U., Noetzli, J., Seppi, R., Scapozza, C., … Zumiani, M. (2024). Acceleration and interannual variability of creep rates in mountain permafrost landforms (rock glacier velocities) in the European Alps in 1995 – 2022. *Environmental Research Letters*, *19*. https://doi.org/10.1088/1748-9326/ad25a4

Kenner, R., Phillips, M., Beutel, J., Hiller, M., Limpach, P., Pointner, E., & Volken, M. (2017). Factors Controlling Velocity Variations at Short-Term Seasonal and Multiyear.pdf. *Permafrost and Periglac. Process.*, *28*, 675–684.

Kenner, R., Pruessner, L., Beutel, J., Limpach, P., & Phillips, M. (2019). How rock glacier hydrology, deformation velocities and ground temperatures interact: Examples from the Swiss Alps. *Permafrost and Periglacial Processes*, *31*(1), 3–14. https://doi.org/10.1002/ppp.2023

Klug, C., Bollmann, E., Sailer, R., Stötter, J., Krainer, K., & Kääb, A. (2012). Monitoring of Permafrost Creep on Two Rock Glaciers in the Austrian Eastern Alps: Combination of Aerophotogrammetry and Airborne Laser Scanning. *Proceedings of the 10th International Conference on Permafrost*, 215–220. https://doi.org/10.13140/RG.2.1.1807.7284

Krautblatter, M., Kellerer-Pirklbauer, A., & Isabelle, G.-R. (2018). Permafrost in den Alpen. *Geographische Rundscahu*, *11*, 22–29. https://doi.org/10.2312/geowissenschaften.1994.12.149

Krummenacher, B., Mihajlovic, D., Nussbaum, A., & Staub, B. (2008). 20 Jahre Furggentälti: Permafrostuntersuchung auf der Gemmi. In *Geographica Bernensia: Vol. G 80.*

Kummert, M., Delaloye, R., & Braillard, L. (2018). Erosion and sediment transfer processes at the front of rapidly moving rock glaciers: Systematic observations with automatic cameras in the western Swiss Alps. *Permafrost and Periglacial Processes*, *29*(1), 21–33. https://doi.org/10.1002/ppp.1960

Lague, D., Brodu, N., & Leroux, J. (2013). Accurate 3D comparison of complex topography with terrestrial laser scanner: Application to the Rangitikei canyon (N-Z). *ISPRS Journal of Photogrammetry and Remote Sensing*, *82*, 10–26. https://doi.org/10.1016/j.isprsjprs.2013.04.009

Lambiel, C., Delaloye, R., & Perruchoud, E. (2005). Yearly and seasonally variations of surface velocities on creeping permafrost bodies. Cases studies in the Valais Alps. In *3rd Swiss Geo- science Meeting, Zürich* (Issue January, pp. 1–2).

Luetschg, M., Lehning, M., & Haeberli, W. (2008). A sensitivity study of factors influencing warm/thin permafrost in the Swiss Alps. *Journal of Glaciology*, *54*(187), 696–704. https://doi.org/10.3189/002214308786570881

Marcer, M., Serrano, C., Brenning, A., Bodin, X., Schoeneich, P., Marcer, M., Serrano, C., Brenning, A., Bodin, X., Goetz, J., Marcer, M., Serrano, C., Brenning, A., Bodin, X., Goetz, J., & Schoeneich, P. (2019). Evaluating the destabilization susceptibility of active rock glaciers in the French Alps. *The Cryosphere*, *13*(1), 141–155. https://doi.org/10.5194/tc-13-141-2019

Mari, S., Delaloye, R., Scapozza, C., & Strozzi, T. (2011). *Inventario dei movimenti di terreno per analisi dei segnali InSAR nelle Alpi meridionali svizzere (periodo 1994-2007)* (pp. 145–159). http://www.unil.ch/igul/page84172.html

Mari, S., Scapozza, C., Delaloye, R., & Lambiel, C. (2012). Il permafrost nelle Alpi Ticinesi (2006–2011). *Bollettino Della Società Ticinese Di Scienze Naturali*, *100*(1), 135–139.

Martínez-Fernández, A., Serrano, E., Pisabarro, A., Sánchez-Fernández, M., de Sanjosé, J. J., Gómez-Lende, M., Rangel-de Lázaro, G., & Benito-Calvo, A. (2022). The Influence of Image Properties on High-Detail SfM Photogrammetric Surveys of Complex Geometric Landforms: The Application of a Consumer-Grade UAV Camera in a Rock Glacier Survey. *Remote Sensing*, *14*(15). https://doi.org/10.3390/rs14153528

McMahon, C., Mora, O. E., & Starek, M. J. (2021). Evaluating the performance of suas photogrammetry with PPK positioning for infrastructure mapping. *Drones*, *5*(2), 1–18. https://doi.org/10.3390/drones5020050

MeteoSchweiz. (2021). *Klimabulletin Jahr 2020*.

MeteoSchweiz. (2023a). *Klimabulletin Jahr 2022*.

MeteoSchweiz. (2023b). *Klimabulletin Winter 2022/23*.

MeteoSchweiz. (2024). *Klimabulletin Jahr 2023*.

Methodenberatung UZH. (n.d.). *Kruskal-Wallis-Test*. https://www.methodenberatung.uzh.ch/de/datenanalyse_spss/unterschiede/zentral/kruskal.html

Micheletti, N., Tonini, M., & Lane, S. N. (2017). Geomorphological activity at a rock glacier front detected with a 3D density-based clustering algorithm. *Geomorphology*, *278*, 287–297. https://doi.org/10.1016/j.geomorph.2016.11.016

Midgley, N. G., & Tonkin, T. N. (2017). Reconstruction of former glacier surface topography from archive oblique aerial images. *Geomorphology*, *282*, 18–26. https://doi.org/10.1016/j.geomorph.2017.01.008

Mosbrucker, A. R., Major, J. J., Spicer, K. R., & Pitlick, J. (2017). Camera system considerations for geomorphic applications of SfM photogrammetry. *Earth Surface Processes and Landforms*, *42*(6), 969–986. https://doi.org/10.1002/esp.4066

Müller, J., Vieli, A., & Gärtner-Roer, I. (2016). Rock glaciers on the run - Understanding rock glacier landform evolution and recent changes from numerical flow modeling. *Cryosphere*, *10*(6), 2865–2886. https://doi.org/10.5194/tc-10-2865-2016

Noetzli, J., & Pellet, C. (2022). *Swiss Permafrost Bulletin 2022* (Issue October 2021). https://doi.org/10.13093/permos-bull-23

Nourbakhshbeidokhti, S., Kinoshita, A. M., Chin, A., & Florsheim, J. L. (2019). A workflow to estimate topographic and volumetric changes and errors in channel sedimentation after disturbance. *Remote Sensing*, *11*(5). https://doi.org/10.3390/rs11050586

Perruchoud, E., & Delaloye, R. (2007). Short-Term Changes in Surface Velocities on the Becs-de-Bosson Rock Glacier (Western Swiss Alps). *Grazer Schriften Der Geographie*, *43*, 131–136.

Peternel, T., Janza, M., Segina, E., Bezak, N., & Macek, M. (2022). Recognition of Landslide Triggering Mechanisms and Dynamics Using GNSS, UAV Photogrammetry and In Situ Monitoring Data. *Remote Sensing*, *14*. https://doi.org/10.3390/rs14143277

Pruessner, L., Huss, M., & Farinotti, D. (2022). Temperature evolution and runoff contribution of three rock glaciers in Switzerland under future climate forcing. *Permafrost and Periglacial Processes*, *33*(3), 310–322. https://doi.org/10.1002/ppp.2149

Rahbek, C., Borregaard, M. K., Antonelli, A., Colwell, R. K., Holt, B. G., Nogues-Bravo, D., Rasmussen, C. M. Ø., Richardson, K., Rosing, M. T., Whittaker, R. J., & Fjeldså, J. (2019). Building mountain biodiversity: Geological and evolutionary processes. *Science*, *365*, 1114–1119. https://doi.org/10.1126/science.aax0151

Ramelli, G., Scapozza, C., Mari, S., & Lambiel, C. (2011). Structure interne et dynamique des glaciers rocheux du massif de la Cima di Gana Bianca, Val Blenio (Tessin). In *La géomorphologie alpine: entre patrimoine et contrainte. Actes du colloque de la Société Suisse de Géomorphologie, 3-5 septembre 2009, Olivone* (Vol. 36, Issue 2011, pp. 177–193).

Redpath, T. A. N., Sirguey, P., Fitzsimons, S. J., & Kääb, A. (2013). Accuracy assessment for mapping glacier flow velocity and detecting flow dynamics from ASTER satellite imagery: Tasman Glacier, New Zealand. *Remote Sensing of Environment*, *133*, 90–101. https://doi.org/10.1016/j.rse.2013.02.008

RGIK. (2021). *Rock Glacier Kinematics as an associated parameter of ECV Permafrost (Version 3.0)* (pp. 1–12).

RGIK. (2022). *Towards standard guidelines for inventorying rock glaciers: baseline concepts (version 4.2.2)*. https://www3.unifr.ch/geo/geomorphology/en/research/ipa-action-group-rock-glacier

RGIK. (2023). Guidelines for inventorying rock glaciers: baseline and practical concepts (version 1.0). In *IPA Action Group Rock glacier inventories and kinematics*. https://doi.org/10.51363/unifr.srr.2023.002

Roer, I., Haeberli, W., Avian, M., Kaufmann, V., Delaloye, R., Lambiel, C., & Kääb, A. (2008). Observations and considerations on destabilizing active rock glaciers in the European Alps. *Ninth International Conference on Permafrost*, 1505–1510.

Sanz-Ablanedo, E., Chandler, J. H., Rodríguez-Pérez, J. R., & Ordóñez, C. (2018). Accuracy of Unmanned Aerial Vehicle (UAV) and SfM photogrammetry survey as a function of the number and location of ground control points used. *Remote Sensing*, *10*(10). https://doi.org/10.3390/rs10101606

Scapozza, C., & Ambrosi, C. (2017). Monitoraggio sistematico del permafrost con il drone ad ala fissa (Cantone Ticino, Svizzera). *Droni Nel Settore Pubblico Fra Presente e Futuro*, 1–36.

Scapozza, C., Antognini, M., & Ambrosi, C. (2018). Il permafrost nelle Alpi Ticinesi (2015/2016 e 2016/2017). *Bollettino Della Società Ticinese Di Scienze Naturali*, *106*(4), 13–22.

Scapozza, C., Baron, L., & Lambiel, C. (2015). Borehole logging in Alpine periglacial talus slopes (Valais, Swiss Alps). *Permafrost and Periglacial Processes*, *26*(1), 67–83. https://doi.org/10.1002/ppp.1832

Scapozza, C., Deluigi, N., Siro, C. Del, Pollo, A., & Antognini, M. (2020). Il permafrost nelle Alpi Ticinesi (2017/2018 e 2018/2019). *Bollettino Della Società Ticinese Di Scienze Naturali*, *108*(5), 33–43.

Scapozza, C., Giaccone, E., Mari, S., Antognini, M., & Fratianni, S. (2016). Il permafrost nelle Alpi Ticinesi (2013/2014 e 2014/2015). *Bollettino Della Società Ticinese Di Scienze Naturali*, *104*(3), 37–44.

Scapozza, C., Lambiel, C., Bozzini, C., Mari, S., & Conedera, M. (2014a). Assessing the rock glacier kinematics on three different timescales: A case study from the southern Swiss Alps. *Earth Surface Processes and Landforms*, *39*(15), 2056–2069. https://doi.org/10.1002/esp.3599

Scapozza, C., Lambiel, C., Gex, P., & Reynard, E. (2011). Prospection géophysique multi-méthodes du pergélisol alpin dans le sud des Alpes suisses. *Géomorphologie: Relief, Processus, Environnement*, *17*(1). https://doi.org/10.4000/geomorphologie.8765

Scapozza, C., Mari, S., Antognini, M., & Lepori, V. (2014b). Il permafrost nelle Alpi Ticinesi (2011/2012 e 2012/2013). *Bollettino Della Società Ticinese Di Scienze Naturali*, *102*, 59–69.

Scherler, M., Schneider, S., Hoelzle, M., & Hauck, C. (2014). A two-sided approach to estimate heat transfer processes within the active layer of the Murtèl-Corvatsch rock glacier. *Earth Surface Dynamics*, *2*(1), 141–154. https://doi.org/10.5194/esurf-2-141-2014

Swiss Permafrost Monitoring Network PERMOS. (n.d.). *Rock glacier velocity*. https://www.permos.ch/data-portal/rock-glacier-velocities

Terzi, S., Torresan, S., Schneiderbauer, S., Critto, A., Zebisch, M., & Marcomini, A. (2019). Multi-risk assessment in mountain regions: A review of modelling approaches for climate change adaptation. *Journal of Environmental Management*, *232*, 759–771. https://doi.org/10.1016/j.jenvman.2018.11.100

Türk, T., Tunalioglu, N., Erdogan, B., Ocalan, T., & Gurturk, M. (2022). Accuracy assessment of UAV-post-processing kinematic (PPK) and UAV-traditional (with ground control points) georeferencing methods. *Environmental Monitoring and Assessment*, *194*(7). https://doi.org/10.1007/s10661-022-10170-0

Ulrich, V., Williams, J. G., Zahs, V., Anders, K., Hecht, S., & Höfle, B. (2021). Measurement of rock glacier surface change over different timescales using terrestrial laser scanning point clouds. *Earth Surface Dynamics*, *9*(1), 19–28. https://doi.org/10.5194/esurf-9-19-2021

Varnes, D. (1978). Slope Movement types and Processes. In R. L. Schuster & R. J. Krizek (Eds.), *TRB Special Report 176, Landslides: Analysis and Control.* (pp. 11–33).

Vivero, S., Bodin, X., Farías-Barahona, D., MacDonell, S., Schaffer, N., Robson, B. A., & Lambiel, C. (2021). Combination of Aerial, Satellite, and UAV Photogrammetry for Quantifying Rock Glacier Kinematics in the Dry Andes of Chile (30°S) Since the 1950s. *Frontiers in Remote Sensing*, *2*, 1–17. https://doi.org/10.3389/frsen.2021.784015

Vivero, S., Hendrickx, H., Frankl, A., Delaloye, R., & Lambiel, C. (2022). Kinematics and geomorphological changes of a destabilising rock glacier captured from close-range sensing techniques (Tsarmine rock glacier, Western Swiss Alps). *Frontiers in Earth Science*, *10*, 1–21. https://doi.org/10.3389/feart.2022.1017949

Vivero, S., & Lambiel, C. (2019). Monitoring the crisis of a rock glacier with repeated UAV surveys. *Geographica Helvetica*, *74*(1), 59–69. https://doi.org/10.5194/gh-74-59-2019

Vonder Mühll, D., Nötzli, J., & Roer, I. (2008). PERMOS – A comprehensive monitoring network of mountain permafrost in the Swiss Alps. *Proceedings of the 9th International Conference on Permafrost*, *July*, 1869–1874.

Wang, Y., Zhao, Y., Mao, X., & Yin, S. (2023). Impact of Climate Change on the Performance of Permafrost Highway Subgrade Reinforced by Concrete Piles. *Future Transportation*, *3*(3), 996–1006. https://doi.org/10.3390/futuretransp3030055

Westoby, M. J., Brasington, J., Glasser, N. F., Hambrey, M. J., & Reynolds, J. M. (2012). "Structure-from-Motion" photogrammetry: A low-cost, effective tool for geoscience applications. *Geomorphology*, *179*, 300–314. https://doi.org/10.1016/j.geomorph.2012.08.021

Wicky, J., & Hauck, C. (2017). Numerical modelling of convective heat transport by air flow in permafrost talus slopes. *Cryosphere*, *11*(3), 1311–1325. https://doi.org/10.5194/tc-11-1311-2017

Wicky, J., & Hauck, C. (2020). Air Convection in the Active Layer of Rock Glaciers. *Frontiers in Earth Science*, *8*, 1–17. https://doi.org/10.3389/feart.2020.00335

Wirz, V., Beutel, J., Gruber, S., Gubler, S., & Purves, R. S. (2014). Estimating velocity from noisy GPS data for investigating the temporal variability of slope movements. *Natural Hazards and Earth System Sciences*, *14*(9), 2503–2520. https://doi.org/10.5194/nhess-14-2503-2014

Wirz, V., Gruber, S., Purves, R. S., Beutel, J., Gärtner-Roer, I., Gubler, S., & Vieli, A. (2016). Short-term velocity variations at three rock glaciers and their relationship with meteorological conditions. *Earth Surface Dynamics*, *4*(1), 103–123. https://doi.org/10.5194/esurf-4-103-2016

Yang, X., Hu, J., Li, P., Gao, C., Latifi, H., Bai, X., Gao, J., Dang, T., & Tang, F. (2024). SCCD: A slicing algorithm for detecting geomorphic changes on topographically complex areas based on 3D point clouds. *Remote Sensing of Environment*, *303*. https://doi.org/10.1016/j.rse.2024.114022

Zahs, V., Hämmerle, M., Anders, K., Hecht, S., Sailer, R., Rutzinger, M., Williams, J. G., & Höfle, B. (2019). Multi-temporal 3D point cloud-based quantification and analysis of.pdf. *Permafrost and Periglac. Process.*, *30*, 222–238.

Zhang, H., Aldana-Jague, E., Clapuyt, F., Wilken, F., Vanacker, V., & Van Oost, K. (2019). Evaluating the Potential of PPK Direct Georeferencing for UAV-SfM Photogrammetry and Precise Topographic Mapping. *Earth Surface Dynamics Discussions*, *January*, 1–34.

Personal declaration

I hereby declare that the submitted thesis is the result of my own, independent work. All external sources are explicitly acknowledged in the thesis.

Morbio Inferiore, 30.04.2024

Giona Crivelli